PRESSURIZED WATER REACTOR OWNERS GROUP

PWROG-15060-NP
Revision 0

WESTINGHOUSE NON-POPRIETARY CLASS 3

Pump Suction Gas Accumulation Operability Criteria Guidance

PWROG SEE Subcommittee

PA-SEE-1280-R1

December 2015

Westinghouse

PWROG-15060-NP
Revision 0

Pump Suction Gas Accumulation Operability Criteria Guidance

PA-SEE-1280-R1

Stephen R. Swantner*

Fluid Systems Engineering

Matthew M. Swartz*

Fluid Systems Engineering

December 2015

Reviewer: Meaghan J. Kirkpatrick*
Fluid Systems Engineering

Approved: Tyler R. Upton*, Manager
Fluid Systems Engineering

Approved: Jay D. Boardman*, Program Director
PWR Owners Group PMO

*Electronically approved records are authenticated in the electronic document management system.

Westinghouse Electric Company LLC
1000 Westinghouse Drive
Cranberry Township, PA 16066, USA

ACKNOWLEDGEMENTS

This report was developed and funded by the Pressurized Water Reactor Owners Group (PWROG) under the leadership of the participating utility representatives of the Systems & Equipment Engineering (SEE) Committee. The following individuals participated in the PWROG core team that guided development of the document: Jeff Brown (APS), Mo Dingler (WCNOC), Anderson Lin (PG&E), and Ed Shore (Dominion). In addition, Steve Wiser (Dominion) and Robert Jacobus (Dominion) are acknowledged for their detailed review and constructive comments on the document.

LEGAL NOTICE

This report was prepared as an account of work performed by Westinghouse Electric Company LLC. Neither Westinghouse Electric Company LLC, nor any person acting on its behalf:

1. Makes any warranty or representation, express or implied including the warranties of fitness for a particular purpose or merchantability, with respect to the accuracy, completeness, or usefulness of the information contained in this report, or that the use of any information, apparatus, method, or process disclosed in this report may not infringe privately owned rights; or

2. Assumes any liabilities with respect to the use of, or for damages resulting from the use of, any information, apparatus, method, or process disclosed in this report.

COPYRIGHT NOTICE

DISTRIBUTION NOTICE

This report was prepared for the PWR Owners Group. This Distribution Notice is intended to establish guidance for access to this information. This report (including proprietary and non-proprietary versions) is not to be provided to any individual or organization outside of the PWR Owners Group program participants without prior written approval of the PWR Owners Group Program Management Office. However, prior written approval is not required for program participants to provide copies of Class 3 Non-Proprietary reports to third parties that are supporting implementation at their plant, and for submittals to the NRC.

PWR Owners Group
United States Member Participation* for PA-SEE-1280-R1

Utility Member	Plant Site(s)	Participant Yes	Participant No
Ameren Missouri	Callaway (W)	X	
American Electric Power	D.C. Cook 1 & 2 (W)	X	
Arizona Public Service	Palo Verde Unit 1, 2, & 3 (CE)	X	
Dominion Connecticut	Millstone 2 (CE)	X	
	Millstone 3 (W)	X	
Dominion VA	North Anna 1 & 2 (W)	X	
	Surry 1 & 2 (W)	X	
Duke Energy Carolinas	Catawba 1 & 2 (W)	X	
	McGuire 1 & 2 (W)	X	
	Oconee 1, 2, & 3 (B&W)	X	
Duke Energy Progress	Robinson 2 (W)	X	
	Shearon Harris (W)	X	
Entergy Palisades	Palisades (CE)	X	
Entergy Nuclear Northeast	Indian Point 2 & 3 (W)	X	
Entergy Operations South	Arkansas 1 (B&W)	X	
	Arkansas 2 (CE)	X	
	Waterford 3 (CE)	X	
Exelon Generation Co. LLC	Braidwood 1 & 2 (W)	X	
	Byron 1 & 2 (W)	X	
	TMI 1 (B&W)	X	
	Calvert Cliffs 1 & 2 (CE)	X	
	Ginna (W)	X	
FirstEnergy Nuclear Operating Co.	Beaver Valley 1 & 2 (W)	X	
	Davis-Besse (B&W)	X	
Florida Power & Light \ NextEra	St. Lucie 1 & 2 (CE)	X	
	Turkey Point 3 & 4 (W)	X	
	Seabrook (W)	X	
	Pt. Beach 1 & 2 (W)	X	
Luminant Power	Comanche Peak 1 & 2 (W)	X	

PWR Owners Group
United States Member Participation* for PA-SEE-1280-R1

Utility Member	Plant Site(s)	Participant	
		Yes	No
Omaha Public Power District	Fort Calhoun (CE)	X	
Pacific Gas & Electric	Diablo Canyon 1 & 2 (W)	X	
PSEG – Nuclear	Salem 1 & 2 (W)	X	
South Carolina Electric & Gas	V.C. Summer (W)	X	
So. Texas Project Nuclear Operating Co.	South Texas Project 1 & 2 (W)	X	
Southern Nuclear Operating Co.	Farley 1 & 2 (W)	X	
	Vogtle 1 & 2 (W)	X	
Tennessee Valley Authority	Sequoyah 1 & 2 (W)	X	
	Watts Bar 1 & 2 (W)	X	
Wolf Creek Nuclear Operating Co.	Wolf Creek (W)	X	
Xcel Energy	Prairie Island 1 & 2 (W)	X	

***Project participants as of the date the final deliverable was completed. On occasion, additional members will join a project. Please contact the PWR Owners Group Program Management Office to verify participation before sending this document to participants not listed above.**

PWR Owners Group
International Member Participation* for PA-SEE-1280-R1

Utility Member	Plant Site(s)	Participant	
		Yes	No
Asociación Nuclear Ascó-Vandellòs	Asco 1 & 2 (W)	X	
	Vandellos 2 (W)	X	
Axpo AG	Beznau 1 & 2 (W)	X	
Centrales Nucleares Almaraz-Trillo	Almaraz 1 & 2 (W)	X	
EDF Energy	Sizewell B (W)	X	
Electrabel	Doel 1, 2 & 4 (W)	X	
	Tihange 1 & 3 (W)	X	
Electricite de France	58 Units	X	
Eletronuclear-Eletrobras	Angra 1 (W)	X	
Eskom	Koeberg 1 & 2 (W)	X	
Hokkaido	Tomari 1, 2 & 3 (MHI)	X	
Japan Atomic Power Company	Tsuruga 2 (MHI)	X	
Kansai Electric Co., LTD	Mihama 1, 2 & 3 (W)	X	
	Ohi 1, 2, 3 & 4 (W & MHI)	X	
	Takahama 1, 2, 3 & 4 (W & MHI)	X	
Korea Hydro & Nuclear Power Corp.	Kori 1, 2, 3 & 4 (W)	X	
	Hanbit 1 & 2 (W)	X	
	Hanbit 3, 4, 5 & 6 (CE)	X	
	Hanul 3, 4 , 5 & 6 (CE)	X	
Kyushu	Genkai 1, 2, 3 & 4 (MHI)	X	
	Sendai 1 & 2 (MHI)	X	
Nuklearna Electrarna KRSKO	Krsko (W)	X	
Ringhals AB	Ringhals 2, 3 & 4 (W)	X	
Shikoku	Ikata 1, 2 & 3 (MHI)	X	
Taiwan Power Co.	Maanshan 1 & 2 (W)	X	

***Project participants as of the date the final deliverable was completed. On occasion, additional members will join a project. Please contact the PWR Owners Group Program Management Office to verify participation before sending this document to participants not listed above.**

TABLE OF CONTENTS

List of Figures

List of Tables

Acronyms

AFM	Air Flow Meter
AIMP	Arch Impedance Meter
DAIMP	Double Arch Impedance Meter
APS	Arizona Public Service
BEP	Best Efficiency Point
BWR	Boiling Water Reactor
BWROG	Boiling Water Reactor Owner's Group
CE	Combustion Engineering
CS	Containment Spray
DHR	Decay Heat Removal
DP	Differential Pressure
ECCS	Emergency Core Cooling System
EPRI	Electric Power Research Institute
FAI	Fauske and Associates, LLC
GL	Generic Letter
HPSI	High Pressure Safety Injection
INPO	Institute of Nuclear Power Operations
LPSI	Low Pressure Safety Injection
MFM	Magnetic Flow Meter
NEI	Nuclear Energy Institute
NI	Nuclear Instruments
NIST	National Institute of Standards and Technology

NPSH	Net Positive Suction Head
$NPSH_A$	Available Net Positive Suction Head
$NPSH_R$	Required Net Positive Suction Head
NRC	United States Nuclear Regulatory Commission
NUREG/CR	Publication prepared by NRC contractor
P	Pressure Instrument
P&ID	Process and Instrumentation Diagram
PW	Parallel Wire Impedance Meter
PWR	Pressurized Water Reactor
PWROG	Pressurized Water Reactor Owner's Group
RAI	Request for Additional Information
RIMP	Ring Impedance Meter
RWT	Refueling Water Tank
RWST	Refueling Water Storage Tank
SE	Safety Evaluation
SER	Significant Event Report
SI	Safety Injection
TC	Thermocouple
VM	Void Meter
WCAP	Westinghouse Commercial Atomic Power

Nomenclature (English Symbols)

A	Area, ft^2
d	pipe diameter, inch
e	specific energy, ft
F	force, lb_f
Fr	Froude Number
g	gravitational acceleration, 32.2 ft/sec^2
g_c	gravitational conversion constant, 32.2 lb_m-ft/lb_f-sec^2
G	mas velocity, $lb_m/sec/ft^2$
h	head, ft
H	height, ft
L	length, ft
M	momentum flux, lb_f
P	static pressure, psia
q	flow rate, ft^3/sec
Q	flow rate, gpm
S	slip ratio
t	time, sec
T	liquid flow area divided by liquid free surface width, ft
u	velocity, ft/sec
V	volume, ft^3
We	Weber Number
y	water level measured normal to datum, ft

Nomenclature (Greek Symbols)

α gas void fraction

β gas volumetric flux ratio

Δ differential

ρ fluid density, lb_m/ft^3

σ surface tension, lb_f/ft

Subscripts

adj adjusted

avg average

c constant

C centroid

crit critical

d downstream

dc down-comer

el elbow

f force

g gas

hp high point gas accumulation location

i initial

id ideal

in inlet

init initial

h homogeneous

l	liquid
L	loss
m	mass
M	measurement location
max	maximum
min	minimum
mix	mixture
op	operation
out	outlet
p	pump
PA	post-accident operation
reqd	required
s	shock
sur	surveillance
u	upstream

1 INTRODUCTION AND PURPOSE

In January of 2008, the U.S. Nuclear Regulatory Commission (NRC) issued Generic Letter (GL) 2008-01, "Managing Gas Intrusion in Emergency Core Cooling, Decay Heat Removal, and Containment Spray Systems" (Reference 1). Each addressee was requested to evaluate their Emergency Core Cooling System (ECCS), Decay Heat Removal (DHR) system, and Containment Spray (CS) system design, operation, and test procedures to assure that gas intrusion is minimized and monitored in order to maintain system operability and compliance with the requirements of Appendix B to 10 CFR 50. In January of 2008, the Institute of Nuclear Power Operations (INPO) also issued Significant Event Report (SER) 2-05 Rev.1 "Gas Intrusion in Safety Systems" (Reference 2), which provides recommendations and guidance for the effective implementation of programs and processes to prevent and manage gas intrusion and accumulation in plant systems.

The Pressurized Water Reactors Owners Group (PWROG) funded analytical and experimental programs to investigate these issues. One of these efforts included an investigation of gas transport in large diameter piping systems. Piping systems with diameters ranging from 4" to 12" were tested to characterize large diameter two phase flow behavior in the presence of flow obstructions in the form of vertical plane elbows. The results of this study were documented in WCAP-17271 (Reference 3 and Reference 4). Phenomena governing the transport process were identified and a scaling study focused on developing empirical correlations to characterize these phenomena was documented. The scaling analysis results provided general correlations for the dominant phenomena observed in the testing, which included flow initialization via a vertical kinematic shock and vertical down-comer to horizontal elbow distribution. The resulting empirical correlations from the scaling analysis are considered acceptable for pipe diameters ranging from 4" to 30". The PWROG also investigated the use of a simplified equation to model gas transport. The results of this investigation are documented in WCAP-17276 (Reference 5).

In April of 2013, the Nuclear Energy Institute (NEI) issued Revision 1a-A of NEI 09-10 (Reference 6), "Guidelines for Effective Prevention and Management of System Gas Accumulation" that provides recommendations and guidance to nuclear generating stations for the effective implementation of programs and processes to prevent and manage gas intrusion and accumulation in plant systems. Appendix 4 of NEI 09-10 established that WCAP-17271 and WCAP-17276 provide suitable methods for calculating gas volume criteria that reasonably assure operability of degraded or nonconforming systems structures and components (SSCs). The NRC safety evaluation (SE) of NEI 09-10 (Reference 7) indicates that qualifications regarding use of WCAP-17271 and WCAP-17276 must be considered when implementing NEI 09-10, Revision 1a-A, and any licensees referencing or using this report should qualify the use of the references.

Recently, NRC inspections and audits have resulted in concerns that licensees may not have adequate guidance to apply the correlations based on WCAP-17271 consistent with limitations and conditions defined as part of the NEI-09-10 SE for gas transport analyses. In an attempt to resolve this issue, members of NEI/PWROG/BWROG met with the NRC on January 15, 2015. The NRC expressed their concurrence with use of the WCAP-17271 empirical correlations and the WCAP-17276 simplified equation to model gas transport in pump suction piping systems for the purpose of establishing acceptance criteria for operability determinations. However, the NRC requested that additional guidance be provided to licensees to ensure the correlations are used within the limitations imposed by the SE.

This document defines a means of applying the correlations in a manner which meets the limitations imposed by the SE.

2 REFERENCES

1. U.S. Nuclear Regulatory Commission, NRC GL 2008-01, "Managing Gas Intrusion in Emergency Core Cooling, Decay Heat Removal, and Containment Spray Systems," Accession No. ML072910759, January 2008.
2. Institute of Nuclear Power Operation, INPO SER 2-05, Revision 1 "Gas Intrusion in Safety Systems," January 2008.
3. Westinghouse WCAP-17271-P, Revision 1, "Testing and Evaluation of Gas Transport to the Suction of ECCS Pumps," Volume I, October 2010.
4. Westinghouse WCAP-17271-P, Revision 0, "Testing and Evaluation of Gas Transport to the Suction of ECCS Pumps," Volumes II and III, August 2010
5. Westinghouse WCAP-17276-P, Revision 1, "Investigation of Simplified Equation for Gas Transport," January 2011.
6. NEI 09-10, Revision 1a-A, "Guidelines for Effective Prevention and Management of System Gas Accumulation," Accession No. ML13136A129, April 2013.
7. NRC Regulatory Issue Summary 2013-09, "NRC Endorsement of NEI 09-10, Revision 1a-A, Guidelines for Effective Prevention and Management of System Gas Accumulation," ADAMS Accession No. ML13178A152, August 2013.
8. Westinghouse FAI/09-130-P, Revision 0, "Technical Basis for Gas Transport to the Pump Suction," December 2010.
9. EPRI Report Number 1026498, "Report of the Expert Panel on the Effect of Gas Accumulation on Pumps," August 2012.
10. Weisman et. al., "Effects of fluid properties and pipe diameters on two-phase flow patterns in horizontal lines," International Journal of Multiphase Flow, Vol. 5, 1979.
11. Westinghouse WCAP-17537-P, Revision 2, "Dynamic Venting of Piping Systems," September 2012.
12. NUREG/CR-2792, Creare TM-825, "An Assessment of Residual Heat Removal and Containment Spray Pump Performance Under Air and Debris Ingesting Conditions," September 1982.
13. Westinghouse WCAP-17167-NP, Revision 0, "Phenomena Identification and Ranking Table (PIRT) to Evaluate Void Fraction / Flow Regime at ECCS, RHR and CS Pump Suctions," December, 2009
14. Taitel, Y. and Dukler, A.E., AIChE Journal, Vol. 22, No. 1, pp. 47-55, "A Model for Predicting Flow Regime Transitions in Horizontal and Near Horizontal Gas-Liquid Flow," January 1976
15. Streeter, Victor L., and Wylie, E. Benjamin, <u>Fluid Mechanics</u>, Seventh Edition, McGraw-Hill Book Company, 1979.

3 PWROG GAS VOLUME ACCEPTANCE CRITERIA METHODOLOGY OVERVIEW

3.1 INTENDED USAGE

The methods provided in this report can be used to predict the volumetric flux of a non-condensable gas at a pump inlet based on the gas volume at an upstream accumulation location for a given set of pump suction piping hydraulic conditions. These methods are intended for operability determinations to show that the system, although degraded, will continue to perform its specified function. These methods are not intended for use in establishing design criteria. Sections 9 and 13 of NEI 09-10 provide more detail on design criteria and operability limits, respectively.

3.2 PUMP GAS INGESTION ACCEPTANCE CRITERIA

Gas ingestion acceptance criteria for pumps are intended to prevent mechanical damage or gas binding of the pump and to assure acceptable hydraulic performance. Transient acceptance criteria are typically presented as maximum allowable void fraction for a maximum specified time interval. Steady state criteria are specified as maximum allowable void fraction for an indefinite time period.

The pump gas ingestion criteria presented in Table 1 of NEI 09-10 represent conservative criteria for gas ingestion, mutually agreed upon by members of the BWROG/PWROG/NEI and the NRC for pump categories commonly encountered in the systems addressed by GL 2008-01 in U.S. operating plants. Pump gas ingestion tolerance criteria for steady state conditions reported in this document are consistent with NUREG/CR 2792 (Reference 12). Gas ingestion tolerance criteria for transient conditions were based on specific sets of test data and vendor inputs that address pump mechanical integrity. The NEI 09-10 criteria are provided as Table 3-1.

The Electric Power Research Institute (EPRI) "Report of the Expert Panel on the Effect of Gas Accumulation on Pumps" (Reference 9) Table 8-1 provides acceptance criteria developed by a panel of pump experts based upon a review of the types of pumps that are in service in the systems addressed by GL 2008-01 in U.S. operating plants. The expert panel used hydraulic and mechanical pump design characteristics to categorize pumps based on the capability to tolerate suction voids. The expert panel developed gas ingestion criteria for each pump category using a "failure mode" approach, in which the potential failure modes were identified and then attributed to each pump category. This allowed an evaluation between categories of relative ability to withstand the effects of the various failure modes and a category-by-category assessment of strengths and weaknesses. Available test data and known operational experience were considered in the evaluation. The EPRI criteria was intended to define more realistic criteria relative to the NEI criteria, and can be used to quantify the conservatism in the NEI 09-10 criteria. Either of these pump ingestion criteria is acceptable for use in the operability determination process. The EPRI criteria are provided as Table 3-2.

Table 3-1 NEI 09-10 Revision 1a-A Pump Criteria

	Q/Q(BEP)	BWR Typical Pumps	PWR Typical Pumps		
			Single Stage (WDF)	Multi-Stage Stiff Shaft (CA)	Multi-Stage Flexible Shaft (RLIJ, JHF)
Steady State Operation > 20 seconds	40% to 120%	2%	2%	2%	2%
Steady State Operation > 20 seconds	<40% or >120%	1%	1%	1%	1%
Transient Operation	70% to 120%	10% for ≤5sec	5% for ≤20sec	20% for ≤20sec	10% for ≤5 sec
Transient Operation	<70% or >120%	5% for ≤5sec	5% for ≤20 sec	5% for ≤20 sec	5% for ≤5 sec

Table 3-2 EPRI Pump Roadmap Criteria			
		Gas Void Fraction for Steady-State and Transient Operation	
Category	Pump Description	Steady-State (> 20 seconds)	Transient (≤ 20 seconds)
1	Centrifugal, overhung, single- stage, horizontal	2%	5%
2a	Centrifugal, overhung, single- stage, vertical, close-coupled	2% (1% if < 40% or >120% BEP)	5%
2b	Centrifugal, overhung, single- stage, vertical, rigidly coupled	2% (1% if < 40% or >120% BEP)	5%
3	Centrifugal, single-stage, double-suction, vertical, between bearings (product-lubricated bottom bearing)	2%	5%
4	Centrifugal, horizontal, between bearings, single-stage, axial or radially split	8%	25%
5a	Centrifugal, horizontal, between bearings, multistage, in-line impeller, balance disk	8%	25%
5b	Centrifugal, horizontal, between bearings, multistage, in-line impeller, balance drum	8%	25%
6	Centrifugal, horizontal, between bearings, multistage, opposed impeller	8%	25%
7	Centrifugal, vertical, multi stage can	2%	5%

3.3 TERMINOLOGY

As indicated in Section 2.1 of WCAP-17271, when pump gas ingestion acceptance criteria is presented in terms of void fraction it actually represents gas volumetric flux ratio, which is the ratio of gas volumetric flux to the total mixture flux. The gas volumetric flux fraction is designated as β in WCAP-17271, WCAP-17276 and this report. In a strict academic sense, gas void fraction is the ratio of flow area occupied by gas to the total flow area, which is designated as α in this report.

The allowable non-condensable gas void fraction at a pump inlet is denoted using the symbol α. For homogenous flow conditions, α_h can be defined in terms of the gas volumetric flux ratio:

$$\alpha_h = \frac{Q_g}{Q_g + Q_l} \qquad \text{Equation 3-1}$$

where Q_g and Q_l are the gas and liquid volume flow rate. Equation 3-1 represents the homogenous flow definition of void fraction, and it assumes that there is no slip between the gas and liquid phases. When the gas and liquid phases move at different velocities then the slip ratio, as defined by Equation 3-2 is not equal to 1.0:

$$S = \frac{u_g}{u_l} \qquad \text{Equation 3-2}$$

where u_g and u_l are the gas and liquid velocity. If slip between the phases exists, the fraction of gas occupying a pipe cross sectional area could not be defined using Equation 3-1. Instead, the definition of α becomes:

$$\alpha = \frac{V_g}{V_g + V_l} = \frac{A_g}{A_g + A_l} \qquad \text{Equation 3-3}$$

Where V_g and V_l are the pipe volume occupied by gas and liquid when defining a volume averaged void fraction and A_g and A_l are the pipe area occupied by gas and liquid for an area averaged void fraction.

For this remainder of this report, the area and volume averaged void fraction, Equation 3-3, will be referred to as α, and the volumetric flux ratio, defined as α in Equation 3-1, will be referred to as β.

$$\beta = \frac{Q_g}{Q_g + Q_l} \qquad \text{Equation 3-4}$$

The following relationship between α, β and S exists:

$$S = \frac{u_g}{u_l} = \frac{Q_g}{A_g}\frac{A_l}{Q_l} = \frac{A_l}{A_g}\frac{Q_g}{Q_l} = \frac{1-\alpha}{\alpha}\frac{\beta}{1-\beta}$$ Equation 3-5

The test programs discussed in this report directly measured α as defined by Equation 3-3. In the testing conducted at Purdue University it was not possible to directly measure the volumetric gas flow rates; therefore, additional analyses were performed to determine β based on measured quantities as will be described later in this report. Portions of the testing conducted to develop criteria for dynamic venting included measurements of the gas flow rate into the system; in these cases the gas volumetric flux ratio, β, would be determined directly from measured values.

3.4 GAS TRANSPORT METHODOLOGIES

Westinghouse has developed methods to predict the volumetric flux of a non-condensable gas at a pump inlet based on the gas volume at an upstream accumulation location for a given set of pump suction piping hydraulic parameters. These methods and their associated bases are documented in WCAP-17276 and WCAP-17271.

WCAP-17276 presents a simplistic approach to model the transport of gas between an accumulation location and the pump suction. The chief advantage of the WCAP-17276 methodology is its ease of use. However, the disadvantage is that the methodology presented in WCAP-17276 does not account for hold-up of gas at piping components that will occur during gas transport to the pump suction. Furthermore, WCAP-17276 does not address all of the limitations and conditions identified in the NRC SE on NEI 09-10. This report will identify methods to address the limitations and conditions identified in the NRC SE on NEI 09-10.

WCAP-17271 presents the results of testing conducted at Purdue University to investigate the transport of gas from a top horizontal accumulation location through a vertical down-comer into a bottom horizontal header. It identifies several key phenomenon observed during the gas transport testing and provides empirical correlations to model two of these phenomena. The first phenomenon is the flow initialization process, in which the initially stratified gas volume is rapidly transported to the downstream end of the top header and into the vertical down-comer, where it is entrained by the liquid stream. The region of separated flow at the top of the vertical down-comer is followed by a bubbly flow region downstream. The abrupt transition between separated flow and bubbly flow within the down-comer is referred to as kinematic shock since the movement of this interface can be defined by a mass balance of gas and is not dependent upon the dynamics of the entrainment process. Figure 3-1 shows a schematic of the scenario modeled by the flow initialization correlation. Figure 3-2 shows the variation in gas void fraction in the vertical down-comer during the flow initialization process. The presence of the kinematic shock in the top of the down-comer and the transition to bubbly flow towards the bottom of the down-comer is evident from the change in void fraction. Figure 3-3 shows the corresponding location of the meters in the vertical down-comer for the 8-inch test at Purdue University.

The second phenomenon analyzed in WCAP-17271 was gas holdup and entrainment at the vertical-to-horizontal elbow located at the down-comer outlet. This phenomenon acts to holdup entrained gas, thereby reducing the gas volumetric flux fraction at the outlet of the elbow. In some cases bubbles coalesce as they transport through the elbow and in other cases, the gas flux reaches a critical point in which a stable gas pocket is formed by the coalesced bubbles followed by a kinematic shock. Figure 3-4 shows a schematic of the scenario modeled by the elbow holdup model. The gas volumetric flux undergoes a significant decrease in magnitude as gas is transported through the elbow due to the hold-up phenomenon.

The chief advantage of the WCAP-17271 correlations is that they can be used to provide a realistic estimate of the impact of gas holdup at elbows in reducing the void fraction at the pump inlet. However, WCAP-17271 does not provide guidance for addressing other features of complex piping systems such as tees, offtakes, and specific pump inlet geometries as identified in the NRC SE.

Sections 4, 5 and 10 provide detailed guidance for applying WCAP-17271 and WCAP-17276 methodologies. Section 6.3 provides a comprehensive set of limitations and conditions that address the NRC SE comments which can be used when applying either methodology.

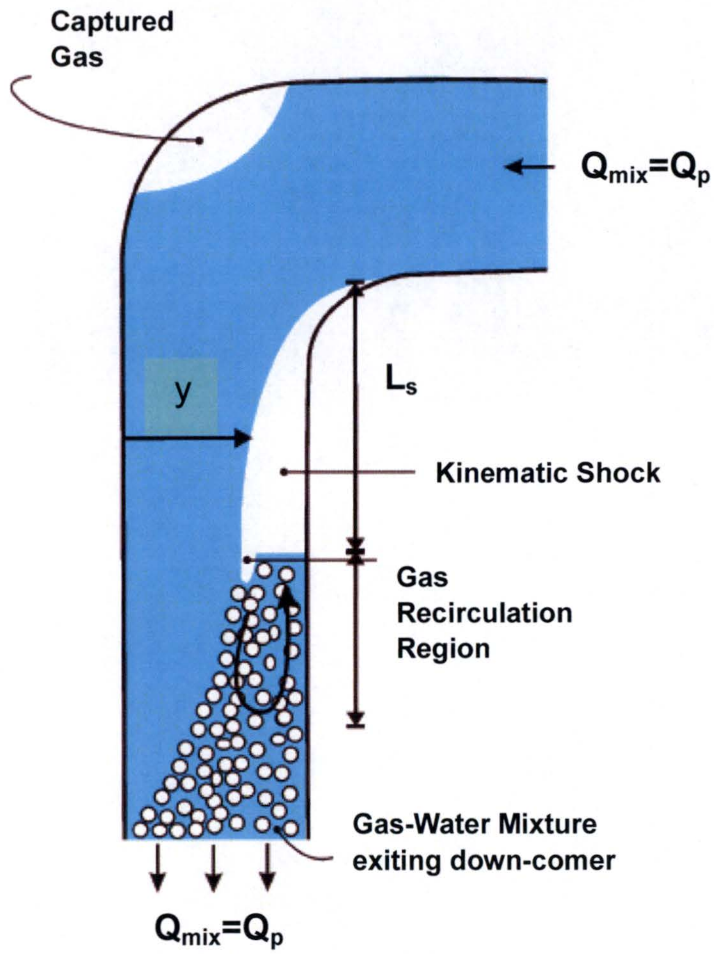

Figure 3-1 Flow Initialization Process

a,c

Figure 3-2 WCAP-17271 Transient Void Fraction Profiles in Vertical Down-comer

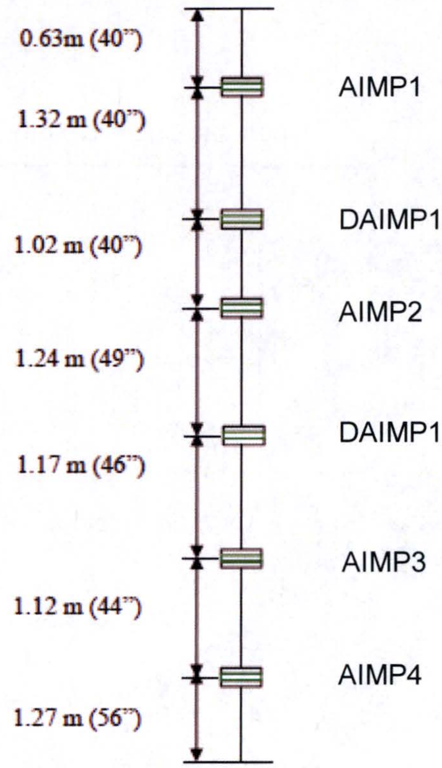

Figure 3-3 P&ID for 8-inch Test at Purdue University

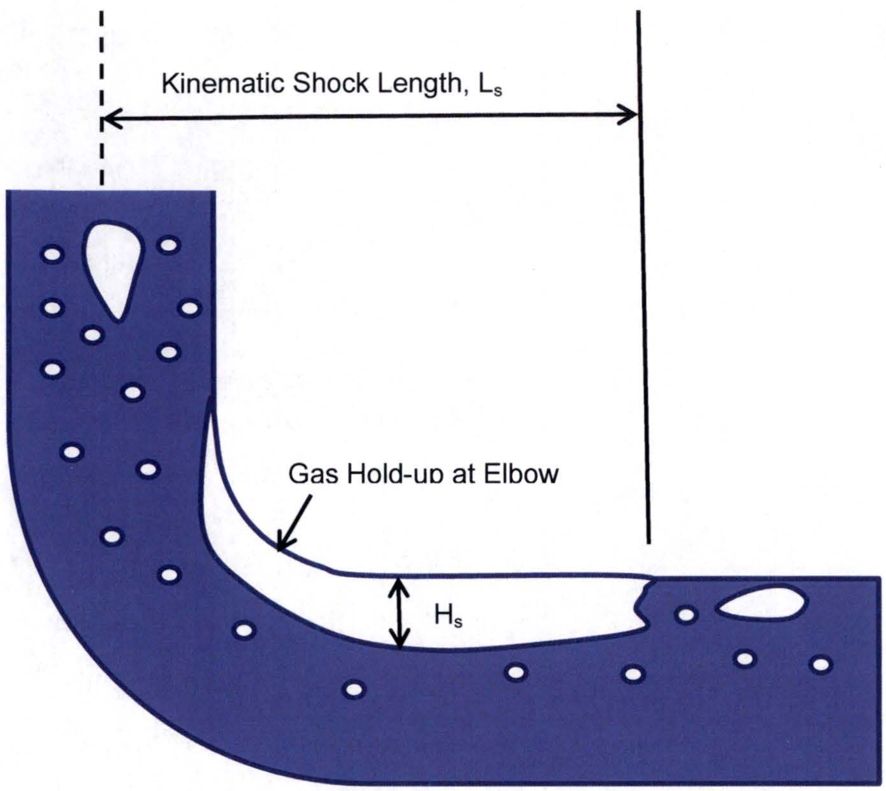

Figure 3-4 Gas Hold-up at Bottom Elbow

4 APPLICATION OF WCAP-17271 EMPERICAL CORRELATIONS

WCAP-17271 provides empirical models of the two key phenomena observed during gas transport testing at Purdue University:

- An initially stagnant gas volume upstream of a vertical down-comer is entrained into the fluid stream through the formation of a kinematic shock at the top of the down-comer. This phenomenon is modeled by the flow initialization correlation.

- As the gas mixture is transported through a vertical-to-horizontal elbow, the gas is held-up by the elbow; that is, the time it takes for the gas to exit the elbow is longer than the time it takes for the gas to enter the elbow. This phenomenon is modeled by the elbow hold-up correlation.

All equations in this section are obtained from WCAP-17271.

4.1 FLOW INITIALIZATION CORRELATION

The flow initialization model assumes the gas void is located upstream of a vertical down-comer. **This model is only valid if a vertical down-comer exists between the gas accumulation location and the pump inlet.** A separated flow regime forms at the top of the vertical down-comer and the gas is entrained at the kinematic shock interface by the liquid at a rate depending on the gas volume, liquid flow rate, and pipe diameter. The intent of the flow initialization model is to determine the average gas volumetric flux at the kinematic shock interface and the amount of time it takes for the liquid flow to completely entrain the gas volume. The flow initialization model is therefore provided in two different forms:

- The first form expresses the average gas volumetric flux at the exit of the kinematic shock as a function of the initial gas volume, mixture velocity, pipe area, and fluid properties.

- The second form expresses the flow initialization time (time to remove the initial gas volume) as a function of the initial gas volume, mixture velocity, pipe area, and fluid properties.

The gas volume used in the flow initialization correlation must be based on the pressure that exists at the top of the vertical down-comer when the transport process is initiated. If the static pressure changes in the suction piping at the initiation of the transport process due to a change in suction source, the gas volume must be adjusted to that which exists once flow has started using the ideal gas law.

The flow initialization time is expressed in terms of the mixture velocity and shock length.

[ ]a, c

Equation 4-1

The ideal shock length, $L_{s,id}$, assumes the initial gas volume in the top header instantaneously moves into the top of the vertical down-comer at 100% void fraction. Equation 4-2 demonstrates how this parameter is calculated:

[ ]a, c

Equation 4-2

where V_i is the initial gas volume, $P_{t,i}$ is the initial pressure in the top header, and P_t is the average pressure in the top header over the flow initialization time period. Note that the initial volume has been corrected for the pressure conditions that would exist when the gas volume is located in the top of the down-comer.

The second form of the flow initialization model expresses the average gas volumetric flow ratio over the initialization process with the gas volume and mixture velocity through a Weber number, as shown in Equation 4-3

[ ]a, c

Equation 4-3

The Weber number, *We*, shown in Equation 4-4, results when Equation 4-1 is expressed in terms of β, as defined by Equation 4-5. In Equation 4-5, Q_g is the average gas volumetric flow rate (gpm), Q_{mix} is the average mixture flow rate (gpm), u_{mix} is average mixture velocity (ft/sec), P_M is the average static pressure at the void fraction measurement location (psia), and 448.8 (gal/min) /(ft^3/sec) is a units conversion factor. Theses parameters are all averaged over the flow initialization time period. During the Purdue tests, Q_{mix} was measured in the water supply to the top header before air was entrained into the mixture. However, it was assumed that Q_{mix} is constant throughout the text section and u_{mix} represents the average mixture velocity over the pipe cross-sectional flow area throughout the test section. This assumption is strictly valid only if the gas is not undergoing significant pressure changes during the transport process. It is acknowledged that during the flow initialization process the actual process deviated from the assumed process due to the gas expansion as the test was initiated. However, the assumption of constant mixture volumetric flow rate is reasonable during the entrainment and subsequent process.

[ ]a, c

Equation 4-4

$$\beta = \frac{Q_g}{Q_{mix}} = 448.8 \frac{V_i \left(\frac{P_{t,i}}{P_M} \right)}{Q_{mix} \Delta t}$$ Equation 4-5

4.2 ELBOW HOLD-UP CORRELATION

WCAP-17271 provides Equation 4-6 for the gas volumetric flux ratio at the elbow outlet as a function of the gas volumetric flux at the elbow inlet, the Froude number and the time over which gas is transported into the elbow. The Froude number is defined by Equation 4-7 where u_{mix} is mixture velocity (ft/sec), g is the gravitational acceleration (ft /sec^2), D is the pipe inside diameter (inch), and 12 inch/foot is a unit conversion factor.

[ ] a, c

Equation 4-6

$$Fr = \frac{u_{mix}}{\sqrt{gd/12}}$$ Equation 4-7

Q_{mix} was measured in the water supply to the top header before air was entrained into the mixture. However, Q_{mix} was constant throughout the text section and u_m represents the average mixture velocity over the pipe cross-sectional flow area throughout the test section. Therefore, the mixture Froude number, as defined by Equation 4-7, is equal to the liquid Froude number at the inlet to the gas accumulation location.

Gas volumetric flux in the vertical down-comer and the associated transport time can be determined using the flow initialization model. The flow initialization transport time is the time over which gas will enter the elbow at the bottom of the down-comer. The gas volumetric flux exiting the kinematic shock will decrease as it transports vertically downward due to the increase in static pressure. The static pressure was assumed to vary linearly over the length of the vertical down-comer from the average pressure in the top header over the transport interval to the average pressure in the bottom header over the transport interval. The gas volumetric flux, β, at the entrance to the elbow is:

$$\beta_{el,in} = \beta_{s,out,} \frac{P_{s,out}}{P_{el,in}}$$ Equation 4-8

The static pressures are in absolute units (psia). Equation 4-6 allows the user to calculate the gas volumetric flux at the elbow outlet based on the gas volumetric flux at the elbow inlet, the time over which gas enters the elbow, and the Froude number based on mixture velocity and elbow outlet diameter. Since the gas holds up at the elbow, the gas transport time will increase at the elbow. The time over which gas leaves the elbow is calculated as:

$$\Delta t_{el,out} = \frac{\beta_{el,in}}{\beta_{el,out}}(\Delta t_{el,in}) \quad \text{Equation 4-9}$$

Section 6.3.4 defines the minimum required down-comer volume to ensure bubbly flow exists at the down-comer exit for a given gas volume, flow rate and pipe diameter. For calculation purposes, the gas volume should be assumed to be located immediately upstream of the first down-comer between the actual accumulation location and the pump inlet which meets the criteria of Section 6.3.4. If multiple vertical to horizontal elbows exist between the accumulation location and the pump inlet the elbow hold-up correlation can be applied at each vertical to horizontal elbow. The outlet transport time from the upstream elbow is the inlet transport time to the downstream elbow. The inlet gas volumetric flux at the downstream elbow is the outlet gas volumetric flux at the upstream elbow corrected by the ratio of static pressures.

Successive application of the elbow hold-up model does not require that the gas remain in the dispersed bubble regime during the entire transport process from the outlet of the first vertical-to-horizontal elbow to the pump suction. Even if the gas flow were to separate from the liquid flow and stratify in a horizontal pipe, the gas volumetric flux ratio will continuously decrease during the transport process to the pump, unless a mechanism exists for gas to accumulate over time at a piping component and subsequently surge downstream as discussed in Section 6.3.

4.3 WCAP-17271 CORRELATION APPLICATION METHOD

In a practical problem the flow initialization and elbow hold-up correlations would be applied in the following manner:

1. Equation 4-1 and Equation 4-2 would be used to predict the time for the gas to be entrained in the flow through the kinematic shock, Δt_{init}
2. Equation 4-3 would be used to predict the average gas volumetric flux at the outlet of the vertical down-comer over the transport time interval, $\beta_{s,out}$
3. Equation 4-8 would be used to predict the average gas volumetric flux ratio at the elbow inlet based on the flux ratio at the shock outlet and the static pressure ratio between the shock outlet and elbow inlet.
4. Equation 4-6 would be used to predict average gas volumetric flux at the elbow outlet, β_{out}, using Δt_{init} and β_{dc} as input variables.
5. Equation 4-9 would be used to predict the gas transport time out of the elbow.

Steps 4 and 5 above could be repeated for subsequent vertically downward to horizontal oriented elbows. However, this simple application method does not consider other complex features of piping systems such as elbows and offtakes. **Furthermore, no consideration for the flow regime that would exist at the pump inlet is given. Therefore, additional limitations on the usage of this methodology are needed. These are discussed in detail in**

Section 6.1 through 6.3. The final outlet transport time is compared with the steady-state criteria in Table 3-1 and Table 3-2, in order to determine if the transient criteria or the steady-state criteria is applicable to pump operation.

4.4 WCAP-17271 CORRELATION UNCERTAINTY CONSIDERATIONS

Uncertainty associated with the application of either the flow initialization or elbow hold-up correlation can be estimated using information provided in WCAP-17271. [

][a,c] These model prediction errors are based on the empirical fit of the correlations to the measured test results. The uncertainty evaluation inherently accounted for test repeatability since all test conditions, including repeat, were included in the fit.

Considering the combined model prediction errors associated with the application of both the flow initialization correlation and the elbow hold-up correlation would require a statistical treatment of the uncertainty. This type of rigorous statistical evaluation is not typically performed for assessing operability. Nonetheless, it is unreasonable to disregard the uncertainty of these correlations in an engineering evaluation. Therefore, recommendations for the treatment of this uncertainty for an operability assessment are provided in Section 8.

5 APPLICATION WCAP-17276 SIMPLIFIED EQUATION

WCAP-17276 documents a simplified approach to model gas transport in pump suction piping. This approach assumes homogenous flow with corrections for system static pressure variations and is referred to as the Simplified Equation. The Simplified Equation, Equation 5-1, can be used to calculate an allowable gas volume at high point locations in pump suction piping based on specified allowable air volume fraction criteria at the pump inlet, system flows and system pressures.

$$V_g = \beta_p \Delta t_p \frac{Q_p}{448.8}\left(\frac{P_p}{P_{hp}}\right)_{PA} \qquad \text{Equation 5-1}$$

where

β_p is the allowable gas volumetric flux ratio at the pump entrance

Δt_p is the time period over which the allowable gas void fraction enters the pump, sec

Q_p is the pump flow rate, gpm

P_p is the absolute static pressure at the pump suction during post-accident operating conditions, psia

P_{hp} is the absolute static pressure at the high point location during post-accident operating conditions, psia

A units conversion factor of 448.8 (gal/min) /(ft^3/sec) is used,

FAI/09-130 provides a technical basis for the gas transport process in pump suction piping. The gas is assumed to be initially trapped at a local high point in the piping system and is transported to the pump upon initiation of flow rate through the system. The essential features of the transport process described in FAI/09-130 are as follows:

1. This combination of the pump suction demand in the down-comer and the supply flow from the water source causes the gas to be transported toward the down-turned downstream elbow which forms the boundary of the high point.

2. The gas continues to expand until the upstream volumetric flow rate equals the suction demand on the down-comer; that is, until the upstream volumetric flow rate equals the pump demand. In addition, the gas rapidly moves to the downstream elbow since the

gas reacts more quickly to the driving head than the liquid as the gas has less inertia than the liquid.

3. As a consequence, the transport of gas into the downstream down-turned elbow results in pulling much of the accumulated gas into the top of the down-comer. For significant initial gas volumes, this gas transport results in a "waterfall" condition in the top of the down-comer, which is a vertically separated flow pattern. Specifically, water pours through the accumulated gas volume causing entrainment of the gas as the waterfall impinges on the accumulated water pool further down in the down-comer.

This transition from a vertically separated flow pattern to a bubbly flow pattern that is transferred toward the pump can be considered a kinematic shock. An essential feature of this kinematic shock is that it involves the entrainment of the air by the "waterfall," as the water plunges into the top of the water column.

FAI/09-130 developed an analytical model for predicting the maximum distance between the top of the down-comer and the bottom of the kinematic shock (L_s), the average gas entrainment rate (Q_g), and the time duration of the transport process (Δt). This model was based on a jet entrainment mechanism, and the coefficients come from a jet impinging an open pool of water. Equation 5-2 provides an implicit expression for L_s as a function of the initial gas volume (V_g) adjusted for static pressure at the high point during post-accident operation, liquid flow rate (Q_l), liquid velocity (u_l) and piping area (A). Equation 5-4 provides a relation between the gas flow rate (Q_g) and the waterfall flow rate (Q_l) as a function of L_s and the pipe diameter. Equation 5-4 provides an expression for the average gas flow rate ($Q_{g,\,avg}$) and was obtained by integration over the total length of the waterfall, and therefore, accounts for the fact that the length varies from L_s to zero as the gas volume is depleted by entrainment. Equation 5-5 simply indicates that the transport time is the initial gas volume divided by the average volumetric entrainment rate over the transport process.

$$L_s = \frac{1}{A}\left\{V_g + \frac{Q_l}{448.8g}\left[\sqrt{2gL_s} - u_l \ln\left(u_l + \sqrt{2gL_s}\right) + u_l \ln(u_l)\right]\right\} \qquad \text{Equation 5-2}$$

$$\frac{Q_g}{Q_l} = 0.049\left(\frac{L_s}{d/12}\right)^{0.68} = \frac{\beta}{1-\beta} \qquad \text{Equation 5-3}$$

$$\frac{Q_{g,\,avg}}{Q_l} = 0.029\left(\frac{L_s}{d/12}\right)^{0.68} = \frac{\beta_{avg}}{1-\beta_{avg}} \qquad \text{Equation 5-4}$$

$$\Delta t = 448.8\frac{V_g}{Q_{g,avg}}$$ Equation 5-5

Equation 5-2 can be re-written in the following form which is convenient for solution.

$$L_s = \frac{1}{A}\left\{V_g + \frac{Q_l u_l}{448.8g}\left[\frac{\sqrt{2gL_s}}{u_l} - \ln\left(1+\frac{\sqrt{2gL_s}}{u_l}\right)\right]\right\}$$ Equation 5-6

Equation 5-3 and Equation 5-4 have the same functional form with different coefficients. This is because Equation 5-4 was obtained by integrating Equation 5-3 and then dividing by L_s to obtain the average value of Q_g. The power law integration properties dictate that the coefficient of Equation 5-4 be a factor of (n+1) lower than the coefficient of Equation 5-3; where n is the exponent of Equation 5-3. Since the exponent of Equation 5-3 is 0.68, the coefficients differ by a factor of 1.68. This is the basis for the 1.7 factor provided in FAI/09-130 and discussed in NRC SE Section 3.15.3 and NRC RAI 2-9 on NEI-09-10. As indicated in NRC SE Section 3.15.3, the intent of the 1.7 criterion was to eliminate slug flow if the actual gas transport time was less than the assumed gas transport time. If, for example, the pump criteria allows a 5% void fraction for 20 seconds, then using 20 seconds in the Simplified Equation could potentially result in allowing a 100 percent void for four seconds with no void for 16 seconds. The response to RAI2-9 indicated that the correlations which form the basis for the 1.7 factor are applicable to gas entrainment due to jet impingement on a pool of water and may not be directly applicable to the formation of a kinematic shock in a piping system. **[**

][a,c]

WCAP-17276 indicates that the best estimate prediction of transport time was obtained using Equation 5-7.

[ ] a,c Equation 5-7

Therefore, if the transport time predicted by Equation 5-7 is less that the allowable transport time in the NEI 09-10 pump acceptance criteria, the Simplified Equation uses Equation 5-7 as input. The NRC SE indicated this is an acceptable method to eliminate the concern that the use of an average void fraction over an assumed time period may allow the formation of slug flow at the pump inlet.

WCAP-17276 Section 3.6 summarized the following limitations on the use of the Simplified Equation:

Limitation 1:Fr $\leq$ 2.5; this can also be expressed as the following limitation between flow rate (gal/min) and inside pipe diameter (inch): $Q \leq 10\ d^{2.5}$.

Limitation 2: Verify that the NEI 09-10 value of Δt_p is not larger than the transport time dictated by the gas volume and flow conditions. This is accomplished by using the lower value of Δt predicted by Equation 5-7 and Δt_p provided in the NEI 09-10 pump criteria.

Limitation 3: The volume of a vertical down-comer located between the high point and the pump must exceed the gas volume by a factor of 4.

Limitation 4: If the gas flow is stratified as it approaches an off-take, then it is necessary to protect against slug flow resulting from a sudden in-surge of gas due to an air entraining vortex. The Simplified Equation cannot be applied under these conditions since the flow distribution model used to establish the transport time is not applicable in this situation.

Limitation 2 will be retained in its current form. However, this report provides alternative means for addressing Limitations 1, 3, and 4 in Section 6.3.

6 GAS TRANSPORT ANALYSIS METHODOLOGY LIMITATIONS

Sections 4 and 5 outline the WCAP-17271 and WCAP-17276 calculation methodologies. WCAP-17271 does not provide guidance for considering complex features of piping systems such as elbows and offtakes. Furthermore, no consideration for the flow regime that would exist at the pump inlet is given. WCAP-17276, which was completed after the WCAP-17271 program, does account for some complex piping features and pump inlet flow regime. However, additional limitations and conditions on the use of WCAP-17276 arose from the NEI-09-10 SE.

To provide clarity and guidance for considering the limitations and conditions associated with the use of WCAP-17271 and WCAP-17276, a review of NEI-09-10 SE is provided in Section 6.1. This is followed by a review of the NEI-09-10 guidance for addressing the limitations and conditions in Section 6.2. Finally, a detailed technical basis for addressing the limitations and conditions is provided in Section 6.3.

6.1 NEI-09-10 SAFETY EVALUATION LIMITATIONS

Section 3.15.3 of the NEI-09-10 SE places limitations on gas void ingestion by pumps to assure bubbly flow at the pump entrance and that the average void fraction meets acceptance criteria defined in NEI-09-10. The following list identifies the issues identified by the NRC in the SE associated with demonstrating bubbly flow exists. Methods to address these issues are provided in Section 6.3.

- Sufficient volume in the vertical down-comer downstream of the gas accumulation location is needed to assure bubbly flow at the down-comer exit if a vertical down-comer exists.
- Other piping configuration can exists between the gas accumulation location and the pump which may result in a transition from a dispersed bubbly flow regime to a separated flow.
- If Froude number is greater than 2.5, there is a potential that a void will be transported as a slug.
- If a vertical down-comer is connected directly to the top of a pump and the down-comer volume is at least four times as large as the original gas volume that existed above the down-comer, then bubbly flow will exist at the pump entrance provided Froude number is small enough to preclude slug flow as identified in the above bullet.
- If a horizontal pipe connects between the bottom of a down-comer and a pump entrance, a methodology should be applied that has a multi-dimensional two phase capability that has been verified by comparison to experimental data. Since phenomena in this region are not well understood, judgment may be a significant factor and a suitable safety factor should be added to predict behavior to reasonably ensure the prediction encompasses actual behavior.
- Horizontal pipes may introduce other concerns. For example, flow stratification in horizontal pipes can lead to an accumulation of gas, such as in an off-take or tee

geometry. Once gas is accumulated, a subsequent instability can lead to a large surge in gas downstream.

In all cases, it is the licensee's responsibility to reasonably and acceptably address the relevant gas transport phenomena. The remainder of this report will provide guidance for assuring that the bubbly flow limitation is met when applying the WCAP-17271 correlations to determine gas void acceptance criteria considering the problems summarized above.

6.2 NEI 09-10 GUIDANCE REGARDING LIMITATIONS

NEI 09-10 indicates that the following approaches for addressing specific configuration limitations are possible:

- Appropriately scaled tests could be used to demonstrate operability.
- Configurations that involve downward flow in a vertical pipe with an elbow to a horizontal pipe that has a small length to diameter ratio with a reducer immediately upstream of the pump entrance can be treated by:
  - Limiting the gas volume to an appropriate fraction of the horizontal pipe volume between elbow and reducer, or
  - Verifying that in all situations of interest the liquid flow rate is sufficient to maintain the gas in a dispersed flow regime.
- Configurations which include pump suction headers with off-takes / tees can be treated by basing the allowable gas volume in the header on the limiting gas volume allowed by each off-take.
- The case of a vertical upward intake residual heat removal pump where flow from a horizontal pipe passes through an elbow and short vertical pipe before entering the pump can be treated by ensuring the liquid flow rate is sufficient to maintain the gas in a dispersed flow regime.
- Lastly, for the case of HPI pumps which take suction direct from a vertical pipe, the factor of four criterion identified in FAI/09-130-P must be applied.

6.3 TECHNICAL GUIDANCE FOR ADDRESSING LIMITATIONS

The following sub-sections outline approaches to address limitations and conditions associated with the use of WCAP-17271 and WCAP-17276. This list can be considered comprehensive. However, due to the nature of flow through complex piping systems, this list does not preclude the possibility of other phenomena that could further limit application of WCAP-17271 and WCAP-17276. Care must be taken to consider unique features associated with a given piping system. An understanding of multiphase flow in piping is necessary to perform a gas transport acceptance criteria analysis.

The limitations and conditions discussed in this section were divided into two categories. The first category consists of limitations based on the available database of test configurations. Limitations based on the available test configuration database are described in Section 6.3.1, 6.3.2 and 6.3.3.

The second category of limitations considers mechanisms that can cause an initially stagnant gas pocket to be swept downstream. As discussed in WCAP-17271 (Reference 3) and WCAP-17167 (Reference 13), there are four known mechanisms which can result in a surge and subsequent increase in the gas flux ratio:

1. Kinematic shock formation in a vertical down-comer which is not large enough to contain the entirety of the separated gas volume (Section 6.3.4)
2. Kinematic shock formation at a vertical elbow preceding a horizontal pump inlet when the inlet pipe is not large enough to contain the entirety of the separated gas volume (Section 6.3.5)
3. Vortex formation at an off-take in a horizontal pipe in which the gas flow has stratified (Section 6.3.6). In this regard, it is noted that a lower flow rate into the off-take may be more limiting than a higher flow rate as it may allow gas to stratify at the inlet to the off-take.
4. Co-current slug flow in a vertical down-comer (Section 6.3.7)

This report provides evaluation tools which allow the user to determine if the potential exists for one of these mechanisms to result in a surge in gas flux and methods to ensure the gas flux at the pump inlet is acceptable. In the absence of these mechanisms, the gas flux will continually decrease during the transport process from the accumulation location to the pump inlet. The presence of piping geometries not directly addressed by this report, such as vertical upwards flow, inclined piping and other complex piping geometries do not prevent the use of the methods provided in this report for operability determinations.

6.3.1 Vertical Down-Comer

The WCAP-17271 test data included 4", 6", 8" and 12" diameter piping that included a large vertical down-comer. The presence of a vertical down-comer is a requirement to apply the methodology of WCAP-17271 and WCAP-17276. The formation of a kinematic shock at the top of the down-comer is the means by which dispersed, bubbly flow is established in the vertical pipe. The flow initialization correlation models this phenomenon and enables the evaluation of the average gas volumetric flux and initialization transport time.

If a vertical down-comer does not exist between the accumulation location and pump inlet, there may be other mechanisms that exist to disperse the gas void in the piping system. For instance, elbows, reducers and check valves may distribute gas along the pipeline. However, methodologies to demonstrate distribution through these components are not currently available to the PWROG. **Therefore, WCAP-17271 and WCAP-17276 are not applicable to this situation. In this case, the guidance provided in Section 7 is applicable.**

6.3.2 Pipe Diameter

The smallest pipe diameter included in the WCAP-17271 test data set was 4 inches. For the tested fluids, WCAP-17271 indicates the maximum stable bubble size can be approximated as 3". This limit can be considered the cutoff between large diameter and small diameter pipe behavior. Below this limit, stable, full diameter slug flow could exist. Slug behavior seemed more pronounced in the 4" testing than the other tests. This is an indication that pipe diameter was starting to influence the transport behavior. **Therefore, the WCAP-17271 correlations should not be used for pipe diameters smaller than 4 inches. In this case, the guidance provided in Section 7 is applicable.**

The largest diameter tested was 12 inches. However, the scaling evaluation documented in WCAP-17271 demonstrated that the correlations could be applied to pipe diameters up to 30 inches. The selection of 30 inches should not be construed as a hard upper limit. This value was selected during project planning with the PWROG as the desired upper limit and the scaling evaluation in WCAP-17271 demonstrated that this objective had been achieved.

6.3.3 Initial Gas Volume and Void Fraction

The tests were conducted with a range of initial void fractions between 5% and 20% and maximum gas volumes of 0.5 ft^3, 2.3 ft^3, 4.4 ft^3, and 10.1 ft^3 for the 4", 6", 8" and 12" tests, respectively. However, these do not constitute limitations for the application of the correlations. An observation of the test was that the initial void fraction was not relevant and was not used as a correlating parameter. The test demonstrated that all of the gas was rapidly transported to the top of the down-comer during flow initialization. **Therefore, as long as the down-comer is large enough to accommodate the kinematic shock formation, the flow initialization correlation is applicable.**

6.3.4 Down-comer Volume

FAI/09-130 suggests that bubbly flow may not exist at the exit of a down-comer if the entire down-comer becomes voided with gas. FAI/09-130 suggests a criterion to preclude this occurrence. The criterion requires that the down-comer volume should be at least four times the volume of the maximum gas accumulation in the high point piping.

Investigation of the WCAP-17271 test data indicates the factor of four criterion is a very conservative limitation. The 8 inch tests incorporated the maximum number of void fraction meters in the vertical down-comer, since the 6 inch test results were not used in the WCAP-17271 correlations due to uncertainties in the initial gas volumes. Table 6-1 shows the location of these meters. The presence of a kinematic shock at a meter location would result in a large void fraction (>0.70) at flow initiation. The data sets for each run in the 8 inch tests were reviewed and the maximum penetration of the kinematic shock was determined for each run. A void fraction $\geq$ 0.7 at the initiation of flow was used as an indication that a kinematic existed at a specific meter. This criterion was confirmed with video observations.

Table 6-1 Location of Void Fraction Meters in Vertical Down-Comer (8 inch Test)

Meter	Distance from top (inch)	Distance from top (feet)	Distance between meters (inch)
AIMP1	40	3.33	
DAIMP1	80	6.67	40
AIMP2	120	10.00	40
DAIMP2	169	14.08	49
AIMP3	215	17.92	46
AIMP4	259	21.58	44

Section 5 of this report indicates that FAI/09-130 provided a method for predicting the maximum depth of the kinematic shock, which is represented by Equation 5-6; bubbly flow is predicted to exist at the outlet of the kinematic shock. Figure 6-1 through Figure 6-4 compare the location of the kinematic shock as predicted by Equation 5-6 with the locations indicated by the measured data for the 8 inch tests. The abscissa in these figures is the ideal shock length (the length occupied by the original gas volume if it were displaced into the down-comer), as defined by Equation 4-2. The ordinate is the ratio of the predicted depth for bubbly flow to the ideal shock length. Since the initial gas volumes varied slightly for each run in a given category, the ideal shock length for each run varied. Also, since the location of the void fraction meters is fixed, the ratio of the void fraction meter location to the ideal shock length changes for a given meter as the ideal shock length changes from run to run.

Figure 6-1 through Figure 6-4 indicate that at low initial gas volumes and low Froude numbers, the amount of gas that cannot be swept from a horizontal header is a function of the full pipe Froude number and pipe diameter and is independent of the initial volume of gas. Therefore, for larger volumes of gas a larger fraction will be forced into the down-comer. Equation 5-6 over-predicts the length of the kinematic shock, since a significant fraction of the gas volume remains in the horizontal header under these conditions. However, as the gas volume and Froude number increase, Equation 5-6 represents the location of the kinematic shock very well.
[

]^{a,c} It is

recommended that Equation 5-6 be used to predict the required length of the kinematic shock.

Figure 6-5 through Figure 6-8 demonstrates the implementation of Equation 5-6 to define vertical down-comer length for pipe diameters between 4 inch and 30 inch and Froude Numbers between 1 and 4. Alternatively, Equation 5-6 can be solved for V_g and the down-comer length (L_{dc}) can be substituted for y to yield an explicit equation for the allowable gas volume for a given down-comer length; this is shown as Equation 6-1.

$$V_g = L_{dc}A - \frac{Q_l U_l}{448.8g}\left[\frac{\sqrt{2gL_{dc}}}{U_l} - \ln\left(1 + \frac{\sqrt{2gL_{dc}}}{U_l}\right)\right] \quad \text{Equation 6-1}$$

[ ]a,c

Figure 6-1 8 Inch Test; Froude Number =0.93 Location of Kinematic Shock

a,c

Figure 6-2 8 Inch Test; Froude Number =1.24 Location of Kinematic Shock

a,c

Figure 6-3 8 Inch Test; Froude Number =1.65 Location of Kinematic Shock

a,c

Figure 6-4 8 Inch Test; Froude Number =2.50 Location of Kinematic Shock

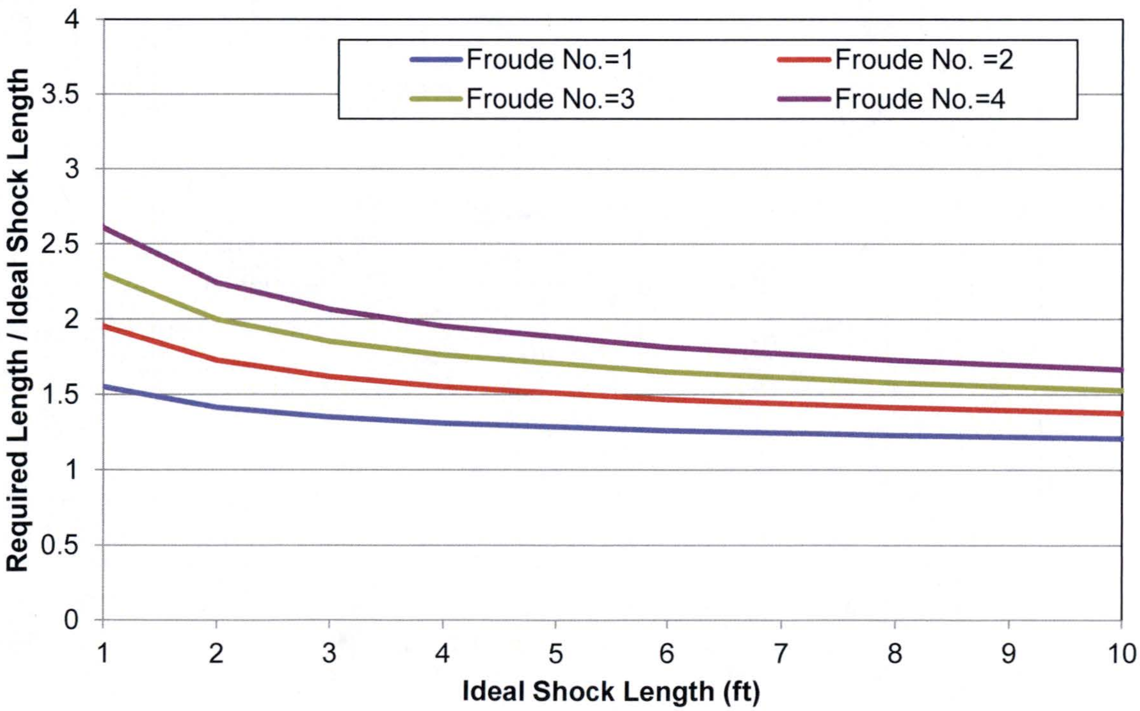

Figure 6-5 4 Inch Diameter Vertical Down-Comer Required Length

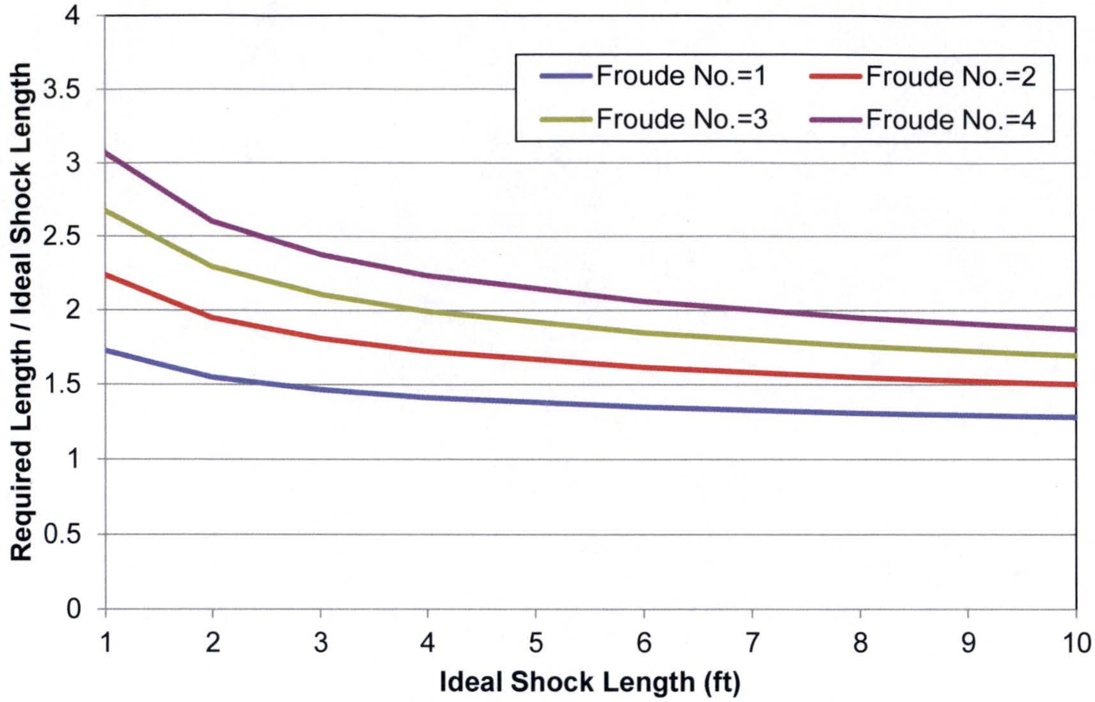

Figure 6-6 8 Inch Diameter Vertical Down-Comer Required Length

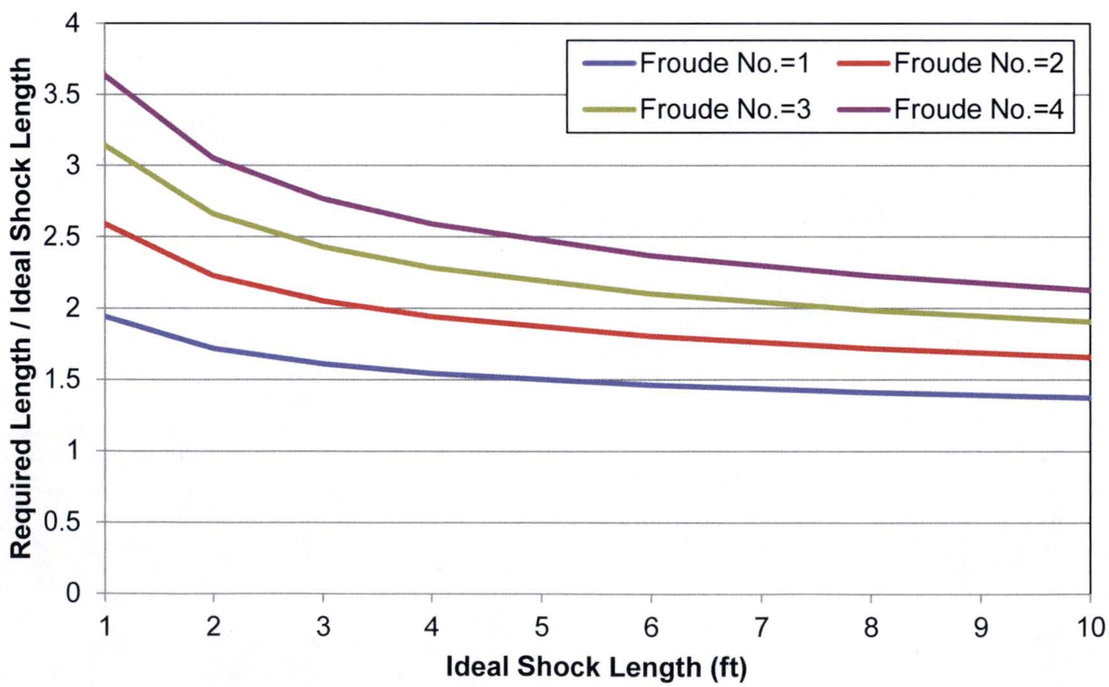

Figure 6-7 16 Inch Diameter Vertical Down-Comer Required Length

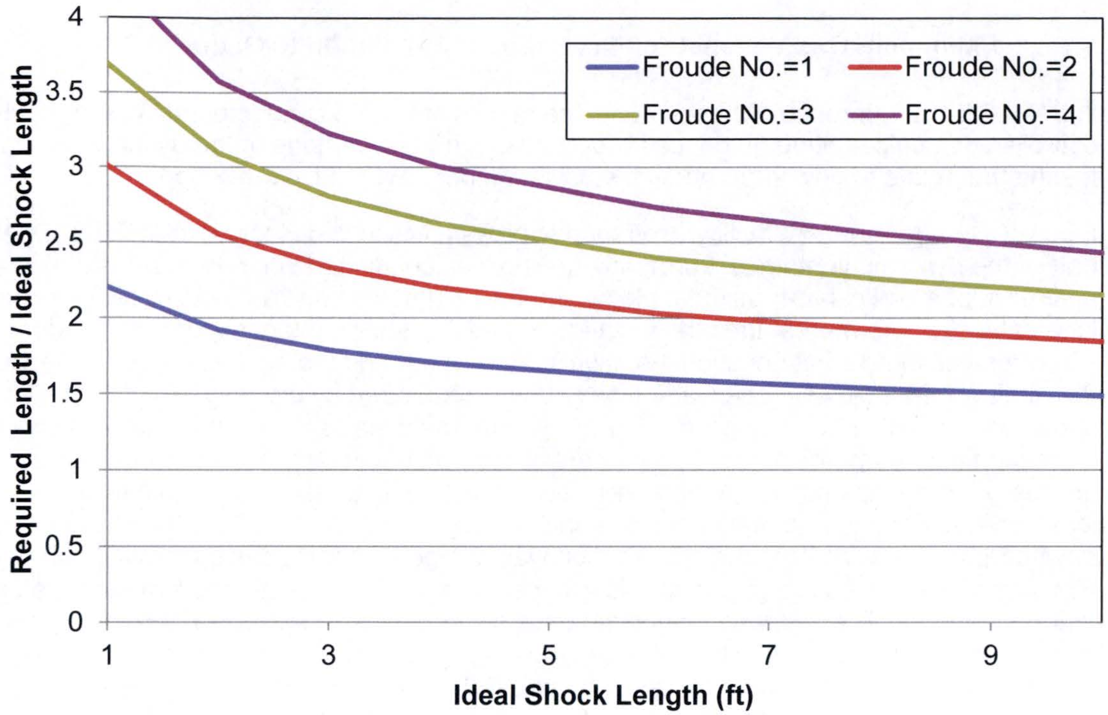

Figure 6-8 30 Inch Diameter Vertical Down-Comer Required Length

6.3.5 Horizontal Pump Inlet

During several of the WCAP-17271 experiments a kinematic shock was observed to form at the vertical to horizontal elbow. If a pump with a horizontal inlet is located downstream of a vertical-to-horizontal elbow and the kinematic shock is sufficiently large, it may impinge upon the pump and result in a slug of gas entering the pump. The NRC SE of NEI 09-10 indicates that if a horizontal pipe connects between the bottom of a down-comer and a pump entrance, a methodology should be applied that has a multi-dimensional two phase capability that has been verified by comparison to experimental data. Since phenomena in this region are not well understood, judgment may be a significant factor and a suitable safety factor should be added to predict behavior to reasonably ensure the prediction encompasses actual behavior.

To develop a better understanding of the separation phenomena leading attachment of a gas pocket at a piping elbow, testing was conducted at the Westinghouse thermal hydraulic laboratory. Section 6.3.5.1 discusses results of this testing that can be used to determine what conditions will cause formation of a separation region. Should a separation region form, guidance in Section 6.3.5.2 can be used to limit the gas volume to an acceptable amount.

6.3.5.1 Flow Separation

6.3.5.1.1 Minimum Gas Volumetric Flux Ratio for Separation to Occur

WCAP-17537 (Reference 11) documents the results of testing conducted at Westinghouse to establish dynamic venting guidance for systems. Only the portions of the dynamic venting testing that relate to flow separation at elbows will be presented in the report.

Figure A-1 shows the test facility used for this project, which is described in APPENDIX A. As a part of the dynamic venting test program, testing was conducted whereby gas was injected upstream of a vertical-to-horizontal elbow and the volumetric flow rate was increased until a kinematic shock formed at the elbow outlet. Figure A-2 shows the configuration used for these tests. Air was injected at Location 1 shown in Figure A-2 and the air flow rate was measured by the air flow meter (AFM). The water flow rate was measured by the magnetic flow meter (MFM) shown in Figure A-1. For a specific liquid flow rate, the tests were started at an air flow rate corresponding to approximately five percent of the water flow rate. The air flow rate was gradually increased until separation occurred at the specified test matrix liquid flow rate. Air injection was continued at the same rate until the separated region was extended to the nearest downstream elbow. At this time, air injection was stopped, allowing the hydraulic jump to entrain air away. Data was collected during this final period of zero air injection to examine the air entrainment rate. The test was completed once all air had been entrained away from the component under test. Table 6-2 provides the averaged measured flow rates and water temperatures for the 6-inch elbow tests. Figure 6-9 shows the required gas volumetric flux ratio to form a kinematic shock as a function of liquid Froude number. The gas volumetric flux was determined using the measured air flow rate required to form the shock and the measured water flow rate. It is noted that the required gas flow rate varies linearly with liquid flow rate.

Table 6-2 6" Elbow Average Data

Test I.D	MFM [gpm]	TC [F]	Test I.D	MFM [gpm]	TC [F]
DVEL318A	309.7	62.8	DVEL513A	505.4	63.9
DVEL318B	309.1	66.0	DVEL513B	504.9	63.9
DVEL318C	309.8	67.7	DVEL513C	504.2	64.0
DVEL363A	355.7	66.3	DVEL563A	556.6	63.7
DVEL363B	356.2	65.6	DVEL563B	556.9	63.7
DVEL363C	355.8	65.4	DVEL563C	555.9	63.6
DVEL363D	355.7	65.1	DVEL613A	608.0	63.6
DVEL363E	355.9	64.5	DVEL613B	608.3	63.7
DVEL413A	406.7	64.9	DVEL613C	607.3	63.7
DVEL413B	406.8	64.9	DVEL663A	656.6	63.4
DVEL413C	406.4	64.7	DVEL663B	654.5	64.2
DVEL463A	453.7	63.7	DVEL663C	656.5	65.3
DVEL463B	453.4	63.7	DVEL727A	718.3	66.5
DVEL463C	453.2	63.8	DVEL727B	719.5	66.2
			DVEL727C	719.3	65.7

As part of the WCAP-17271 testing, videos were recorded at key locations. One of the video locations was the outlet of the vertical-to-horizontal elbow. For each run of the 4-inch, 6-inch, 8-inch and 12-inch tests, these videos were reviewed to determine which cases resulted in the formation of a kinematic shock. The following observations were made: a,c

[ ]

The specific runs for which shocks formed and did not form were catalogued. Figure 6-10 compares the average gas volumetric flux for runs which did and did not result in formation of a kinematic shock. Also shown is the dynamic venting data. **[**

] a,c

Therefore, the maximum gas volumetric flux ratio is the more relevant parameter to indicate shock formation. This parameter was not measured during the tests. However, the peak void fraction at each meter was a metric that was determined during the analytical effort to develop WCAP-17271. Equation 3-5 relates the gas volumetric flux, β, with the void fraction, α, and the slip ratio, S. The gas slip ratio was calculated based on mass conservation principles and was recorded as a metric for each run, along with the peak void fraction. The slip ratio was calculated using the following method.

The gas flow rate was calculated over the transport time interval, Δt, by assuming a constant gas velocity over the entire transport interval. With the known initial injected gas volume, V_i, corrected to the pressure at the instrument location, the gas flow rate is the total volume, corrected for pressure, of gas divided by the transport time interval.

$$q_g\left(ft^3/s\right)=\frac{V_i}{\Delta t}\left(\frac{P_{t,init}}{P_M}\right) \qquad \text{Equation 6-2}$$

The gas velocity is then the gas flow rate divided by the gas flow area:

$$u_g\left(ft/s\right)=\frac{q_g}{\alpha_{avg}\cdot A\cdot \Delta t} \qquad \text{Equation 6-3}$$

The measured flow rate, Q (gpm), indicates the combined gas and liquid flow rates. Therefore, the total liquid flow rate is equal to:

$$q_l\left(ft^3/s\right)=\frac{Q}{448.8}-u_g\cdot\alpha_{avg}\cdot A$$ Equation 6-4

The liquid velocity is the liquid flow rate divided by the liquid flow area:

$$u_l\left(ft/s\right)=\frac{q_l}{\left(1-\alpha_{avg}\right)A}$$ Equation 6-5

The slip ratio was calculated by substituting u_g and u_l into Equation 3-2. The maximum gas volumetric flux based on substituting the peak void fraction and average slip ratio into Equation 3-5 and solving for the peak volumetric flux ratio. The results are shown in Figure 6-11 which demonstrates that the peak gas volumetric flux ratio for shock formation is consistent with the dynamic venting data.

A regression analysis of the data in Figure 6-9 yields the relation provided in Equation 6-6 with an R-squared value of 0.99.

[ ]a,c Equation 6-6

[

]a,c

6.3.5.1.2 Correlation for Maximum Gas Volumetric Flux at Kinematic Shock Outlet

The correlations in WCAP-17271 provide the average gas volumetric flux for the flow initialization process and elbow holdup processes. The flow initialization correlation relates the average gas flux ratio to the Weber number, which is a function of the gas volume and mixture velocity. [

]a,c

[ ]a,c Equation 6-7

Using Equation 6-7 and Equation 6-6, the allowable gas volume to preclude a kinematic shock can be determined for a given pipe diameter and flow rate. Figure 6-13 and Figure 6-14 illustrate the results of these calculations.

Equation 6-7 provides a correlation for the maximum gas volumetric flux as a function of the kinematic shock length. Strictly speaking, this equation is only appropriate to use if the gas accumulation location is located directly upstream of the vertical down-comer preceding the pump inlet. This expression can be integrated to yield the average gas volumetric flux as shown in Equation 6-8.

[ ] a,c Equation 6-8

[ ] a,c Equation 6-9

[ ]^{a,c} Equation 6-9 is useful in situations where the gas accumulation location is not located directly upstream of the vertical down-comer supplying the pump inlet. **The WCAP-17271 or WCAP-17276 methodology can be used to predict the average gas flux ratio at the pump inlet and Equation 6-9 can be used to predict the maximum gas flux ratio for comparison with allowable limit (Equation 6-6). If the gas accumulation location is immediately upstream of the vertical down-comer supplying the pump inlet then Equation 5-6 should be used to predict the kinematic shock length and Equation 6-7 should be used to predict the maximum gas volumetric flux ratio for comparison with the Equation 6-6 limit.**

a,c

Figure 6-9 Conditions for Kinematic Shock; WCAP-17537 6-Inch Elbow Tests

a,c

Figure 6-10 8-Inch Tests Conditions for Shock Formation in terms of Average Beta

a,c

Figure 6-11 8-Inch Tests Conditions for Shock Formation in terms of Maximum Beta

a,c

Figure 6-12 Maximum Beta as a Function of L_s/D

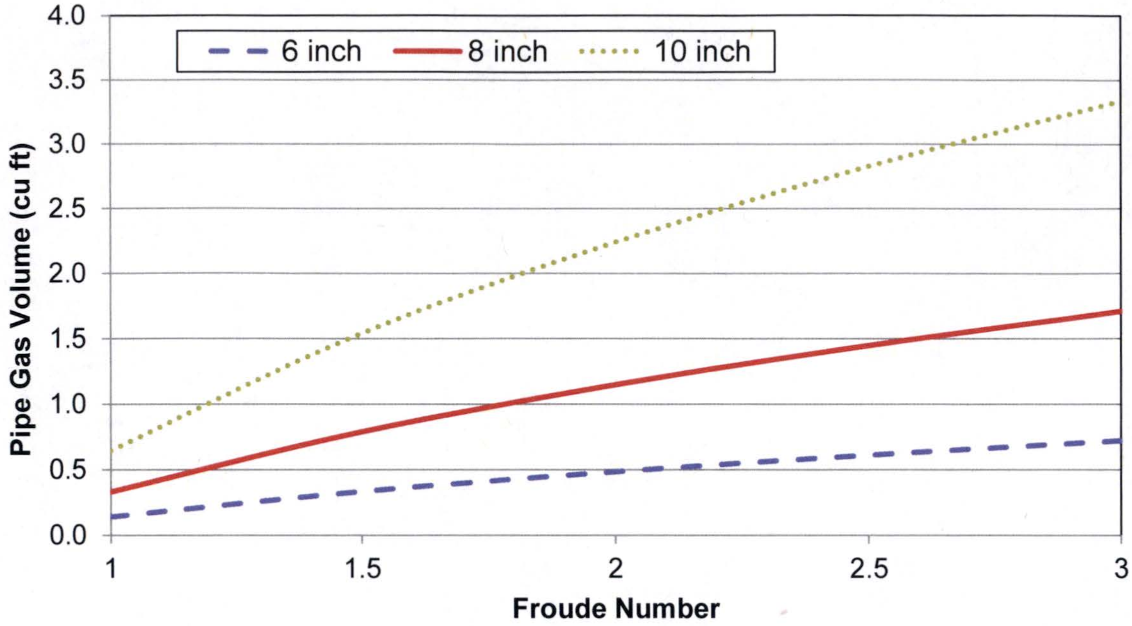

Figure 6-13 Maximum Gas Volume to Prevent Kinematic Shock (6", 8" 10")

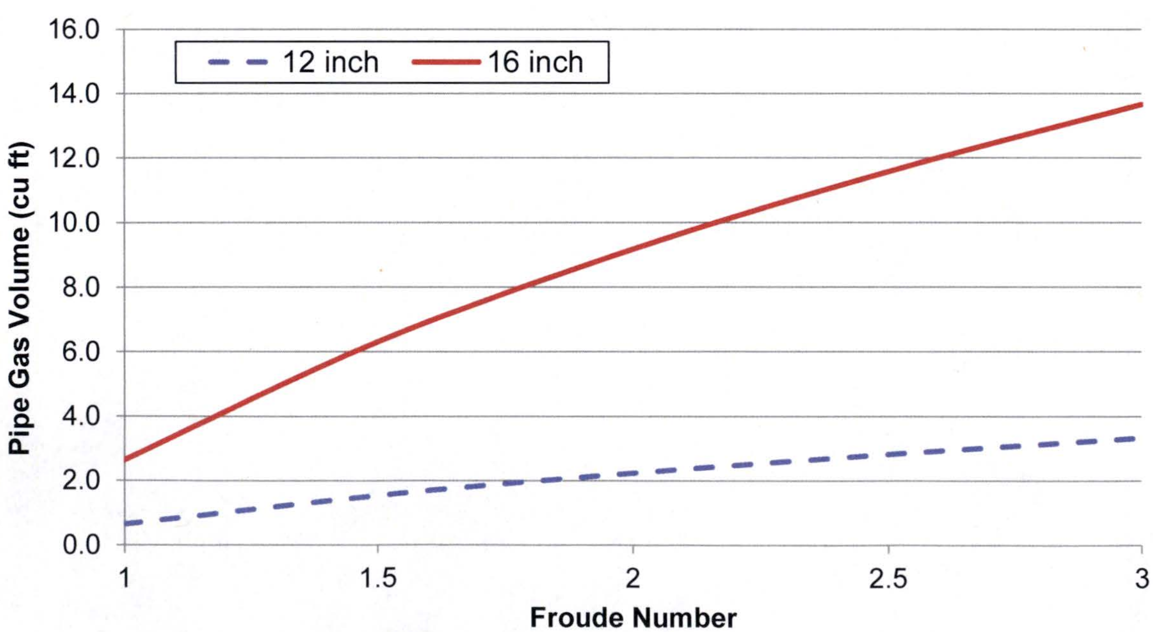

Figure 6-14 Maximum Gas Volume to Prevent Kinematic Shock (12", 16")

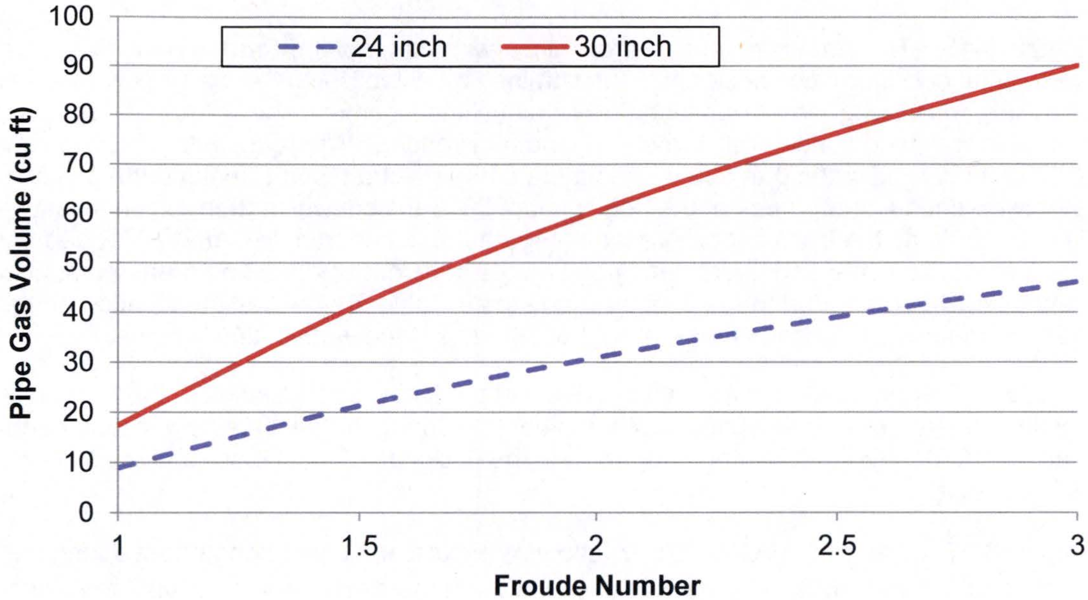

Figure 6-15 Maximum Gas Volume to Prevent Kinematic Shock (24", 30")

6.3.5.2 Piping Length assuming flow Separation at Elbow Upstream of Pump Inlet

In applications involving a pump with a horizontal inlet which is preceded by a vertical down-comer, it is necessary to demonstrate that either a kinematic shock does not form or that the length of horizontal pipe is long enough to contain the kinematic shock without allowing it reach the pump inlet. Section 6.3.5 provides criteria to prevent a kinematic shock from occurring at the outlet of a vertical down-comer. This section will provide the information necessary to estimate the length of a kinematic shock, should it form in the horizontal pipe.

Figure 6-16 shows the maximum void fraction in the kinematic shock region for those cases where a kinematic shock occurred in the Purdue tests. It is noted that results for the 6 inch Purdue tests are presented in

Figure 6-16 since the measured void fraction does not rely on the initial gas volume. Therefore, concerns about the validity of the initial gas volume do not affect this data. The maximum void fraction was used instead of the average void fraction over the transport interval since this better represents the void fraction in the kinematic shock. This is because the parallel wire meter at the inlet to the bottom horizontal header was installed in the elbow outlet flanges for the 4 inch, 6 inch, 8 inch and 12 inch tests. Therefore, this meter will always detect the presence of a kinematic shock formation. Since the average void fraction would be determined based on a period which is longer than the kinematic shock duration, use of this parameter would result in a value that is biased low. For each data set, the maximum void fraction appears to linearly decrease with Froude number. The average void fraction measured at locations VM8 (RIMP8) and VM9 (RIMP9) during the dynamic venting 6 inch elbow test is also presented in

Figure 6-16. This data is seen to represent a lower bound of the Purdue data. This dynamic venting elbow kinematic shock data was obtained by establishing the water flow rate and gradually increasing the air injection flow rate until the kinematic shock formed. The air injection flow rate was held constant as the shock length increased. Whereas, in the Purdue tests WCAP-17271 indicates that due to the nature of the gas transport transient, the gas flux to the elbow reached a sharp peak at the beginning of the transient which then exponentially decayed in magnitude as the transient progressed. Figure 3-2, taken from WCAP-17271, demonstrates the effect of flow rate and hydrostatic head on the transient void fraction measurements in the vertical down-comer during the 8 inch Purdue tests. Table 6-1 defines the location of the void fraction meters referenced in Figure 3-2 from the top of the vertical down-comer.

Figure 6-16 appears to indicate that the effect of the large initial gas flux in the Purdue tests is to result in a large kinematic shock depth. In addition, during the 4-inch elbow testing conducted as part of WCAP-17537, vortexing of air around the backside of each electrode in PW1 and PW2 was observed.

Figure 6-17, taken from WCAP-17537, shows a picture of the vortexing effect during a test run. It is expected that since more air was in contact with the electrodes, additional resistance (impedance) in the current path between the electrodes would result in a higher void fraction reading. The degree to which this may have occurred at the parallel wire meters during the Purdue testing is unknown, but the tendency for this phenomenon to occur would indicate that the parallel wire meters may over-predict the actual gas void fraction.

It is noted in

Figure 6-16 that the RIMP9 meter, which is approximately 8 feet downstream of the elbow and 6 feet downstream of RIMP8, indicates a lower void fraction than RIMP8. This implies that the water level was increasing in the direction of flow. This is consistent with the fact that the liquid flow in the region upstream of the kinematic shock is supercritical. Reference 15 indicates that the behavior of supercritical open-channel flow and the transition to subcritical flow by means of a hydraulic jump is governed by changes in the specific energy and conservation of momentum. Equation 6-10 indicates the head loss is the change in specific energy, e, and is equal to the difference in the elevation of the liquid surface (y_l) and liquid velocity head upstream and downstream of the hydraulic jump. In addition, Equation 6-11 indicates that momentum, expressed as the sum of the liquid hydrostatic force (F) and momentum flux (M) does not change across the jump. Equation 6-12 defines the hydrostatic force (F), which is based on the centroid elevation for a non-uniform cross-section. Equation 6-13 defines the momentum flux of liquid. Equation 6-14 indicates that the critical Froude number is equal to 1 at the transition from supercritical to subcritical flow. The appropriate length in the transition Froude number is based on the liquid flow area, A_l, divided by the width of the liquid free-surface, T; this quantity equals the rate of change of liquid area divided by the liquid area.

$$\Delta e = \left(y_{l,u} + \frac{u_{l,u}^2}{2g} \right) - \left(y_{l,d} + \frac{u_{l,d}^2}{2g} \right) = h_L$$ Equation 6-10

$$F_{l,u} + M_{l,u} = F_{l,d} + M_{l,d}$$ Equation 6-11

$$F = \rho_l \frac{g}{g_c} y_C A_l$$ Equation 6-12

$$M = \rho_l \frac{u_l^2}{g_c} A_l$$ Equation 6-13

$$Fr_{crit}^{\;2} = \left(\frac{u_l^2}{g \frac{A_l}{T}} \right)_{crit} = 1$$ Equation 6-14

Figure 6-18 shows the Froude number based on Equation 6-14 as a function of water depth for 100 gpm flow rate in a 6-inch pipe. The Froude number reaches unity at a water level of 2.84 inches. Supercritical flow exists below this water level and subcritical flow exists above it.

Figure 6-19 provides the specific energy as a function of water level for this case. Flow proceeds in the direction of decreasing specific energy due to irreversible losses in the system. The specific energy is on the abscissa (x-axis), which is numbered in reverse order, so that proceeding from left-to-right is in order of decreasing energy. Below a level of 2.84 inches, in the supercritical regime, level increases in the direction of flow. This is consistent with the observations made in the dynamic venting testing which demonstrates that the void fractions measured at the downstream meter (RIMP9) were lower than those measured at the upstream meter (RIMP8). Above the critical level, water level decreases in the direction of flow, consistent with subcritical behavior. Figure 6-20 depicts the sum of hydrostatic force acting on the water depth and the momentum flux as a function of water depth. The total momentum flux is on the abscissa (x-axis), which is numbered in reverse order, so that a vertical line represents conservation of momentum; a condition which must exist across the kinematic shock. Two vertical dashed lines are represented. The first is at the critical point where total momentum flux reaches a minimum. The second vertical line is at a momentum flux of 3.55 lb_f. In the supercritical region, this flux corresponds to 1.2 inches of water. In the subcritical region, this flux corresponds to a depth of 6 inches, which is the pipe diameter. The significance is that the closed pipe conduit would preclude the transition from supercritical to subcritical from occurring at a water depth of less than 1.2 inches, as the closed channel would preclude the stream from expanding to the extent necessary to dissipate the requisite energy.

This illustrates an important distinction between a hydraulic jump and a kinematic shock. The hydraulic jump is a dynamic shock, and the energy and momentum balances dictate the energy which will be dissipated across the jump. At the high flow rates (full pipe Froude number greater than 1) achieved during the Purdue tests and dynamic venting tests, the pipe sizes tested precluded the possibility of a hydraulic jump from occurring. The kinematic shocks observed in these tests were strictly driven by the difference in magnitude between the influx of air to the elbow and the rate at which the liquid could entrain air into the downstream flow. The formation of the shock was unrelated to energy dissipation due to a dynamic shock. However, the presence of the stratified air layer at the upstream end of the kinematic shock did cause the liquid flow to experience the head loss associated with a sudden expansion as it exited the shock into the full pipe. Equation 6-15 is the classic equation for the pipe flow (closed channel) head loss due to a sudden expansion (Reference 15). It is expressed in terms of the liquid flow area upstream of the expansion ($A_{l,u}$) the liquid flow area downstream of the expansion ($A_{l,d}$) , and the liquid flow velocity upstream of the expansion ($V_{l,u}$).

$$h_L = \frac{\left(1 - \frac{A_{l,u}}{A_{l,d}}\right)^2 u_{l,u}^2}{2g}$$ Equation 6-15

The liquid flow area can be related to the void fraction by means of Equation 6-16, which allows the area ratio term in Equation 6-15 to be expressed as Equation 6-17, since $\alpha_{l,d} << \alpha_{l,u}$.

$$A_L = (1 - \alpha)A$$ Equation 6-16

$$1 - \frac{A_{l,u}}{A_{l,d}} = 1 - \frac{(1 - \alpha_{l,u})}{(1 - \alpha_{l,d})} \approx 1 - \frac{(1 - \alpha_{l,u})}{1} = \alpha_{l,u}$$ Equation 6-17

The upstream velocity term can be expressed in terms of the downstream velocity by means of Equation 6-18, which allows the head loss to be expressed in terms of the upstream void fractions and downstream Froude number.

$$V_{l,u}^2 = \left(\frac{A_{l,d}}{A_{l,u}}\right)^2 u_{l,d}^2 = \frac{(1 - \alpha_{l,d})^2}{(1 - \alpha_{l,u})^2} u_{l,d}^2 \approx \frac{u_{l,d}^2}{(1 - \alpha_{l,u})^2}$$ Equation 6-18

$$h_L = \frac{\left(1 - \frac{A_{l,u}}{A_{l,d}}\right)^2 u_{l,u}^2}{2g} \approx \frac{\left(\alpha_{l,u}\right)^2 u_{l,d}^2}{2g\left(1-\alpha_{l,u}\right)^2} = \left(\frac{d}{12}\right) \frac{\left(\alpha_{l,u}\right)^2 Fr_{l,d}^2}{2\left(1-\alpha_{l,u}\right)^2}$$ Equation 6-19

Figure 6-21 demonstrates the behavior of the term in Equation 6-19 as a function of void fraction for different values of Froude number. This head loss would tend to get extremely large with increasing void fraction and Froude number. As shown in Figure A-2, the differential pressure drops across the kinematic shock were recorded during the dynamic venting tests. These tests indicated that the head loss across the shock only slightly increased with increasing Froude number. This behavior is the result of decreasing void fraction with increasing Froude number that leads to a relatively constant head loss. This explains the behavior shown in

Figure 6-16.

The measured void fraction at the downstream location (RIMP9) during the dynamic venting test will be used as the basis for the kinematic shock depth. It is noted that using the dynamic venting kinematic shock depth as the basis for determining the required pump inlet piping length is conservative, since a lower gas volume fraction requires a longer pipe length. **[**

][a,c] The maximum allowable gas volume is given by Equation 6-21, where V is the volume of the horizontal pump inlet pipe.

[ ] a,c Equation 6-20

[ ] a,c Equation 6-21

a,c

Figure 6-16 Maximum Void Fraction in Horizontal Kinematic Shock

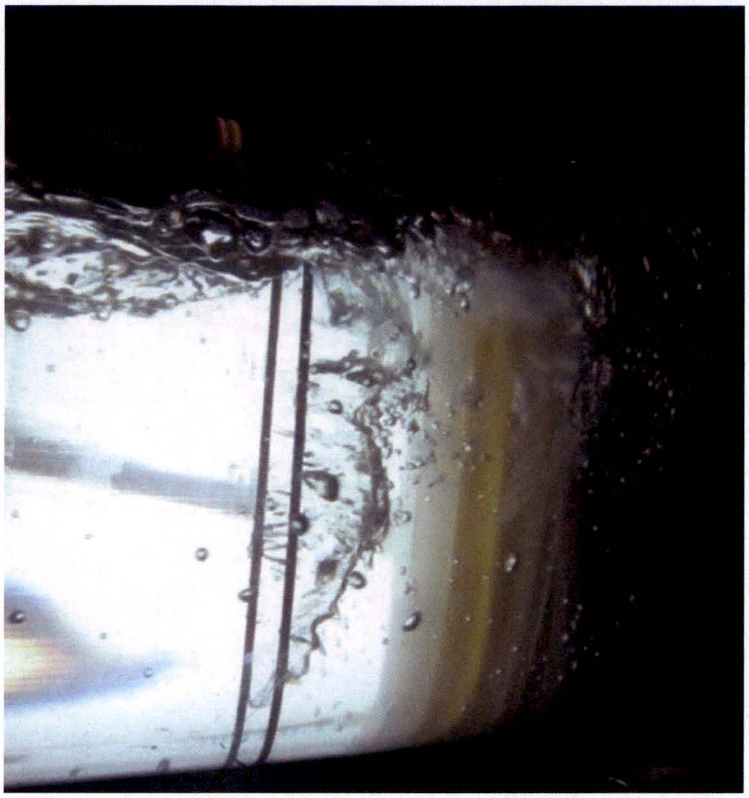

Figure 6-17 WCAP-17537 Vortexing at Parallel Wires

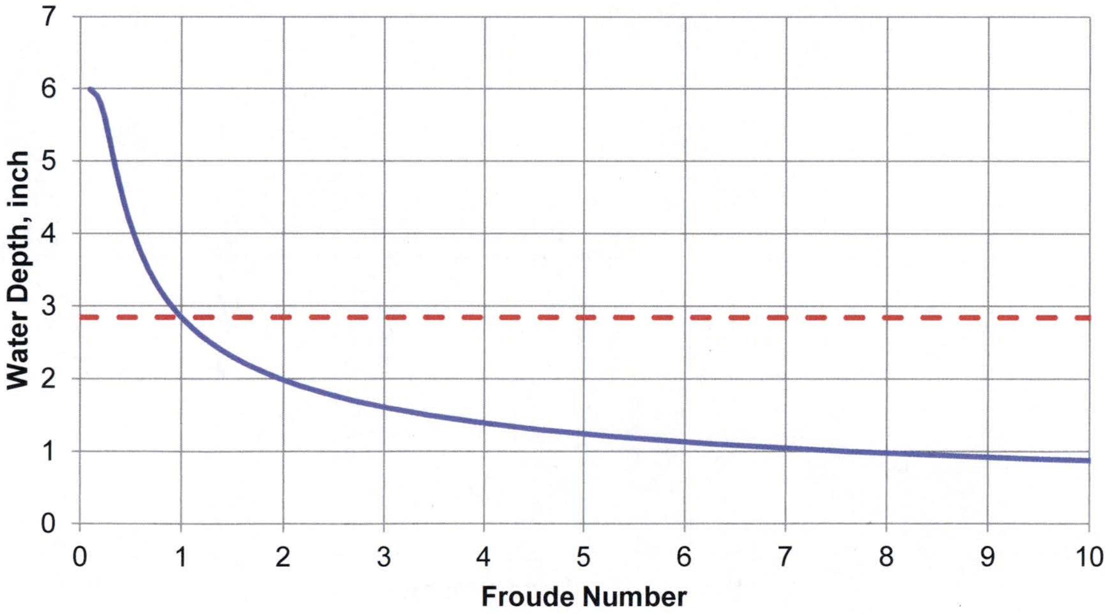

Figure 6-18 Froude Number as a function of water depth (100 gpm in 6 inch pipe)

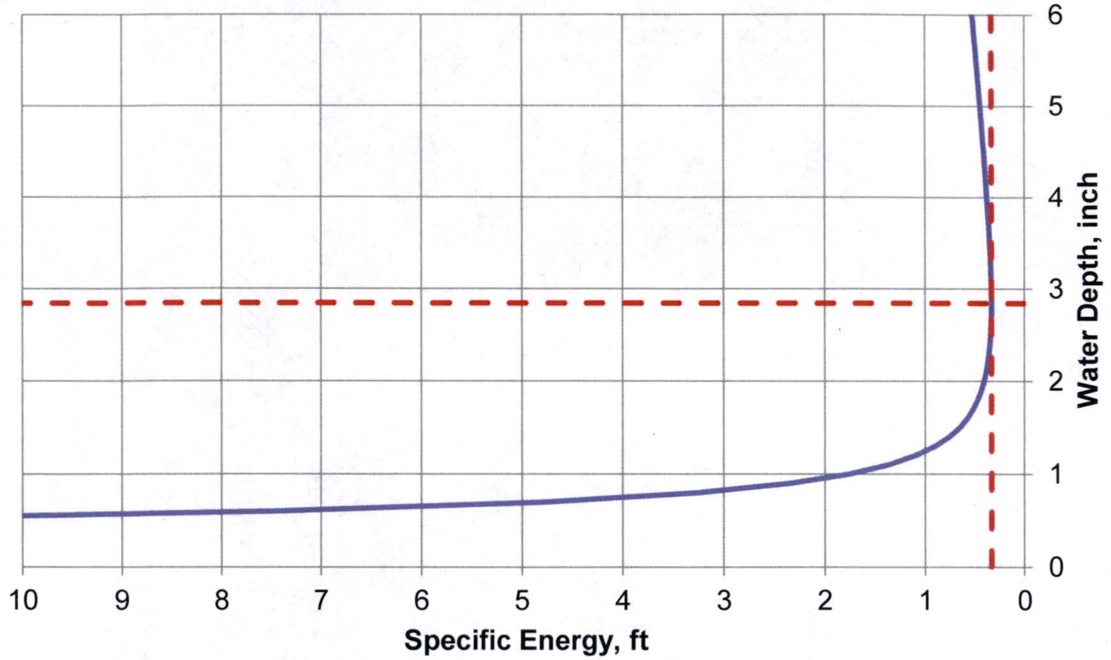

Figure 6-19 Specific Energy as a Function of Water Depth (100 gpm in 6 inch pipe)

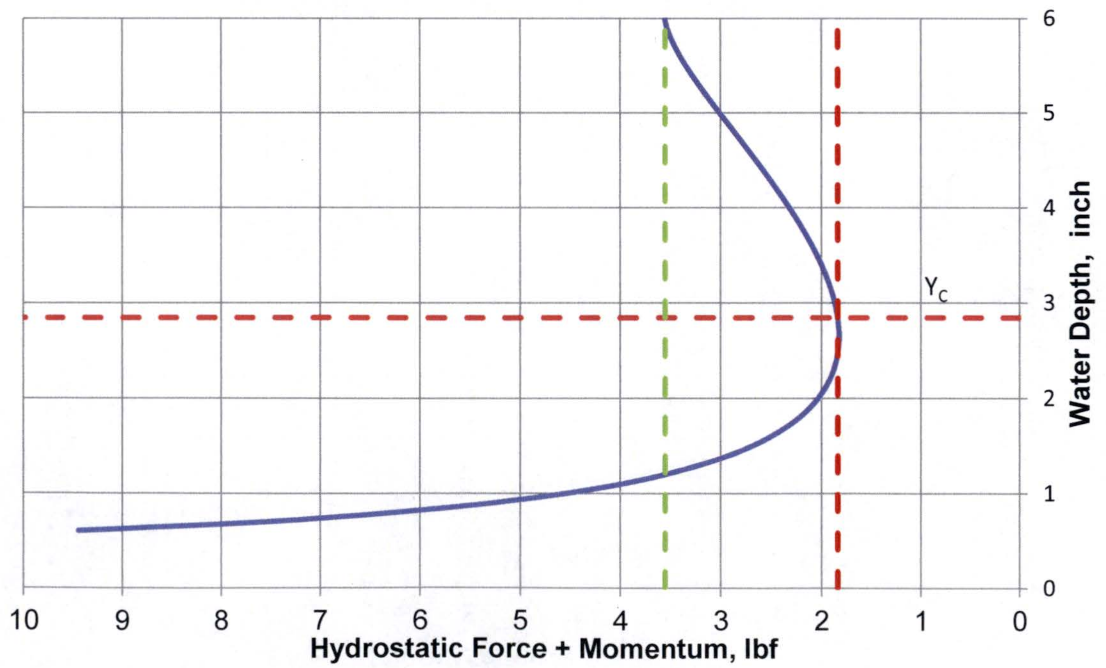

Figure 6-20 Force and Momentum as a Function of Water Depth (100 gpm in 6 inch pipe)

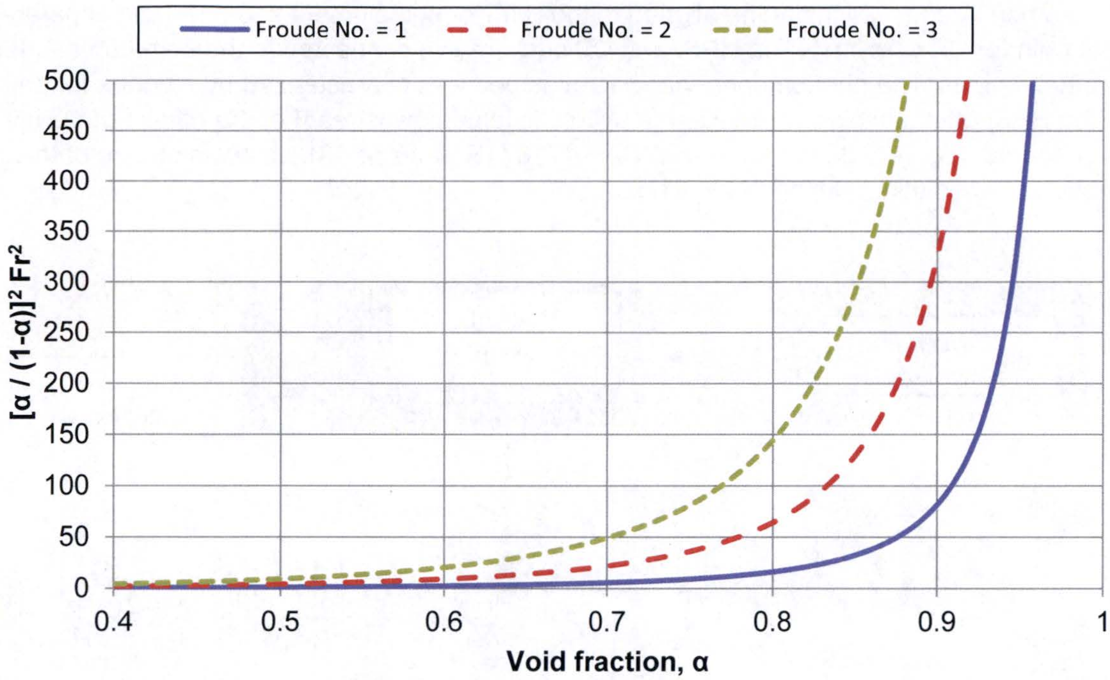

Figure 6-21 Sudden Expansion Loss Coefficient Behavior

6.3.6 Horizontal Off-takes

This section pertains to off-takes from a horizontal pipe. The off-take may be any type of branch connection within a horizontal plane or oriented at an angle downwards from the horizontal plane. Off-takes oriented vertically upwards would not result in vortex formation as the gas will freely transport upwards due to buoyancy.

WCAP-17167 (Reference 13) discusses a scale model test program of the Palo Verde Nuclear Generating Stations ECCS system conducted by Fauske and Associates Inc. (FAI) for Arizona Public Service (APS). The test program investigated the potential to transport an air volume initially trapped in a horizontal segment of the containment sump outlet line through a vertical down-comer and subsequently into the ECCS and CS pump suction lines. The testing modeled the pump suction transfer from the RWT to the containment sump. The first phase investigated the manner in which the liquid outflow from the sump interacted with the air volume, the ability of the liquid outflow to transport air through the vertical down-comer, and the flow pattern of the two-phase mixture in the down-comer. The second phase investigated the nature of the two-phase flow pattern produced in the pump suction piping for the HPSI, LPSI, and CS systems.

In addition to the observation of the kinematic phenomenon and the transition region after the vertical to horizontal elbow, which were also observed in the WCAP-17271 testing, an additional phenomenon was also observed. The HPSI, LPSI and CS systems take suction from the common header which can be aligned to the RWT or containment sump (A train separated from B train for CE systems). The HPSI and CS suctions are connected to the common header with offtake pipes. The phenomenon that was observed was characterized by a vortex formation at the HPSI offtake piping. In addition, a hydraulic jump downstream of the offtake pipe was observed. Figure 6-22, taken from WCAP-17167 (Reference 13), shows a picture of this phenomenon taken during the testing.

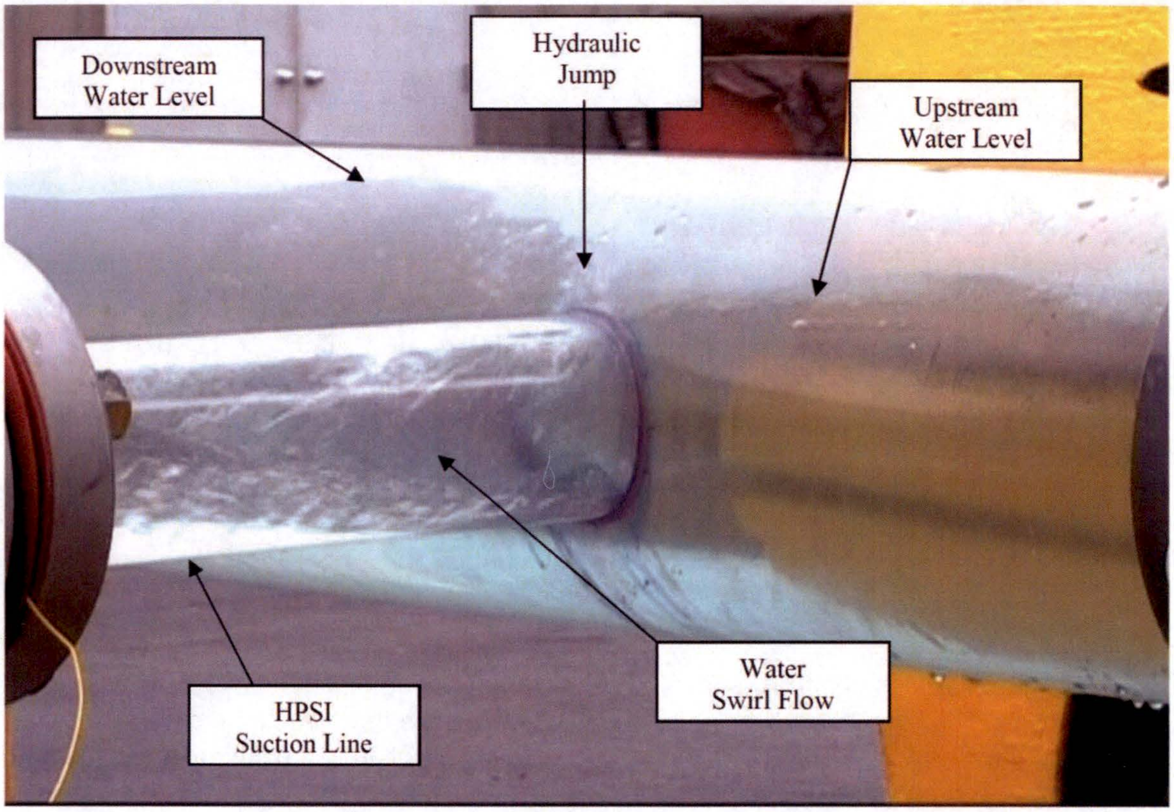

Figure 6-22 Off-Take Vortexing observed during APS Testing

However, it is important to note that the flow rate in the common header upstream of the HPSI off-take corresponded to a Froude number of 0.66 during the test when this phenomenon was observed. This is a relatively low Froude number which would allow a stratified gas layer to form. This situation is not consistent with the basis for the WCAP-17271 correlations and their implementation as documented in this report. Data sets collected with Froude numbers less than unity were not used in the development of the WCAP-17271 correlations since, in these cases, the gas was not completely flushed from the top horizontal header which did not allow mass balance computations to be performed with the requisite degree of accuracy. **Therefore, the WCAP-17271 methodology is only applicable for cases when the Froude number is at least unity.**

Flow stratification in horizontal pipes can lead to an accumulation of gas, such as at off-take or tee geometry. Once gas is accumulated, a subsequent instability can lead to a surge in gas downstream of the off-take. The flow regime map shown below in Figure 6-23 was reproduced from data provided in Figure 3a of Reference 10. This flow regime map uses the liquid and gas mass velocities to determine the flow regime. The following observations are made regarding Figure 6-23.

- For gas mass velocities of less than 1000 lb/hr/ft^2, Stratified flow occurs when liquid mass velocities are less than 1.5 x 10^5 lb/hr/ft^2; this is the value at which stratified flow transitions to plug flow.

- Plug flow transitions to bubbly flow when the gas mass velocity is less than around 100 lb/hr/ft^2 and the liquid mass velocity increases to 1.0 x 10^6 lb/hr/ft^2.

- For gas mass velocities of less than 1000 lb/hr/ft^2, plug flow transitions to dispersed flow when the liquid mass velocities reaches 2.0 x 10^6 lb/hr/ft^2.

Figure 6-24 shows the relation between liquid mass velocity and Froude number as a function of pipe diameter. The following observations are made.

- For all pipe diameters under consideration and for all Froude numbers greater than or equal to unity, the liquid mass velocity exceeds7.0 x 10^5 lb/hr/ft^2 which is well above1.5 x 10^5 lb/hr/ft^2, the transition from stratified flow to plug flow.

- For all pipe diameters under consideration and for all Froude numbers greater than or equal to 2.5, the liquid mass velocity exceeds 2.0 x 10^6 lb/hr/ft^2 which is the transition from plug flow to dispersed flow.

- For all pipe diameters under consideration and for all Froude numbers greater than or equal to 1.5, the liquid mass velocity exceeds 1.0 x 10^6 lb/hr/ft^2 which is the transition from plug flow to bubbly flow, assuming the gas mass velocity is less than around 100 lb/hr/ft^2.

- For all pipe diameters at least 8 inches in diameter and for all Froude numbers greater than or equal to unity, the liquid mass velocity exceeds 1.0 x 10^6 lb/hr/ft^2 which is the transition from plug flow to bubbly flow, assuming the gas mass velocity is less than around 100 lb/hr/ft^2.

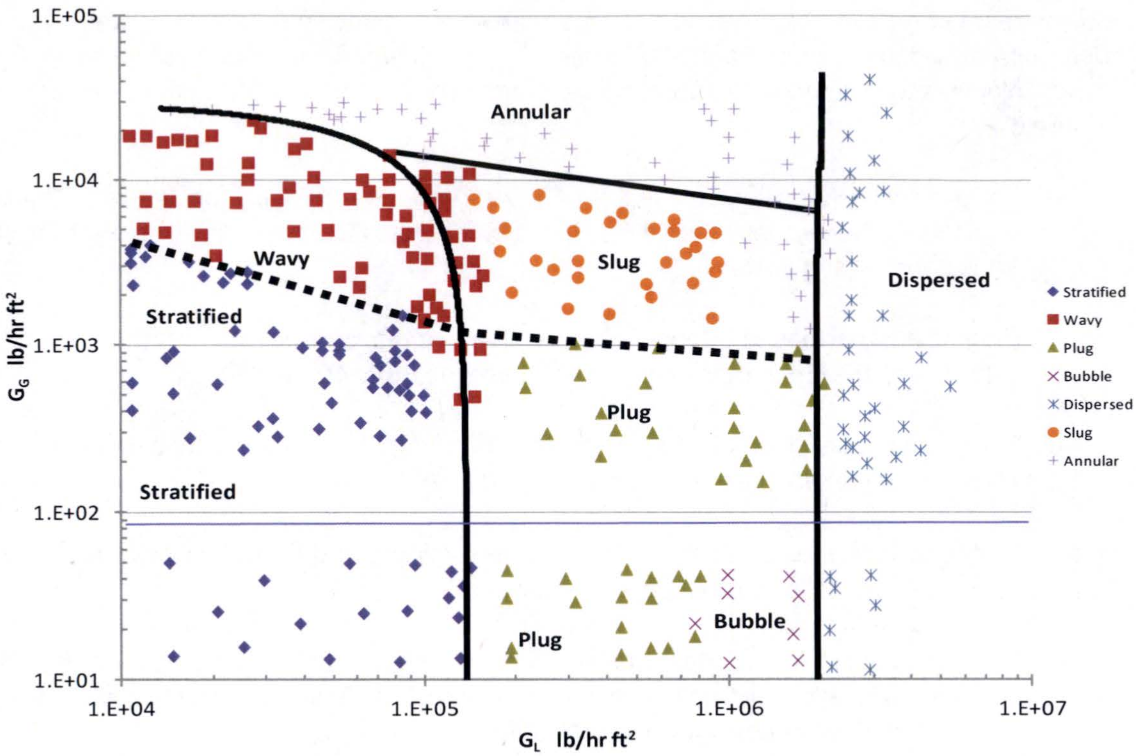

Figure 6-23 Horizontal Flow Regime Map

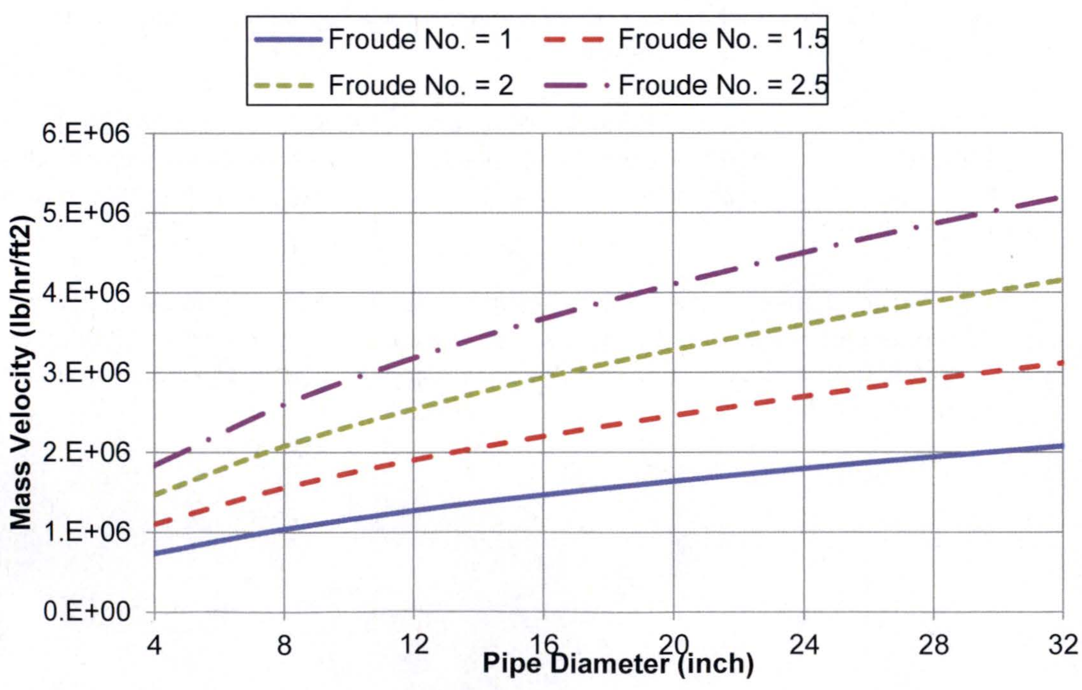

Figure 6-24 Relation between Froude number and Mass Velocity

These observations are significant, since the gas transport methodology being used required the Froude number to be at least unity, which corresponds to liquid mass velocities well above the transition from stratified flow to plug flow and oft exceed the transition from plug flow to bubbly flow or dispersed flow as shown by the Figure 6-23 flow regime map. Reference 10 indicates that the Figure 6-23 flow regime map was based on data from air-water tests in a 2 inch pipe. In Reference 14, Taitel and Dukler provide a theoretical model for predicting flow regime transitions in horizontal pipes. Five major flow regimes are identified: smooth stratified, wavy stratified, intermittent (plug and slug), annular with dispersed liquid, and dispersed bubble flow. Annular flow with dispersed liquid occurs at high gas flow rates and is therefore not applicable to the case at hand. In addition, smooth stratified and wavy stratified flow regimes are both separated flow regimes, which must both be avoided in pump suction piping. Therefore, the transition between these regimes is not relevant. However, the transition between stratified and intermittent and between intermittent and dispersed bubble flow is very important to consider in pump suction piping. Taitel and Dukler indicate the transition from stratified to intermittent flow occurs as liquid flow rate increases and a wave is formed which rapidly grows to block the gas flow path. At lower gas flow rates, intermittent (plug or slug) flow will result. At higher gas flow rates, the liquid is swept up and around the circumference of the pipe to form an annulus with some entrainment if the gas flow rate is high enough. The transition criteria between stratified and intermittent flow is developed by extending infinitesimal wave stability analysis to finite wave in a circular pipe. In the intermittent flow regime, waves form which bridge the pipe flow area and a liquid slug is formed with an adjacent gas bubble. At high liquid flow rates and low gas flow rates, the equilibrium level is near the top of the pipe and the transition from intermittent to dispersed bubble flow occurs when the turbulent fluctuations overcome the buoyant forces tending to keep the gas at the top of the pipe. The transition criterion is expressed in terms of the ratio of the pressure gradient based on the liquid superficial velocity and the buoyancy force per unit length and unit gas flow area. Figure 6 of Reference 14 demonstrates the effects of pipe diameter on transition boundaries for water-air at 1 atm and 77°F, and is reproduced as Figure 6-25, below. Figure 6-26 provides the same information as Figure 6-25 in the same format as the flow regime map of Figure 6-23. It is noted that the transition criteria between stratified and intermittent and between intermittent and dispersed bubble flow as predicted by Taitel and Dukler for a two-inch pipe air-water flow (Figure 6-26) is consistent with Figure 6-23. Furthermore, Figure 6-26 indicates that as the pipe diameter increases from 2 inches to 12 inches, the stratified-intermittent transition at low gas flow rates increases slightly, whereas the intermittent-dispersed bubble transition shifts by a more substantial amount. Therefore, using criteria that the Froude number is greater than or equal to unity ensures that the liquid mass velocity remains substantially above the transition value for stratified – intermittent flow and near the transition from intermittent – dispersed bubble flow. Since the off-take criteria will be applied well upstream of the pump suction, it is not necessary to ensure that the flow regime is in the dispersed bubble regime. As long as the flow is sufficient to ensure that gas bubbles will not coalesce into a stratified flow regime that could result in vortex formation at the off-take.

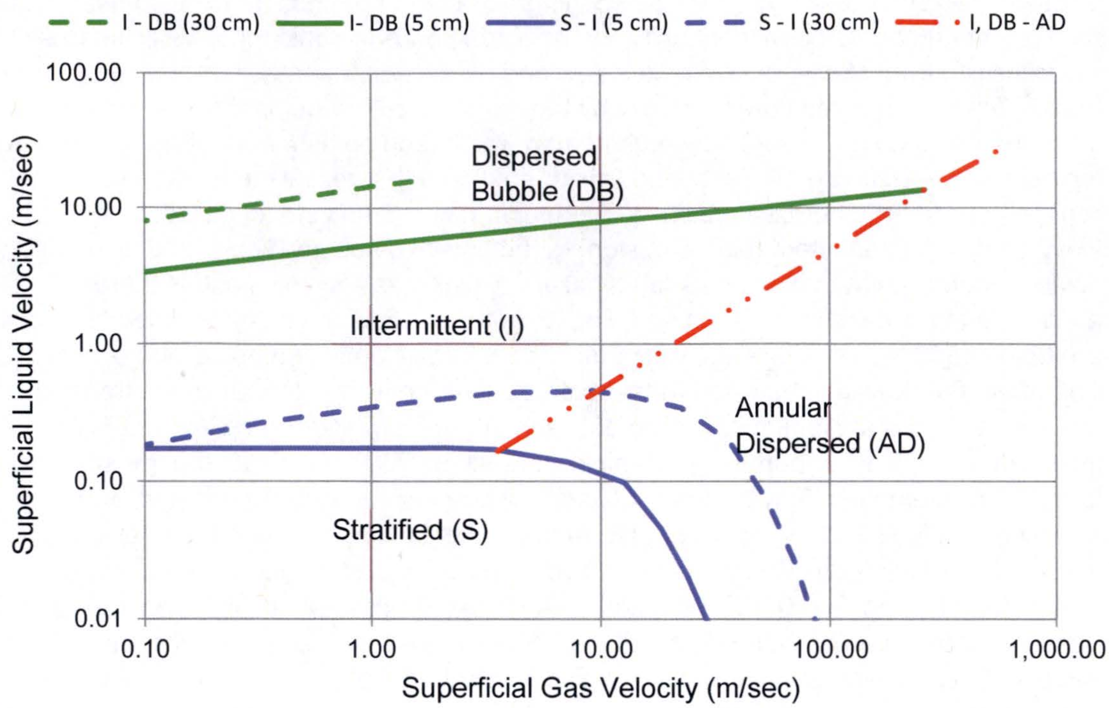

Figure 6-25 Figure 6 of Reference 14

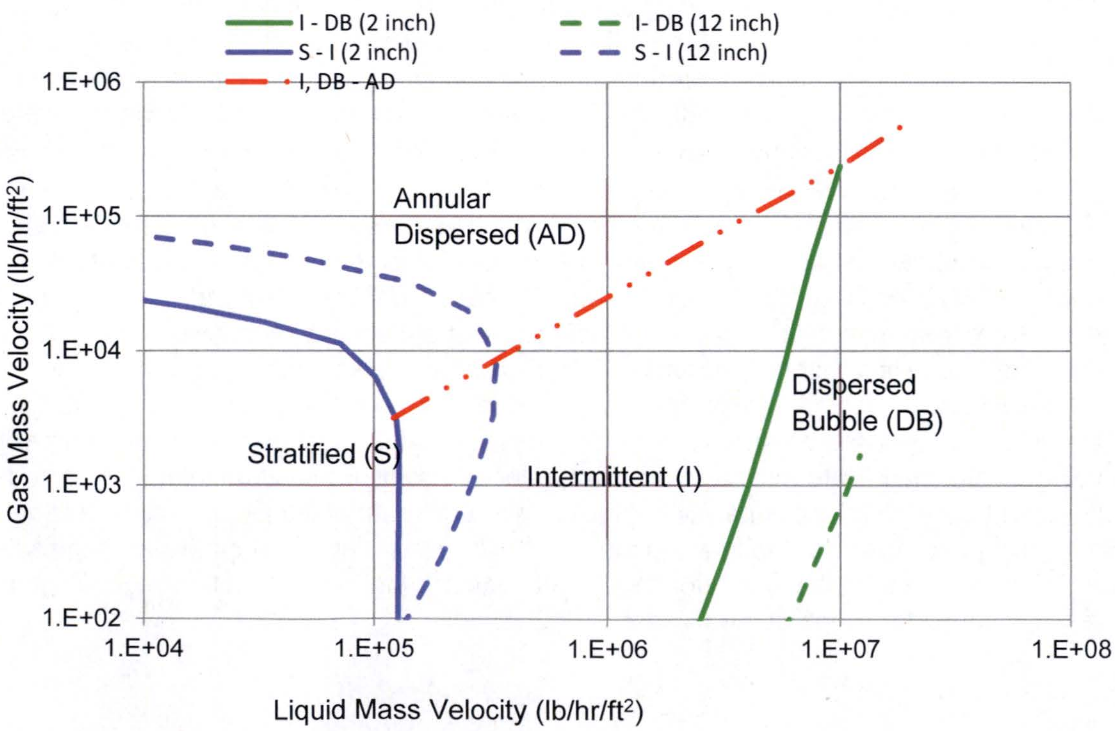

Figure 6-26 Reformatted Version of Figure 6 of Reference 14

The gas volumetric flux ratio is defined by Equation 3-4. The liquid mass velocity is defined by Equation 6-22 and the gas mass velocity is defined by Equation 6-23. These can be substituted into Equation 3-4, resulting in Equation 6-24.

$$G_l = \frac{\rho_l q_l}{A} \qquad \text{Equation 6-22}$$

$$G_g = \frac{\rho_g q_g}{A} \qquad \text{Equation 6-23}$$

$$\beta = \frac{q_g}{q_g + q_l} = \frac{1}{1 + \frac{q_l}{q_g}} = \frac{1}{1 + \frac{G_l}{G_g}\frac{\rho_g}{\rho_l}} \qquad \text{Equation 6-24}$$

Using values of ρ_l=62.4 lb/ft^3 and ρ_g=0.075 lb/ft^3, corresponding to standard pressure and temperature, Equation 6-24 can be used to determine β as a function of G_g and G_l. The results are shown in Table 6-3.

Table 6-3 Relation between G_g and β

	Gas Volumetric Flux Ratio (β)		
G_g (lb/hr/ft^2)	G_l =1.0 x 10^6 lb/hr/ft^2	G_l =2.0 x 10^6 lb/hr/ft^2	G_l =3.0 x 10^6 lb/hr/ft^2
50	0.040	0.020	0.014
100	0.077	0.040	0.027
150	0.111	0.059	0.040
200	0.143	0.077	0.053
250	0.172	0.094	0.065
300	0.200	0.111	0.077
500	0.294	0.172	0.122
1000	0.454	0.294	0.217
1200	0.500	0.333	0.250

As the gas mass velocity increases at constant liquid mass velocity (1.0 x 10^6 lb/hr/ft^2), the flow regime transitions from bubbly flow to plug flow as the gas mass velocity increases to 100 lb/hr/ft^2 (β=0.08) and from plug flow to slug flow as the gas mass velocity increases to 1000 lb/hr/ft^2 (β=0.45). As the gas mass velocity increases at constant liquid mass velocity (2.0 x 10^6 lb/hr/ft^2), the flow regime transitions from bubbly flow to plug flow as the gas mass velocity increases to 100 lb/hr/ft^2 (β=0.03) and from plug flow to slug flow as the gas mass velocity increases to 1000 lb/hr/ft^2 (β=0.29). In all these cases, we know the gas is moving along with the liquid since the Froude number is greater than unity. However, in bubbly flow the gas is dispersed throughout the liquid, in plug flow the gas is moving in separated pockets along the top of the pipe, and in slug flow the gas is moving in separated slugs which occupy the majority of the flow area.

Therefore, the following criteria will be used to treat off-takes from horizontal headers upstream of pump inlets.

- **With the following flow conditions:**
  - **Froude number $\geq$ 1**
  - **Calculated gas volumetric flux ratio, $\beta \leq 0.25$**
- **It can be assumed that the gas is moving with the liquid in either a bubbly or incipient plug flow regime and will not accumulate or stratify at a tee**
- **It will be assumed that the gas is entirely transported though the off-take in the flow direction being considered.**

6.3.7 Co-Current Slug Flow

The 4", 6" and 8" Purdue University tests covered a range of Froude numbers between 0.6 and 2.5. The 12" testing was limited to Froude numbers between 0.6 and 1.0 due to pumping limitations. WCAP-17271 indicates that co-current slugging was observed in the vertical section of the 6" and 8" tests for some cases at a Froude number of 2.5. These slugs tended to be unstable (i.e., rapid break up) and did not result in an increase in downstream gas flux for the geometries tested as part of this program. However, since it was not possible to define the formation and stability of co-current slugging based on the data collected, an upper Froude number limit of 2.5 was placed on the correlations.

Many systems have flow rates which correspond to a Froude number of 2.5 or greater. As noted in WCAP-17271, the slugs tended to be very unstable and broke up in the vertical pipe. For pipe diameters 6 inch and greater, a Froude number of 2.5 corresponds to a mass velocity greater than $2x10^6$ lb_m/hr_{ft}^2. Figure 6-23 indicates that the mass velocity corresponds to the dispersed flow regime for horizontal header; therefore, the slug would tend to quickly break up in the horizontal header if it made it to the bottom of the vertical down-comer. In addition, WCAP-17271 notes that the vertical-to-horizontal elbow tends to hold-up gas at the elbow, and the tendency for a kinematic shock to form increases with gas flux. All of these phenomenon act to break up a co-current gas slug. **Therefore, if the vertical down-comer is followed by an elbow and a horizontal run (that is, the vertical pipe does not go directly into the pump), it can be safely assumed a co-current slug would be broken up quickly, and the Froude number limit of 2.5 is not applicable. This limit remains applicable for pumps with vertically downward inlets when the gas accumulation location is immediately upstream of the pump inlet.**

7 GUIDANCE IF LIMITATIONS CANNOT BE MET

If the conditions specified in Section 6 cannot be met, one option is to use the method prescribed in Section 3.15.2.5 of the NRC SE on NEI 09-10. This was approved by the NRC for determining upstream void volume that will not jeopardize operability without limitations or conditions specified. The acceptable volume is obtained by multiplying the allowable void fraction given in the NEI 09-10 pump acceptance criteria times the total volumetric flow rate times 0.5 seconds. The method should be applied to the conditions expected to exist when the pump is started or is running, not to the void measurement conditions. The NRC equation is provided as Equation 7-1:

$$V_g = \alpha_p \frac{Q_p \frac{gal}{min}}{\left(7.48 \frac{gal}{ft^3}\right)\left(60 \frac{sec}{min}\right)} \frac{P_p}{P_{hp}} (0.5\ sec) \qquad \text{Equation 7-1}$$

Equation 7-1 results in a relatively small allowable gas volume. If Equation 7-1 results in an unacceptably small void volume, appropriately scaled testing is the preferred approach to demonstrate larger allowable gas volume. This does not preclude the use of other data sets that may be available to justify operability.

8 TREATMENT OF UNCERTAINTIES

WCAP-17271 indicates that the flow initialization correlation has an uncertainty of ± 45% with a 90% confidence and the elbow hold-up correlation has an uncertainty of ± 55% with a 90% confidence. The correlations are not independent as parameters calculated from the flow initialization correlation are inputs for the elbow hold-up correlation. In addition, the elbow hold-up correlation may be applied multiple times for a give transport configuration. Therefore, determination of the overall uncertainty through a statistical combination of uncertainties would not be straightforward. However, since the correlations are intended for use in operability determinations, a precise determination of the overall uncertainty is unnecessary. Instead, it will be demonstrated that there are significant inherent conservatisms in the evaluation method which offset the correlation uncertainty.

8.1 PUMP CRITERIA

The EPRI Pump Roadmap Document (Reference 9) indicates the pump criteria used in NEI 09-10 (Reference 6) is conservative by a factor of approximately two in most cases. **Therefore, use of the NEI 09-10 pump criteria introduces a large factor of safety.** In addition, many licensees use the steady state criteria provided in NEI 09-10 as the basis for the operability limits. This results in an additional factor of safety of approximately two.

8.2 TREATMENT OF TEES AND OFF-TAKES

The PWROG has not provided guidance on the manner in which gas separates at tees and off-takes. Therefore, in order to simplify the evaluations, licensees typically make the conservatism assumption that all of the gas is transported through the off-take connection aligned to the pump. This is a very conservative assumption. **Therefore, the assumption that the entire gas quantity travels towards the pump under evaluation is conservative.**

8.3 HOLD-UP AT COMPONENTS

As the mixture travels through the system, components may be encountered which allow gas to be held up. Some examples are:

- Heat exchanger plenums
- Valve bonnets
- Vertically upward off-takes
- Tees with no flow through one branch
- Low pressure recirculation zones downstream of orifices, partially throttled valves, elbows, etc

Some of the gas will be held up in these locations, thereby reducing the gas void fraction that is transported to the pump suction. This is typically not taken into account in the gas transport evaluation, and results in a conservative prediction of the gas flux to the pump.

9 COMPARISON OF WCAP-17271 WITH SYSTEM TEST

System tests were conducted as part of the WCAP-17537 (Reference 11) test plan. The pump flow rate was set at 500 gpm. Prior to initiation of liquid flow, an initial volume fraction of gas was established in the top horizontal header where Void Meter 7 (VM7) was located; refer to Figure A-1. The pump was then turned on and the gas volume fractions at VM7 and VM11 were measured throughout the duration of the transient. Tests were run with initial void fractions of 0.02, 0.20, and 0.50. The gas volume fractions correspond to 0.1 ft^3, 1.14 ft^3, and 2.48 ft^3 of gas. The resulting traces from VM7 and VM11 were reviewed and it is estimated that the times to entrain air from the system were 66 seconds, 69 seconds, and 74 seconds, respectively. The traces are provided as Figure 9-1, Figure 9-2, and Figure 9-3.

a,c

Figure 9-1 System Test: 2 Percent Initial Gas Volume Fraction, 500 gpm

a,c

Figure 9-2 System Test: 23 Percent Initial Gas Volume Fraction, 500 gpm

a,c

Figure 9-3 System Test: 50 Percent Initial Gas Volume Fraction, 500 gpm

The WCAP-17271 correlations were used to model this process. The flow initialization model was applied once and the vertical-to-horizontal elbow hold-up model was applied three times. In addition, the time to homogeneously transport the gas through the system piping volumes was taken into account. Figure 9-4 compares the results with the measured transport times and the transport times predicted by WCAP-17271. It is observed that the WCAP-17271 predicted times are slightly lower than the measured times, but follow the trend of the measured data. This indicates that the correlations correctly model the key behavior. They are also conservative in the sense that a lower transport time corresponds to a higher predicted average gas volumetric flux.

a,c

Figure 9-4 System Test Results

10 IMPLEMENTATION PROCESS

10.1 BACKGROUND

This section will outline a general process and an example will be provided in the following section.

10.2 INPUTS REQUIRED

10.2.1 Gas Accumulation Locations

The high points and potential gas accumulation locations in the pump suction piping should be identified in accordance with Section 8 of NEI 09-10. It is recommended that one-line pipe diagrams be used in this process. The purpose of these drawings is to identify pipe elevation changes, pipe lengths, and major components throughout the piping system.

The following list of locations should be identified for evaluation:

- Inverted "U" Piping
- Heat Exchangers
- Valves (Check, Isolation, Throttle, ...)
- Vent Locations
- Branch Lines
- Orifices
- Relief Valves
- Reducers
- Interfaces with Other Systems
- Points identified as local high points as a result of laser scanning or other detection methods.

10.2.2 Flow paths and Flow Rates

After identifying the high point location, determine the flow path(s) and locate the potentially effected pumps. This can be done by looking at the one-line pipe drawings, isometric drawings, flow drawings, flow models, and initial system configurations. The intent of this process is to use the WCAP-17271 and WCAP-17276 correlations in conjunction with the limitations established in this document to demonstrate that the maximum gas volumetric flux ratio at the pump inlet is within the limits of Table 3-1 or Table 3-2. Since we are interested in demonstrating that maximum allowable gas volumetric flux limits are met, the evaluation process uses the maximum expected flow rates, as these will always result in the highest gas volumetric flux. As a result, the lowest allowable gas volume will occur in conjunction with the highest system flow rates, based on observations made during the gas transport testing conducted at Purdue University (WCAP-17271).

The term header is used to designate a pipe which supplies flow to more than one pump. For example, the RWST outlet provides flow to multiple pumps. Header flow rates should be identified assuming all pumps operate (that is, no single failure) and assuming the limiting single failure. The larger flow rate should be used in the gas transport evaluation. The lower flow rate should be used to demonstrate to meet that flow does not stratify in horizontal pipes.

10.2.3 Vertical Down-comers

The flow path(s) from the high point location to pump suction should be examined for vertical down-comer piping. The volume of each vertical down-comer pipe segment should be calculated for use in demonstrating that the criteria in Section 6.3.4 is met. If credit is taken for an intermediate down-comer volume to meet the Section 6.3.4 criteria, the gas volume must be adjusted for the static pressure which exists at the intermediate down-comer.

The number of vertical-to-horizontal elbows between the gas accumulation location and the pump inlet should be identified if the WCAP-17271 methodology will be used. If credit is taken of an intermediate down-comer volume to meet the Section 6.3.4 criteria, only the vertical-to-horizontal elbows downstream of the intermediate down-comer can be credited in the WCAP-17271 methodology.

10.2.4 Off-takes from Horizontal Pipes

Identify any system off-takes between the high point and pump inlet. If the off-takes are located in a horizontal run of pipe it will be necessary to demonstrate the criteria in Section 6.3.6 is met.

10.2.5 Static Pressure Distribution during Gas Transport Conditions

The minimum static pressure at the pump inlet must be identified since this will result in the largest gas volumetric flux at the pump inlet. This value is usually determined from the minimum $NPSH_A$ calculation. However, since the gas volume is assumed to be present when the system is first actuated, the minimum $NPSH_A$ results can be adjusted to credit suction source levels existing at the time of system actuation. The corresponding static pressure distribution throughout the system must be identified. In particular, the static pressure at the top and bottom of each vertical down-comer must be known to apply the WCAP-17271 methodology. Since the gas void fractions are expected to be relatively small, the hydrostatic heads during gas transport will be approximately equal to the hydrostatic heads due to a water solid condition. If the static pressure distribution from a hydraulic model accounting for friction and form losses is unavailable, the static pressure distribution can be estimated by using the pump inlet pressure as the datum and making adjustments for hydrostatic head due to elevation changes.

10.2.6 Static Pressure Distribution during Surveillance Test Conditions

The allowable gas volumes are determined based on the static pressure distribution during system operation in the applicable mode. However, the allowable gas volume criteria to be used during gas monitoring surveillance tests must be based on the static pressures existing during the surveillance test. Therefore, the calculated gas volume should be adjusted to account for the change in static pressure from pump operating conditions to surveillance test conditions at the gas accumulation location.

10.2.7 Fluid Properties

The WCAP-17271 methodology requires knowledge of the liquid density (ρ_l) and the surface tension (σ) at the operating liquid pressure and temperature. The flow regime chart in Section 6.3.6 requires calculating the liquid and gas mass velocities. This requires identification of the liquid density (ρ_l) and gas density (ρ_g).

10.2.8 Pump Inlet Piping Configuration

For each pump to be evaluated, the configuration of the pump inlet piping should be identified. If the pump has a vertical downward inlet, it is necessary to demonstrate that the criteria in Section 6.3.7 is met. If the pump has a horizontal inlet, it is necessary to demonstrate that the criteria in Section 6.3.5 is met.

10.2.9 Pump Data

Pump data should be acquired for each pump that has the potential to be affected by the gas void. This information includes the pump type, best efficiency point flow rate, pump operating flow rate for the scenario being evaluated, manufacturer pump head curve, and test limit pump head curve.

The NRC SE on NEI 09-10 requires that if the steady-state criteria in Table 3-1 is used to develop the allowable gas volume the pump head margin should be evaluated, to verify that at least 3% margin exists between the pump developed operating head and the minimum head required to meet operability conditions. Since the gas transport time is expected to be small, it is anticipated that the impact will be negligible in most cases.

One of the inputs into determining the allowable void volume and transient transport time from Table 3-1 is the ratio of the Pump Operating Flow Rate, Q_{PUMP}, and the Best Efficiency Point Flow Rate, Q_{BEP}.

10.3 METHOD TO ADJUST GAS FLUX DUE TO CHANGE IN FLOW RATE

The existing methodology does not incorporate a correlation to determine the gas flow distribution at an off-take. Therefore, it is conservatively assumed that all of the gas goes through the off-take in the direction of the pump under evaluation. Therefore, based on conservation of gas mass, the gas volumetric flux ratio at the off-take exit can be calculated assuming the gas volumetric flow rate remains constant. The mixture flow rate at the inlet to the off-take is the pumped system flow rate at the off-take inlet. Likewise, the mixture flow rate at the outlet of the off-take is the pumped system flow rate at the off-take outlet.

$$\beta_{in} = \frac{q_{g,in}}{q_{mix,in}} \qquad \text{Equation 10-1}$$

$$\beta'_{out} = \frac{q_{g,in}}{q_{mix,out}} \qquad \text{Equation 10-2}$$

$$\beta_{out} = \frac{q_{mix,in}}{q_{mix,out}} \beta_{in} \qquad \text{Equation 10-3}$$

10.4 ALLOWABLE GAS VOLUME CALCULATION PROCESS

10.4.1 Pump Allowable Gas Volumetric Flux Ratio and Transport Time

Based on the pump operating flow rate and pump best efficiency flow, determine the allowable gas volumetric flux ratio from Table 3-1 (or Table 3-2) based on the applicable pump type. A transport time of 20 seconds is applicable to the steady state criteria.

10.4.2 Estimate Initial Gas Volume

10.4.2.1 WCAP-17276 (Simplified Equation) Methodology

The initial gas volume is estimated using Equation 5-1 based upon the allowable values of β_p and Δt_p from Table 3-1 and the values of Q_p, P_p, and P_{hp}, where the static pressures are those that exist during pump operation.

It is now necessary to determine if the allowable gas transport time, Δt_{Pump} from Table 3-1, is consistent with the expected transport time. This is done by using Equation 5-6 to calculate y based on the gas volume (V_g) and liquid flow rate (Q_l), velocity (U_l) and pipe cross-section area (A) at the high-point location. The expected transport time (Δt) is calculated using Equation 5-7 based on the liquid flow rate, gas volume (V_g) and pipe diameter (D) existing at the high point location. If the expected transport time is less than the allowable transport time, the gas volume should be adjusted using Equation 10-4.

$$V_{g,adj} = \frac{\Delta t}{\Delta t_g} V_g \qquad \text{Equation 10-4}$$

10.4.2.2 WCAP-17271Methodology

Application of the WCAP-17271 requires guessing an initial gas volume, V_{GAS}.

1. Equation 4-2 is used to determine the ideal shock length (L_S) based on the assumed V_{GAS} and the pipe area (A) in the vertical down-comer downstream of the gas volume. It is noted that the pressure ratio in Equation 4-2, corrects the gas volume from static to operating conditions. Therefore, a value of unity should be used for this ratio. The correction from the operating pressure to the surveillance test pressure will be performed at a later step.
2. Equation 4-1 is then used to predict the time for the gas to be entrained in the flow through the kinematic shock (Δt_{init}) based on the ideal shock length and fluid properties.
3. Equation 4-4 is used to calculate the Weber number (We) based on L_S and fluid properties
4. Equation 4-3 would be used to predict the average gas volumetric flux ($\beta_{shock\ outlet}$) at the outlet of the vertical down-comer over the transport time interval based on the Weber number.
5. Equation 4-8 would be used to predict the average gas volumetric flux ratio at the elbow inlet ($\beta_{el,in}$) based on the flux ratio at the shock outlet ($\beta_{s,out}$) and the static pressure ratio between the shock outlet ($P_{s,\ out}$) and elbow inlet ($P_{el,in}$).
6. Equation 4-7 would be used to calculate the Froude number (Fr) based on the mixture velocity (u_{mix}) and down-comer pipe diameter (d).
7. Equation 4-6 is then used to predict the average gas volumetric flux at the elbow outlet ($\beta_{el,out}$) using $\Delta t_{el,in} = \Delta t_{init}$, $\beta_{el,in}$, and Fr as input variables.
8. Equation 4-9 is then used to calculate $\Delta t_{el,out}$ based on $\Delta t_{el,in}$, $\beta_{el,in}$, and $\beta_{el,out}$.
9. Steps 5 through 8 are repeated for each vertical-to-horizontal elbow between the gas accumulation location and the pump inlet.
10. Equation 10-3 is used to adjust the gas volumetric flux ratio each time the flow rate changes due to an off-take.
11. By repeated application of these steps, the gas volumetric flux ratio at the pump inlet (β_p) and transport time (Δt_p) can be calculated.
12. The assumed initial gas volume is iterated upon until the Equation 10-5 or Equation 10-6 are satisfied.

$$\beta_p \le \beta_{Transient} \text{ and } \Delta t_p \le \Delta t_{Transient} \quad \text{Equation 10-5}$$

$$\beta_p \le \beta_{Steady\text{-}State} \text{ and } \Delta t_p \ge 20 \text{ sec} \quad \text{Equation 10-6}$$

10.4.3 Verify Vertical Down-comer Limitation

The gas volumes calculated in Section 10.4.2 meet the pump criteria provided in Table 3-1 or Table 3-2. However, it must be demonstrated that the vertical down-comer limitation is met to ensure the separated flow region remains in the down-comer and bubbly flow exits the bottom. This can be done directly by using Equation 5-6 to calculate y based on the gas volume (V_g) and liquid flow rate (Q_l), velocity (U_l) and pipe cross-section area (A) at the down-comer location. The parameter y is the required down-comer length. Alternatively, Figure 6-5 through Figure 6-8 can be used to estimate the allowable gas volume.

If credit is taken of an intermediate down-comer volume to meet the Section 6.3.4 criteria, then the gas volume must be adjusted for the static pressure which exists at the intermediate down-comer.

In addition, if credit is taken of an intermediate down-comer volume to meet the Section 6.3.4 criteria, only the vertical-to-horizontal elbows downstream of the intermediate down-comer can be credited in the WCAP-17271 methodology.

10.4.4 Verify Horizontal Off-take Limitation

The gas volumes calculated in Section 10.4.2 meet the pump criteria provided in Table 3-1 or Table 3-2. However, it must be demonstrated that if an off-take is located in a horizontal run of pipe, the criteria in Section 6.3.6 is met. As long as the Froude Number in the horizontal header is greater than or equal to unity and the gas volumetric flux ratio is less than or equal to 25% the limitation is met.

If the Froude number is less than unity, then it is recommended that the Taitel-Dukler methodology (Reference 14) be used to demonstrate that the flow regime is in the intermittent flow regime, preferably close to the dispersed bubble regime than the stratified regime. This approach is recommended since it matches available test data and accounts for the effects of pipe diameter, which may be significant.

10.4.5 Verify Pump Inlet Limitation

10.4.5.1 Horizontal Inlet

If the pump has a horizontal inlet preceded by a vertical down-comer, it should be verified that either a kinematic shock does not form in the horizontal pipe downstream of the elbow, or that the length of horizontal pipe is sufficient to prevent the kinematic shock from directly entering the pump.

Equation 6-6 provides the minimum required allowable gas volumetric flow ratio to form a kinematic shock at the outlet of a vertical-to-horizontal elbow in terms of the Froude number. Equation 6-7 provides a relation between the maximum gas volumetric flux at the down-comer outlet and the shock length y calculated by Equation 5-6 divided by the diameter of the down-comer. A kinematic shock will not form if the calculated gas volumetric flux ratio is less than the minimum required flux ratio. Alternatively, Figure 6-13 through Figure 6-15 can be used to determine if a kinematic shock will form.

If a kinematic shock does form, Equation 6-21 provides the necessary pipe volume to prevent the kinematic shock from directly entering the pump as a function of Froude number.

10.4.5.2 Vertical Downwards Inlet

If the pump has a vertical downwards inlet, the methodology provided in Section 10.4.6 should be used to demonstrate that the liquid flow rate is not sufficient to transport a co-current gas slug directly to the pump inlet.

10.4.6 Verify Maximum Flow Limitation

This limitation ensures that the liquid flow rate will not be high enough to transport a co-current slug of gas directly to the pump inlet. Many systems have flow rates which correspond to a Froude number of 2.5 or greater. As noted in WCAP-17271, the slugs tended to be very unstable and broke up in the vertical pipe. For pipe diameters 6 inch and greater, a Froude number of 2.5 corresponds to a mass velocity greater than $2x10^6$ $lb_m/hr\text{-}ft^2$. Figure 6-20 indicates that the mass velocity corresponds to the dispersed flow regime for horizontal header; therefore, the slug would tend to quickly break up in the horizontal header if it made it to the bottom of the vertical down-comer. In addition, WCAP-17271 notes that the vertical-to-horizontal elbow tends to hold-up gas at the elbow, and the tendency for a kinematic shock to form increases with gas flux. All of these phenomenon act to break up a co-current gas slug. Therefore, if the vertical down-comer is followed by an elbow and a horizontal run (that is, the vertical pipe does not go directly into the pump), it can be safely assumed a co-current slug would be broken up quickly, and the Froude number limit of 2.5 is not applicable. This limit remains applicable for pumps with vertically downward inlets when the gas accumulation location is immediately upstream of the pump inlet.

10.5 GAS VOLUME BASED ON SURVEILLANCE STATIC PRESSURE

The gas volume calculated in Section 10.4 is based on the static pressure at the accumulation location during operating conditions. The surveillance tests are usually conducted when the pumps are not in operation, or when the system is aligned to a different suction source. As a result, a different static pressure may exist at the accumulation during surveillance testing than during operation. The allowable gas volume must be adjusted to the static pressure which will exist during surveillance testing using the ideal gas law.

11 EXAMPLE PROBLEM

11.1 INPUTS REQUIRED

11.1.1 Gas Accumulation Locations

The one line drawing for the evaluation is shown in Figure 11-1, which is applicable to the RWST supply to two Safety Injection pumps. There are two gas accumulation locations. The first gas accumulation location is formed by the inverted U-tube caused by the down-turned elbow in the RWST. The second gas accumulation location is formed by the 8 inch check valve at elevation 170 feet, which does not allow the gas to vent back to the RWST.

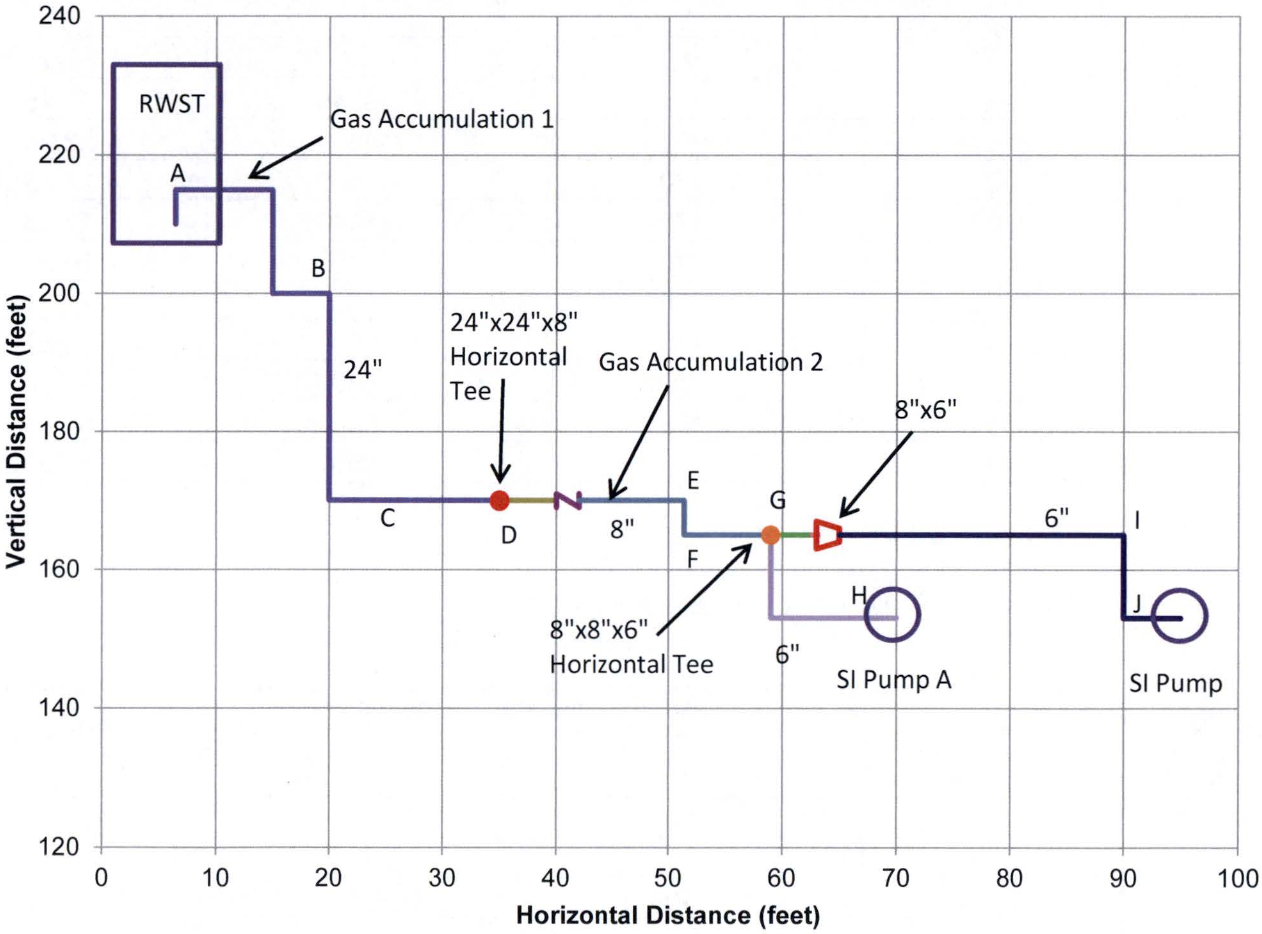

Figure 11-1 One-Line Drawing

11.1.2 Flow paths and Flow Rates

Table 11-1 identifies the system flow rates for the case to be evaluated. The location identifiers refer to identifiers on Figure 11-1. The flow out of the RWST is 18,548 gpm in a 24 inch pipe. At the off-take at Location D, 17,678 gpm is diverted to the RHR, CS, and Charging pumps and 870 gpm is supplied to the two SI pumps. It is noted that at Locations E, F, G the header flow rate of 870 gpm is used. However, at Locations H, I, and J the single pump operating flow rate of 660 gpm is used. This allows the evaluation to be bounding for both two pump and single pump operation, since the maximum system flow rates will result in a lower allowable gas volume.

Table 11-1 System Flow Rates

Location	Y	Q	D
	ft	gpm	inch
A	215	18548	23.25
B	200	18548	23.25
C	170	18548	23.25
D	170	18548	23.25
E	170	870	7.981
F	165	870	7.981
G	165	870	7.981
H	153	660	6.065
I	165	660	6.065
J	153	660	6.065

11.1.3 Vertical Down-comers

There are five vertical down-comers in Figure 11-1 as shown in Table 11-2.

Table 11-2 Vertical Down-Comers

Down-comer Location	L	D	A	V
	ft	inch	ft^2	ft^3
A-B	15	23.25	2.9483	44.23
B-C	30	23.25	2.9483	88.45
E-F	5	7.981	0.3474	1.74
G-H	12	6.065	0.2006	2.41
I-J	12	6.065	0.2006	2.41

11.1.4 Off-takes from Horizontal Pipes

There are two horizontal off-takes in Figure 11-1 as shown in Table 11-3. The ratio of inlet flow to outlet flow is also provided since this will be needed to adjust the gas volumetric fraction using Equation 10-3.

Table 11-3 Horizontal Off-takes				
Horizontal Off-take	Description	Q_{in}	Q_{out}	Q_{in} / Q_{out}
	ft	gpm	gpm	
D	24"x24"x8" tee	18548	870	21.32
G	8"x8"x6" tee	870	660	1.32

11.1.5 Static Pressure Distribution during Gas Transport Conditions

The minimum static pressure at the pump inlet must be identified since this will result in the largest gas volumetric flux at the pump inlet. This value is usually determined from the minimum $NPSH_A$ calculation. However, since the gas volume is assumed to be present when the system is first actuated, the minimum $NPSH_A$ results can be adjusted to credit suction source levels existing at the time of system actuation. Table 11-4 identifies the static pressure distribution during operation. The values were obtained from the $NPSH_A$ calculation and adjusted by the difference in hydrostatic head due to the RWST elevation assumed during the $NPSH_A$ (223 ft) and the RWST elevation during normal operation when surveillance testing is performed (270 ft).

Table 11-4 Static Pressure Distribution during Pump Operation		
LOC	Y	PADJ
	ft	psia
A	215	36.12
B	200	38.33
C	170	42.76
D	170	42.76
E	170	42.24
F	165	41.97
G	165	41.24
H	153	40.08
I	165	40.24
J	153	39.04

11.1.6 Static Pressure Distribution during Surveillance Test Conditions

The allowable gas volumes are determined based on the static pressure distribution during system operation in the applicable mode. However, the allowable gas volume criteria to be used during gas monitoring surveillance tests must be based on the static pressures existing during the surveillance test. Therefore, the calculated gas volume should be adjusted to account for the change in static pressure from pump operating conditions to surveillance test conditions at the gas accumulation location. Table 11-5 identifies the static pressure distribution during surveillance testing and was obtained by using an RWST water level static pressure of 14.7 psia and adding the hydrostatic head between the RWST level (270 ft) and the Location elevation.

Table 11-5 Static Pressure Distribution during Surveillance Testing		
Location	Y	PADJ
	ft	psia
A	215	38.50
B	200	44.98
C	170	57.96
D	170	57.96
E	170	57.96
F	165	60.13
G	165	60.13
H	153	65.32
I	165	60.13
J	153	65.32

11.1.7 Fluid Properties

The WCAP-17271 methodology requires knowledge of the liquid density (ρ_l) and the surface tension (σ) at the operating liquid pressure and temperature. The flow regime chart in Section 6.3.6 requires calculating the liquid and gas mass velocities. This requires identification of the liquid density (ρ_l) and gas density (ρ_g). These values are provided in Table 11-6.

Table 11-6 Fluid Properties		
Parameter	Units	Value
T	$^{\circ}F$	70
ρ_l	lb_m/ft^3	62.3
ρ_g	lb_m/ft^3	.075
σ	lb_f/ft	0.005

11.1.8 Pump Inlet Piping Configuration

Table 11-7 identifies the pump inlet configurations. The inlet volumes were determined for use in Equation 6-21.

Table 11-7 Pump Inlet Configurations				
Pump	Inlet type	Diameter	Length	Volume
		Inch	ft	Ft^3
SI Pump 1	Horizontal	6.065	11	2.2
SI Pump 2	Horizontal	6.065	5	1.0

11.1.9 Pump Data

The NRC SE on NEI 09-10 requires that if the steady-state criteria in Table 3-1 is used to develop the allowable gas volume the pump head margin should be evaluated, to verify that at least 3% margin exists between the pump developed operating head and the minimum head required to meet operability conditions.

Table 11-8 provides the required pump data. Both pumps have 12.5 % margin between actual operating head and the required head for pump operability, which exceeds the 4% requirement imposed by the NRC SE on NEI 9-10.

Table 11-8 Data for SI Pump 1 and 2		
SI Pump 1 and 2		
Manufacturer	Flowserve	
Model	JHF	
Q_{BEP}	450	gpm
Q_{Pump}	660	gpm
Q_{Pump}/Q_{BEP}	1.47	
Table 3-1 Steady State β	0.01	
Table 3-1 Transient β	0.05	
Table 3-1 Transient Δt	5	sec
Pump Head at Q_{Pump}	1800	ft
Pump Min Head for Operability	1600	ft
Margin	12.5	%

11.1.9.1 WCAP-17276 (Simplified Equation) Methodology

The initial gas volume is estimated using Equation 5-1 based upon the allowable values of β_{Pump} and Δt_{Pump} from Table 3-1 and the values of Q_{Pump}, P_{Pump}, and $P_{High\text{-}Point}$, where the static pressures are those that exist during pump operation. Table 11-9 provides the inputs and output of Equation 5-1.

Table 11-9 Equation 5-1 Results			
Input	B_p	0.05	
Input	Δt_p	5.00	sec
Input	Q_p	660.00	gpm
Input	P_p	39.04	psia
Input	P_{hp}	36.12	psia
Output	V_g	0.40	ft^3

An initial guess of the gas volume divided by the down-comer area, 0.4ft^3 / 2.9483 ft^2 =0.1357 ft, is used in the right hand side of Equation 5-6 and a new value of y is calculated. This is used as a new estimate for y, and this sequence of successive approximations results in a value of y=0.6035 ft. Substituting this value back into Equation 5-6 demonstrates the procedure has converged. Table 11-10 provides the inputs and output of Equation 5-6.

Table 11-10 Equation 5-6 Results			
Input	$Q_{hp'}$	18548	gpm
Input	U_l	14.0	ft/sec
Input	d	23.25	inch
Input	A	2.9483	ft^2
Input	V_g	0.40	ft^3
Input	L_s	0.6035	ft
Output	L_s	0.6035	ft

The largest calculated gas volume can be used as long as all limitations can be met. Based on this value of L_s, the transport time is calculated using Equation 5-7. Table 11-11provides the inputs and output of Equation 5-7.

Table 11-11 Equation 5-7 Results			
Input	Q'	18548	gpm
Input	d	23.25	inch
Input	V_g	0.40	ft^3
Input	L_s	0.6035	ft
Output	Δt	0.3	sec

Therefore, the gas will transport much more quickly than the allowable transient transport time based on Table 3-1. As a result, the allowable gas volume must be adjusted as shown below.

$$V_{g,adj}' = \frac{\Delta t}{\Delta t_p} V_g = \left(\frac{0.3 \sec}{5 \sec} \right) 0.4 \, ft^3 = 0.024 \, ft^3$$

11.1.9.2 WCAP-17271Methodology

Application of the WCAP-17271 requires guessing an initial gas volume, V_{GAS}.

Equation 4-2 is used to determine the ideal shock length (L_S) based on the assumed V_{GAS} and the pipe area (A) in the vertical down-comer downstream of the gas volume. It is noted that the pressure ratio in Equation 4-2, corrects the gas volume from static to operating conditions. Therefore, a value of unity should be used for this ratio. The correction from the operating pressure to the surveillance test pressure will be performed at a later step. Equation 4-1 is then used to predict the time for the gas to be entrained in the flow through the kinematic shock (Δt_{init}) based on the ideal shock length and fluid properties. Equation 4-4 is used to calculate the Weber number (We) based on L_S and fluid properties. Equation 4-3 would be used to predict the average gas volumetric flux ($\beta_{shock\ outlet}$) at the outlet of the vertical down-comer over the transport time interval based on the Weber number. Table 11-12 shows the results of these calculations.

Table 11-12 WCAP-17271 Calculation of $\beta_{Shock\ Outlet}$

Input		$Q_{dc'}$	18548	gpm
Equation 4-2	input	V_g	0.43	ft^3
	Input	A	2.9483	ft^2
	Output	L_s	0.1458	ft
Equation 4-1	Input	L_s	0.1458	ft
	Input	U_{mix}	14.0	ft/sec
	Input	ρ_l	62.3	lb/ft^3
	Input	σ	0.005	lb/ft
	Output	Δt	0.32	sec
Equation 4-4	Input	L_s	0.1458	ft
	Input	U_{mix}	14.0	ft/sec
	Input	ρ_l	62.3	lb/ft^3
	Input	σ	0.005	lb/ft
	Output	We	11089	
Equation 4-3	Input	We	11089	
	Output	$B_{s,out}$	0.0327	

Equation 4-8 would be used to predict the average gas volumetric flux ratio at the elbow inlet ($\beta_{elbow\ inlet}$) based on the flux ratio at the shock outlet ($\beta_{s,out}$) and the static pressure ratio between the shock outlet ($P_{s,out}$) and elbow inlet ($P_{el,in}$). Equation 4-7 would be used to calculate the

Froude number (Fr) based on the mixture velocity (u_m) and down-comer pipe diameter (d). Equation 4-6 is then used to predict the average gas volumetric flux at the elbow outlet ($\beta_{el,out}$) using $\Delta t_{el,in}=\Delta t_{init}$, $\beta_{elbow\ inlet}$, and Fr as input variables. Equation 4-9 is then used to calculate $\Delta t_{el,}$out based on $\Delta t_{el,in}$, $\beta_{el,in}$, and $\beta_{el,out}$. Steps 5 through 8 are repeated for each vertical-to-horizontal elbow between the gas accumulation location and the pump inlet. Table 11-13 shows the results for the 1st elbow.

Table 11-13 WCAP-17271 Calculation of $\beta_{el,out}$ and $\Delta t_{el,out}$ for 1st elbow				
Equation 4-8	Input	$\beta_{s,out}$	0.0327	
	Input	P_s	36.12	psia
	Input	P_{el}	38.33	psia
	Output	$\beta_{el,in}$	0.0308	
Equation 4-7	Input	Q	18548	gpm
	Input	d	23.25	inch
	Input	U_{mix}	14.0	ft/sec
	Output	Fr	1.77	
Equation 4-6	Input	Fr	1.77	
	Input	$\beta_{el,in}$	0.0308	
	Input	$\Delta t_{el,in}$	0.32	sec
	Output	$\beta_{el,out}$	0.0013	
Equation 4-9	Input	$\beta_{el,in}$	0.0308	
	Input	$\Delta t_{el,in}$	0.32	sec
	Input	$\beta_{el,out}$	0.0013	
	Output	$\Delta t_{el,out}$	7.73	sec

Table 11-14 shows the results for the 2nd elbow.

Table 11-14 WCAP-17271 Calculation of $\beta_{el,out}$ and $\Delta t_{el,out}$ for 2nd elbow				
Equation 4-8	Input	$\beta_{s,out}$	0.0013	
	Input	P_s	38.33	psia
	Input	P_{el}	42.76	psia
	Output	$\beta_{el,in}$	0.0011	
Equation 4-7	Input	Q	18548	gpm
	Input	d	23.25	inch
	Input	um	14.00	ft/sec
	Output	Fr	1.77	
Equation 4-6	Input	Fr	1.77	
	Input	$\beta_{el,in}$	0.0011	
	Input	$\Delta t_{el,in}$	7.73	sec
	Output	$\beta_{el,out}$	0.0007	
Equation 4-9	Input	$\beta_{el,in}$	0.0011	

Table 11-14 WCAP-17271 Calculation of $\beta_{el,out}$ and $\Delta t_{el,out}$ for 2nd elbow				
	Input	$\Delta t_{el,in}$	7.73	sec
	Input	$\beta_{el,out}$	0.0007	
	Output	$\Delta t_{el,out}$	12.08	sec

Equation 10-3 is used to adjust the gas volumetric flux ratio each time the flow rate changes due to an off-take. Table 11-15 shows the results for the 1st off-take.

Table 11-15 WCAP-17271 Calculation of $\beta_{el,out}$ and $\Delta t_{el,out}$ for 1st off-take				
Equation 10-3	Input	β_{in}	0.0007	
	Input	Q_{in}	18548	gpm
	Input	Q_{out}	870	gpm
	Output	β_{out}	0.0156	

Table 11-16 shows the results for the 3rd elbow.

Table 11-16 WCAP-17271 Calculation of $\beta_{el,out}$ and $\Delta t_{el,out}$ for 3rd elbow				
Equation 4-8	Input	$\beta_{s,out}$	0.0156	
	Input	P_s	42.76	psia
	Input	P_{el}	41.97	psia
	Output	$\beta_{el,in}$	0.0159	
Equation 4-7	Input	Q	870	gpm
	Input	d	7.981	inch
	Input	um	5.57	ft/sec
	Output	Fr	1.20	
Equation 4-6	Input	Fr	1.20	
	Input	$\beta_{el,in}$	0.0159	
	Input	$\Delta t_{el,in}$	12.08	sec
	Output	$\beta_{el,out}$	0.0059	
Equation 4-9	Input	$\beta_{el,in}$	0.0159	
	Input	$\Delta t_{el,in}$	12.08	sec
	Input	$\beta_{el,out}$	0.0059	
	Output	$\Delta t_{el,out}$	32.39	sec

Equation 10-3 is used to adjust the gas volumetric flux ratio each time the flow rate changes due to an off-take. Table 11-17 shows the results for the 2nd off-take.

Table 11-17 WCAP-17271 Calculation of $\beta_{el,out}$ and $\Delta t_{el,out}$ for 2nd off-take				
Equation 10-3	Input	β_{in}	0.0059	
	Input	Q_{in}	870	gpm
	Input	Q_{out}	660	gpm
	Output	β_{out}	0.0078	

Table 11-18 shows the results for the 4th elbow.

Table 11-18 WCAP-17271 Calculation of $\beta_{el,out}$ and $\Delta t_{el,out}$ for 4th elbow				
Equation 4-8	Input	$\beta_{s,out}$	0.0078	
	Input	P_s	41.97	psia
	Input	P_{el}	39.04	psia
	Output	$\beta_{el,in}$	0.0084	
Equation 4-7	Input	Q	660	gpm
	Input	d	6.065	inch
	Input	um	7.32	ft/sec
	Output	Fr	1.81	
Equation 4-6	Input	Fr	1.81	
	Input	$\beta_{el,in}$	0.0084	
	Input	$\Delta t_{el,in}$	32.39	sec
	Output	$\beta_{el,out}$	0.0083	
Equation 4-9	Input	$\beta_{el,in}$	0.0084	
	Input	$\Delta t_{el,in}$	32.39	sec
	Input	$\beta_{el,out}$	0.0083	
	Output	$\Delta t_{el,out}$	32.72	sec

By repeated application of these steps, the gas volumetric flux ratio at the pump inlet ($\beta_{Pump\ Calc}$) and transport time ($\Delta t_{Pump\ Calc}$) can be calculated. It is noted that the overall transport time exceeds 20 seconds. Therefore, the steady state pump criteria must be applied. The allowable steady state gas volumetric flux ratio for this pump is 0.01, which is satisfied by a void volume of 0.43 ft^3.

11.1.10 Verify Vertical Down-comer Limitation

The gas volume calculated in Section 10.4.2 meets the pump criteria provided in Table 3-1 or Table 3-2. However, it must be demonstrated that the vertical down-comer limitation is met to ensure the separated flow region remains in the down-comer and bubbly flow exits the bottom. This can be done directly by using Equation 5-6 to calculate y based on the gas volume (V_g) and liquid flow rate (Q_l), velocity (u_l) and pipe cross-section area (A) at the down-comer location. The parameter y is the required down-comer length. Alternatively, Figure 6-5 through Figure 6-8 can be used to estimate the allowable gas volume.

If credit is taken of an intermediate down-comer volume to meet the Section 6.3.4 criteria, then the gas volume must be adjusted for the static pressure which exists at the intermediate down-comer.

In addition, if credit is taken of an intermediate down-comer volume to meet the Section 6.3.4 criteria, only the vertical-to-horizontal elbows downstream of the intermediate down-comer can be credited in the WCAP-17271 methodology.

Table 11-10 indicates that the length of the kinematic shock for a gas volume of 0.4 ft^3 is 0.6 ft of 24 inch pipe. The allowable gas volume of 0.43 ft^3 will therefore require a down-comer which is slightly large than 0.6 ft. The length of the first down-comer is 15 ft., which exceeds the required length by a substantial amount. Therefore, the first down-comer length is acceptable.

11.1.11 Verify Horizontal Off-take Limitation

The gas volume calculated in Section 10.4.2 meets the pump criteria provided in Table 3-1 or Table 3-2. However, it must be demonstrated that if an off-take is located in a horizontal run of pipe, the criteria in Section 6.3.6 is met. As long as the Froude Number in the horizontal header is greater than or equal to unity and the gas volumetric flux ratio is less than or equal to 25% the limitation is met.

Table 11-14 indicates the Froude number is 1.77 in the 24 inch pipe upstream of the first off-take. Table 11-15 indicates the gas volumetric flux is 0.0007 at the inlet and 0.0156 at the outlet of the off-take. Table 11-16 indicates the Froude number is 1.20 at the outlet of the off-take.

Table 11-16 indicates the Froude number is 1.20 in the 8 inch pipe upstream of the second off-take. Table 11-17 indicates the gas volumetric flux is 0.0059 at the inlet and 0.0078 at the outlet of the off-take.

Therefore, both off-takes are well within the limits to ensure the gas does not stratify.

11.1.12 Verify Pump Inlet Limitation

11.1.12.1 Horizontal Inlet

If the pump has a horizontal inlet preceded by a vertical down-comer, it should be verified that either a kinematic shock does not form in the horizontal pipe downstream of the elbow, or that the length of horizontal pipe is sufficient to prevent the kinematic shock from directly entering the pump.

Equation 6-6 provides the required allowable gas volumetric flow ratio to form a kinematic shock at the outlet of a vertical-to-horizontal elbow in terms of the Froude number. Equation 6-7 provides a relation between the maximum gas volumetric flux at the down-comer outlet and the shock length y calculated by Equation 5-6 divided by the diameter of the down-comer. A kinematic shock will not form if the calculated gas volumetric flux ratio is less than the required flux ratio. Alternatively, Figure 6-13 through Figure 6-15 can be used to determine if a kinematic shock will form.

If a kinematic shock does form, Equation 6-21 provides the necessary pipe volume to prevent the kinematic shock from directly entering the pump as a function of Froude number.

Table 11-7 indicates both pumps have a horizontal inlet and that pump 2 has a horizontal inlet pipe with a volume of 1.0 ft^3. Equation 6-21 is used to determine the allowable gas volume if a kinematic shock forms. Table 11-19 summarizes the results of these calculations. The allowable gas volume if a kinematic shock occurred is 0.21 ft^3, which is less than the value of 0.43 ft^3 based on the pump limits. The minimum required volumetric flux to create a kinematic shock is 0.13. A 0.43 ft^3 gas volume in a 6-inch pipe at with a flow rate of 660 gpm creates a kinematic shock of 3.797 feet which results in a maximum volumetric flux of 0.1295, which is less that the allowable value of 0.13; therefore, a kinematic shock will not occur. In addition, the 3.797 foot shock length is well less than the 12 feet vertical down-comer at the pump inlet. Therefore, the pump inlet criteria are met.

Table 11-19 Horizontal Inlet Limits				
Equation 6-21	Input	V	1.00	ft^3
	Input	Fr	1.81	
	Output	V	0.21	ft^3
Equation 6-6	Input	Fr	1.81	
	Output	$\beta_{min\ reqd}$	0.13	
Equation 5-6	Input	Q	660	gpm
	Input	U_l	7.329968	ft/sec
	Input	d	6.065	inch
	Input	A	0.2006	ft^2
	Input	V_g	0.43	ft^3
	Input	L_s	3.797	ft
	Output	L_s	3.797	ft
Equation 6-7	Input	V_g	0.43	ft^3
	Input	d	6.065	inch
	Input	Q	660	gpm
	Input	L_s	3.797	ft
	Output	β_{max}	0.1295	ft^3

11.1.13 Verify Maximum Flow Limitation

This is not applicable since the Froude number does not exceed 2.5 throughout the system and the pump does not have a vertical downwards inlet.

11.1.14 Adjust Allowable Gas Volume to Surveillance Static Pressure

Table 11-4 indicates the static pressure at accumulation location A (Figure 11-1) is 36.12 psia during pump operation. Table 11-5 indicates static pressure at accumulation location A (Figure 11-1) is 38.50 psia during surveillance testing. The calculated allowable gas volume of 0.43 ft^3 is based on the static pressure during operating conditions. This gas volume must be adjusted to the static pressure that exists during surveillance tests using Equation 11-1.

$$V_{g,sur} = \left(\frac{P_{op}}{P_{sur}}\right) V_{g,op} = \left(\frac{36.12}{38.50}\right)\left(0.43\ ft^3\right) = 0.40\ ft^3 \qquad \text{Equation 11-1}$$

11.2 SUMMARY OF RESULTS

The WCAP-17276 methodology initially allowed a gas volume of 0.4 ft^3. However, this was limited to 0.024 ft^3 due to the fact that the very high gas velocity (14 ft/sec) in the gas accumulation location would entrain the gas at a much faster rate (0.3 sec) than the pump transient limit (5 sec). Therefore, a significant reduction in void fraction was necessary to limit the average void fraction to 0.05 over the transport time period. Since the gas transport time predicted by the WCAP-17276 methodology is less than the minimum 0.5 second transport time limit allowed by the NRC (Section 7), the gas volume could be increased to (0.5 sec/ 0.3 sec) (0.024 ft^3)=0.04 ft^3.

The WCAP-17271 methodology allowed a gas volume of 0.43 ft^3 during operating conditions. The allowable gas volume was limited based on the horizontal pump inlet. As a point of comparison with the WCAP-17271 method, the flow initialization model for WCAP-17271 also predicted a flow initialization time of 0.32 seconds for a 0.43 ft^3 gas volume. However, due to the presence of several elbows, the predicted transport time to the pump was 33 sec. This is well above the transient time limit of 5 seconds. Due to the fact that the operating flow rate of the pump under evaluation was 47% beyond the best efficiency flow rate, Table 3-1 limits the steady state pump gas volumetric flux ratio to 0.01. Using an iterative procedure, it was demonstrated that the 0.43 ft^3 void meets this limit.

The methodologies documented in this report were used to evaluate the potential impact of various configurations on the allowable gas volume. The results are summarized as follows:

- Vertical down-comer limitation: Equation 5-6 was used to determine that the kinematic shock length is 0.6 feet as compared with the down-comer length of 15 feet.
- Horizontal off-take limitation: There are two horizontal pipe runs with horizontal off-takes. It was demonstrated that the Froude number at the inlet to the off-take was greater than 1 in both cases. In addition, the gas volumetric flux was 0.01 which is well less than the allowable limit of 0.25.
- Horizontal pump inlet configuration: Both pumps in the sample evaluation had horizontal inlets. Equation 6-21 was used to demonstrate that if a kinematic shock were to occur,

the pump inlet piping would limit the gas volume to 0.21 ft^3 to prevent the kinematic shock from directly entering the pump. Equation 6-6 was used to determine that a gas flux ratio of 0.13 is required to form a kinematic shock at the vertical-to-horizontal elbow at the pump inlet. Equation 6-7 was used to determine that the gas volumetric flux at the entrance to the vertical-to-horizontal elbow was 0.1295 based on the shock length y calculated using Equation 5-6. This is less than the allowable limit of 0.13.
- Vertical pump inlet configuration: There are no pumps with vertical downwards inlets in the sample evaluation. Therefore, it was not necessary to demonstrate that the gas volume was limited to preclude a kinematic shock for entering the pump or demonstrating that the Froude number at the pump inlet did not exceed 2.5.

The allowable gas volume of 0.43 ft^3 during operating conditions was adjusted to account for the difference in static pressure between operating conditions and surveillance testing. The corresponding allowable gas volume during surveillance testing is 0.40 ft^3.

12 ROAD MAP FOR DETERMINING OPERABILITY LIMITS

The intent of this section is to provide a road map to the overall process of developing operability limits using flow charts to clarify the process. Figure 12-1 depicts the overall process which includes developing the inputs, choosing an evaluation tool, and determining if piping layout geometry limits the gas volume. Figure 12-2 elaborates on the process for developing the input parameters.

Figure 12-3 outlines the process to determine which evaluation methodology is chosen. It is noted that there are four potential conditions that can preclude the use of either the WCAP-17271 or WCAP-17276 methodologies:

1. If a vertical down-comer does not exist between the gas accumulation location and the pump inlet, then nether the WCAP-17271 or WCAP-17276 methodologies can be applied. Both the WCAP-17271 and WCAP-17276 methodologies rely upon the presence of a vertical down-comer to entrain the gas from an initially separated regime into a dispersed bubble flow.
2. If flow conditions allow the gas to stratify in a horizontal pipe which contains an off-take (and the off-take is either horizontal or rotated downwards), this can result in a downstream surge of gas if a vortex were to occur. The conditions for stratification are addressed in Section 6.3.6 of this report. If the Section 6.3.6 methods indicate flow can stratify in the horizontal pipe, then the following options exist:
    a. If there is a vertical down-comer in the flow path downstream of off-take, the allowable gas volume can be calculated using WCAP-17271 or WCAP-17276 by assuming the accumulation location is downstream of the off-take.
    b. If the off-take is vertically upwards then a vortex will not occur and WCAP-17271 or WCAP-17276 can be used.
    c. If conditions a) or b) do not apply, then WCAP-17271 or WCAP-17276 cannot be used.
3. If the pump has a vertical downwards inlet and the gas accumulation location is immediately upstream of that down-comer, WCAP-17271 or WCAP-17276 cannot be applied if the Froude number is greater than 2.5. This situation can result in co-current slug flow of gas directly into the pump inlet.
4. If the pump has a horizontal inlet preceded by a vertical down-comer, and the Froude number is less than 1, WCAP-17271 or WCAP-17276 cannot be applied since criteria are not available for determining if a kinematic shock or hydraulic jump would occur in the horizontal inlet piping.

Figure 12-4 outlines the WCAP-17276 methodology, commonly referred to as the Simplified Equation. Figure 12-5 outlines the WCAP-17271 methodology, also referred to as the Purdue method or Purdue correlations. Figure 12-6 shows the method used to determine if the allowable gas volume is limited by the down-comer volume. Figure 12-7 provides a method for evaluating horizontal pump inlet. Figure 12-8 provides a method for determining if a horizontal off-take limits the allowable gas volume.

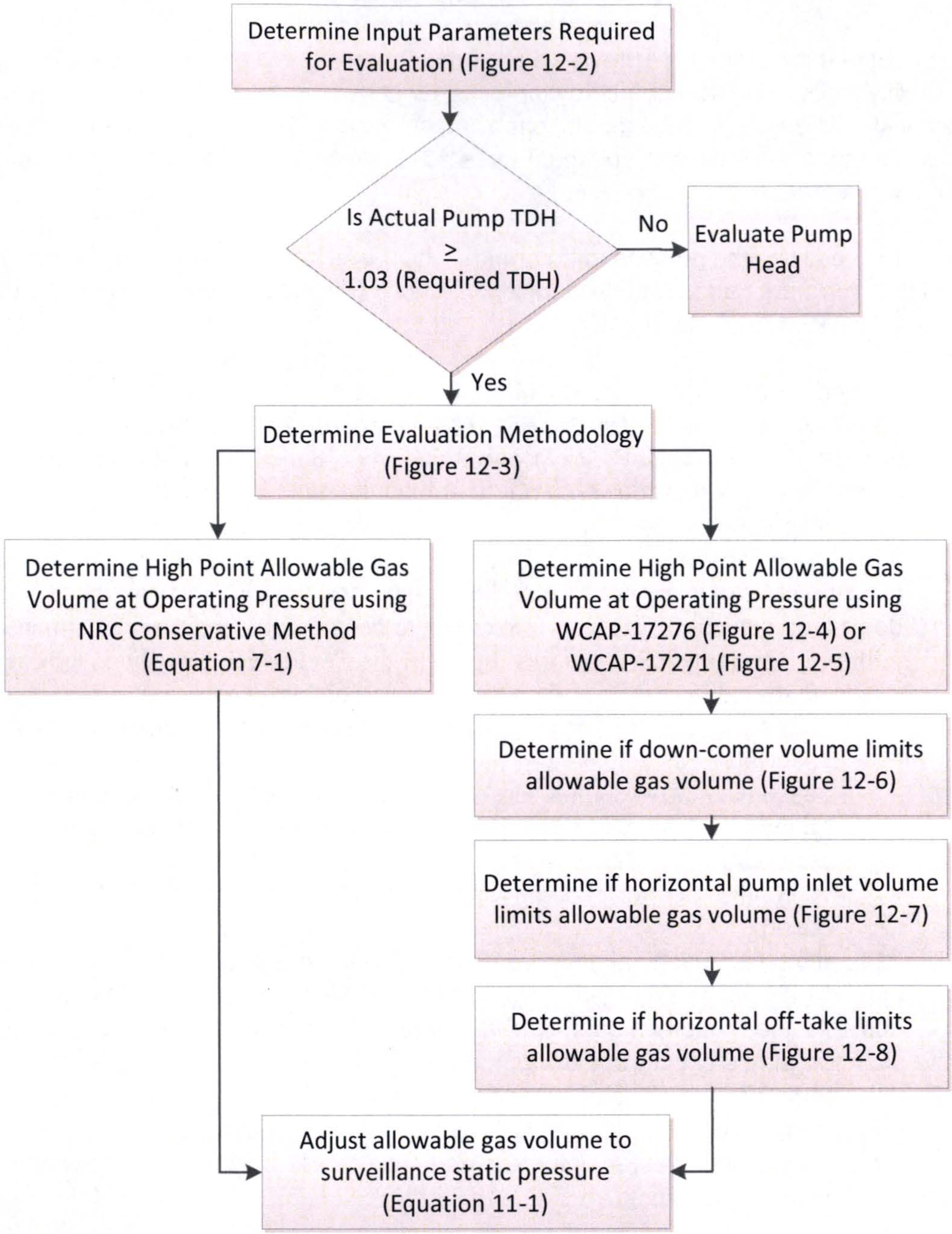

Figure 12-1 Overall Process to Determine Operability Limits

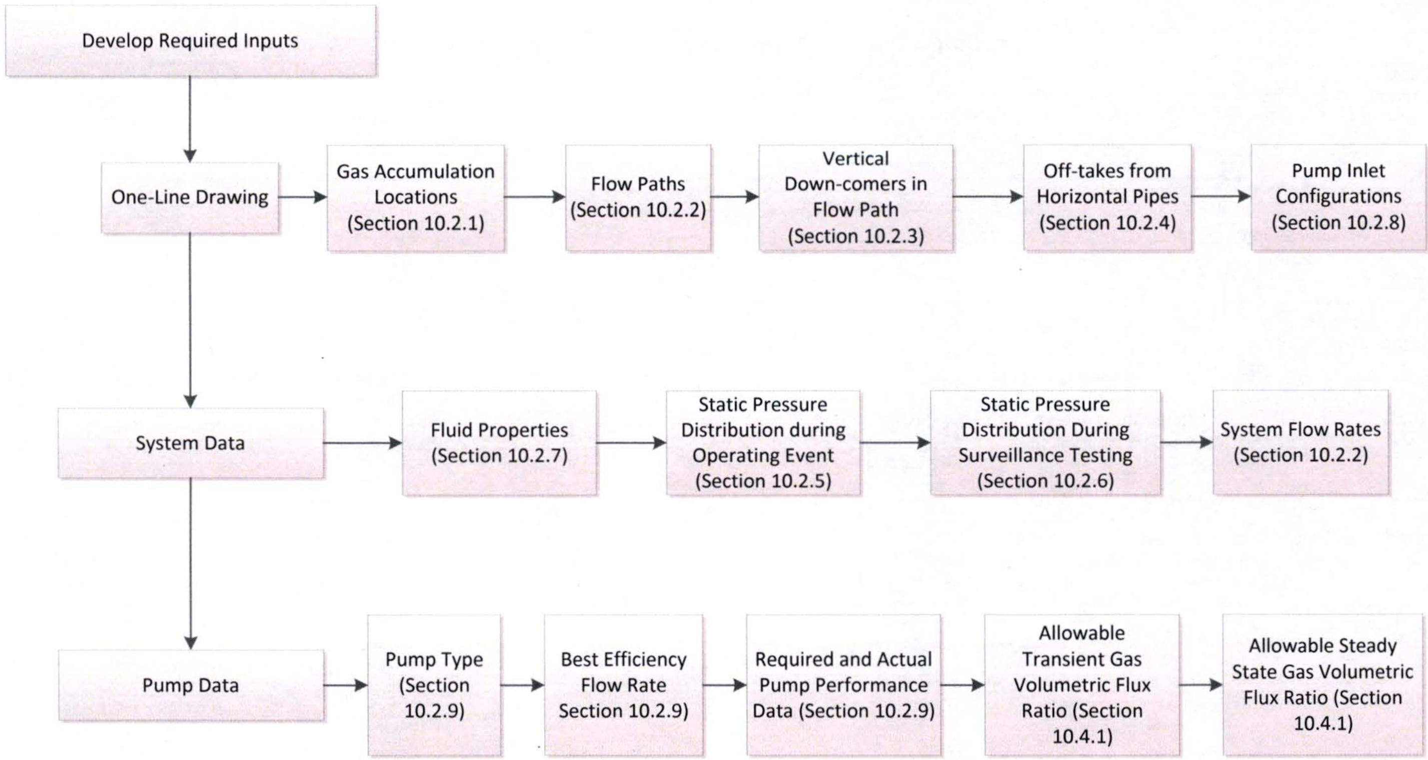

Figure 12-2 Develop Required Input Parameters for Evaluation

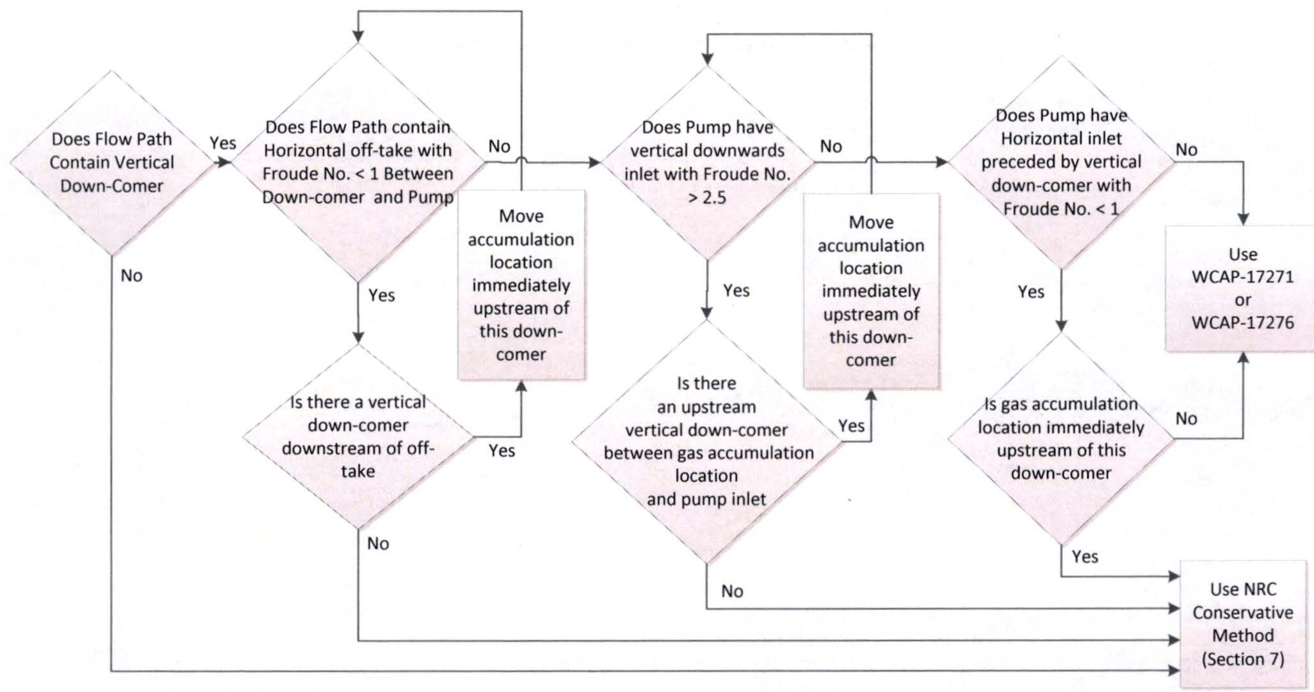

Figure 12-3 Determine Evaluation Methodology

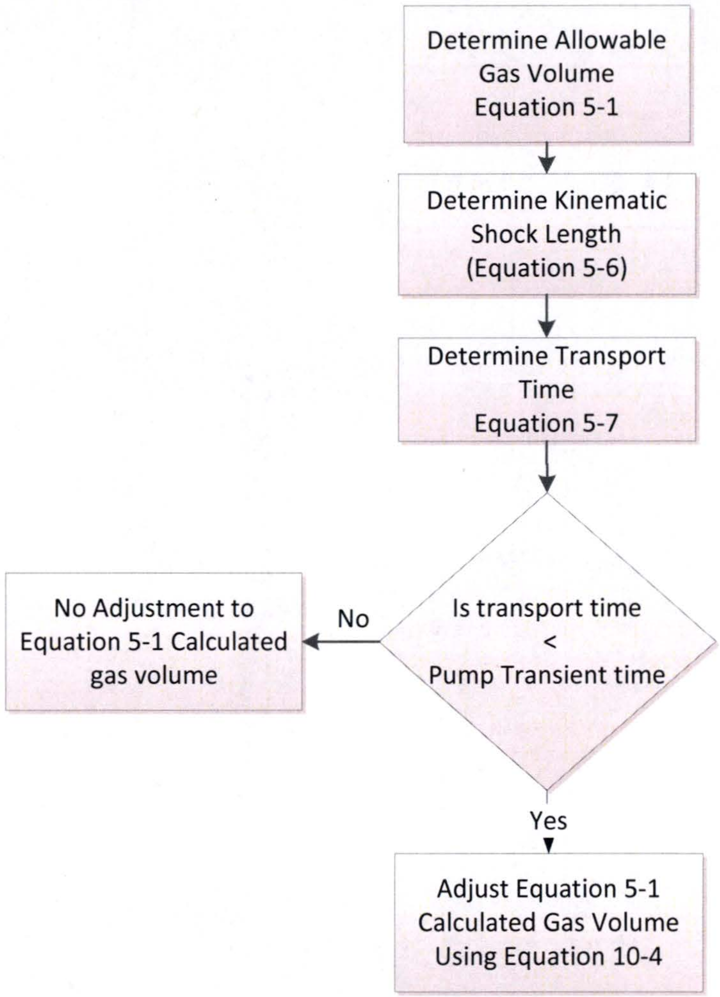

Figure 12-4 WCAP-17276 Evaluation Methodology

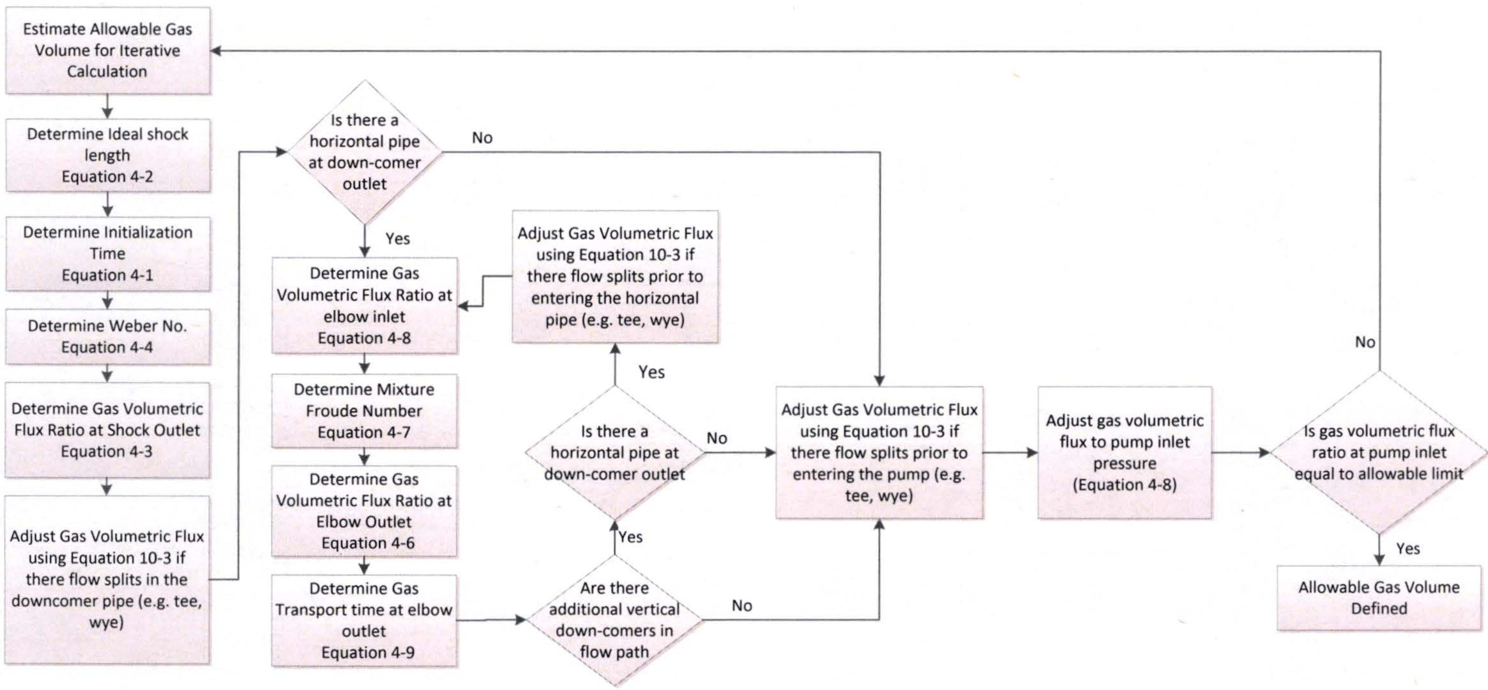

Figure 12-5 WCAP-17271 Evaluation Methodology

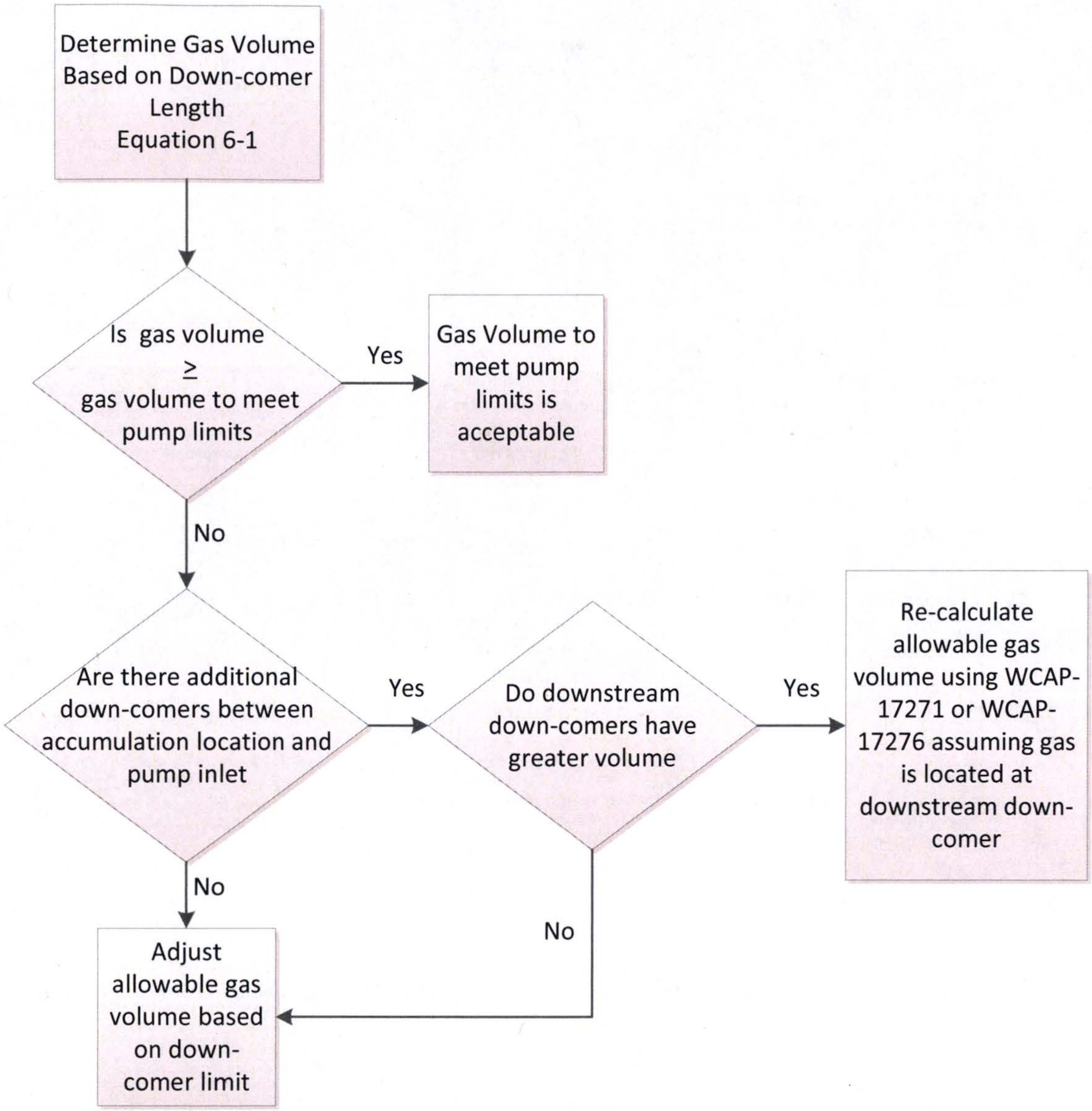

Figure 12-6 Determine if Down-comer Volume Limits Allowable Gas Volume

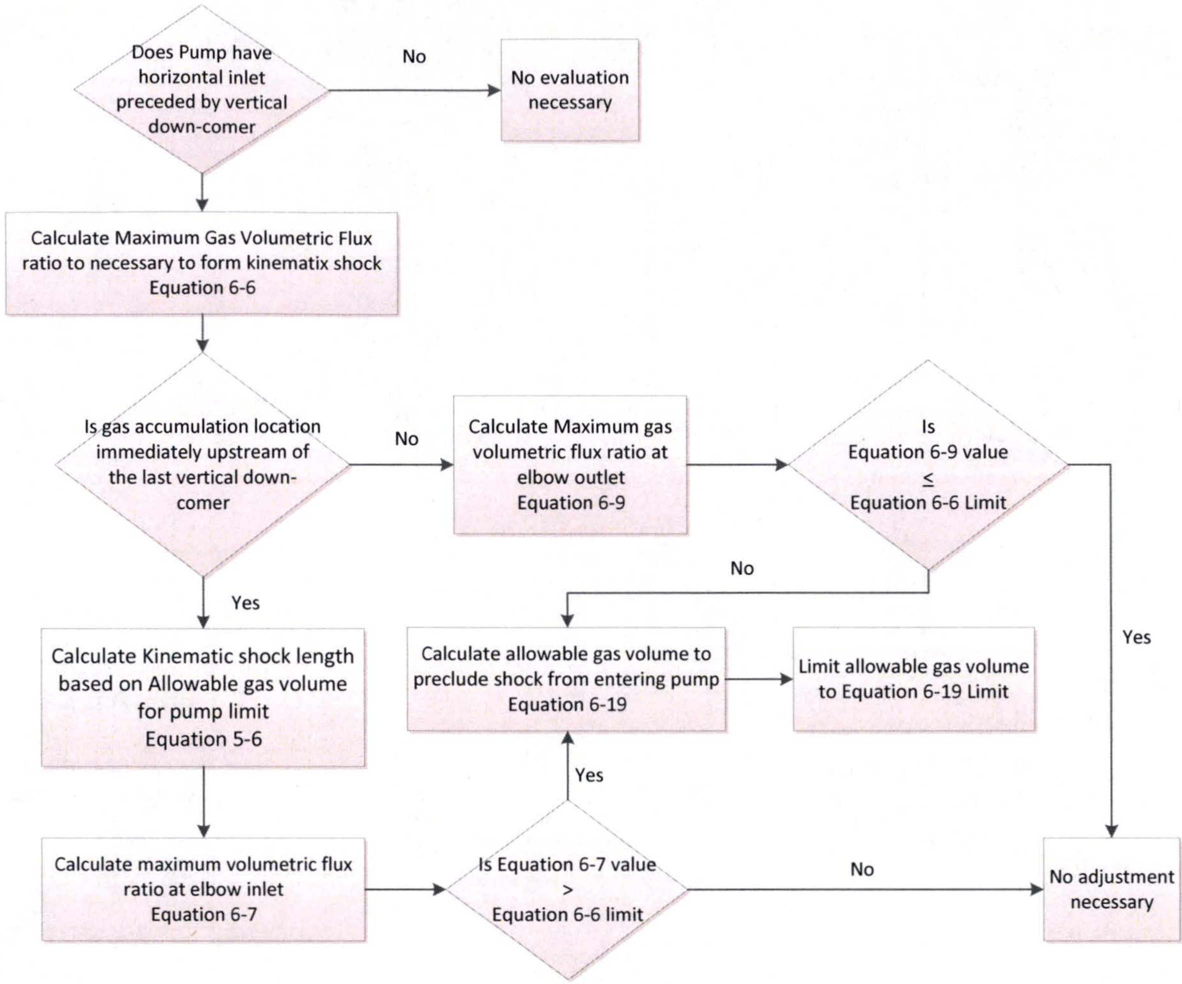

Figure 12-7 Determine if Horizontal Pump Inlet Volume limits Allowable Gas Volume

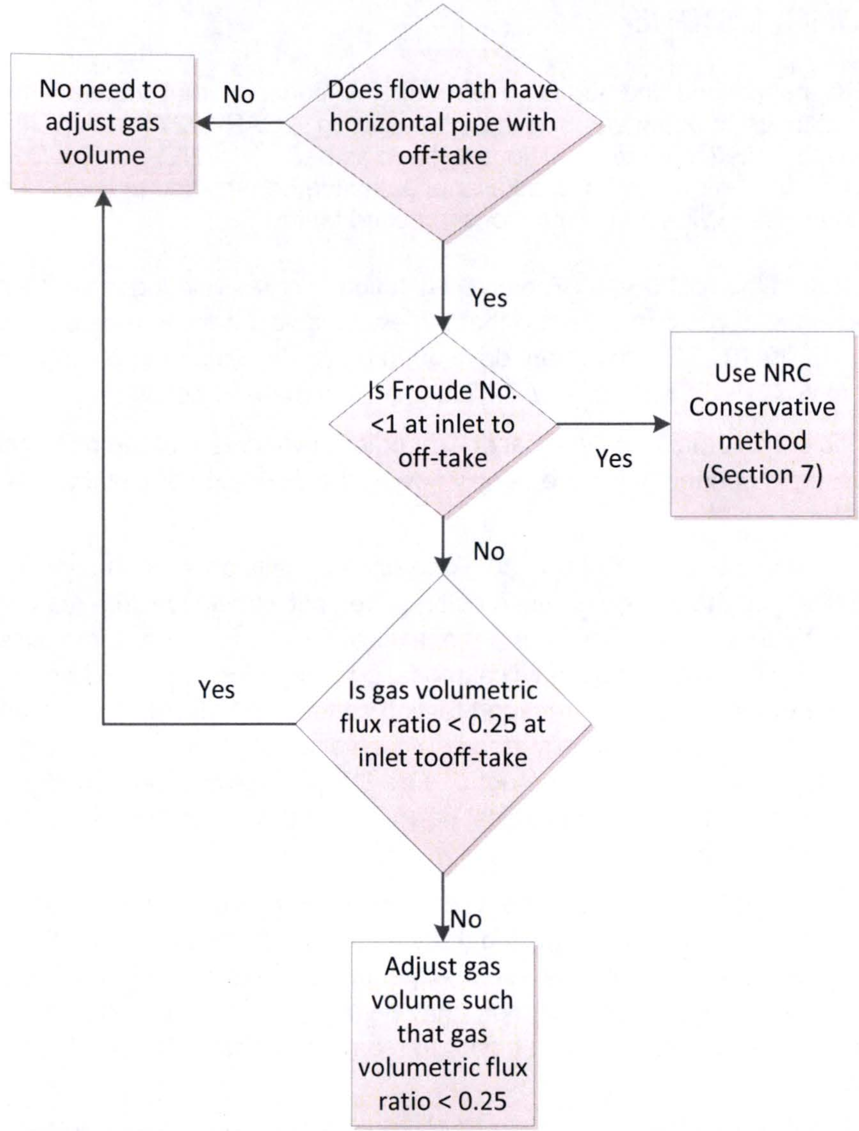

Figure 12-8 Determine if Horizontal Off-take limits Allowable Gas Volume

13 CONCLUSIONS

Recent NRC inspections and audits have resulted in concerns that licensees may not have adequate guidance to apply the correlations based on WCAP-17271 and WCAP-17276 consistent with limitations and conditions defined as part of the NEI-09-10 SE for gas transport analyses. The NRC requested that additional guidance be provided to licensees to ensure the correlations are used within the limitations imposed by the SE.

Section 3.15.3 of the NEI-09-10 SE places limitations on gas void ingestion by pumps to assure bubbly flow at the pump entrance and that the average void fraction meets acceptance criteria defined in NEI-09-10. This document developed methodologies to address these limitations on the usage of WCAP-17271 and WCAP-17276, as summarized below.

1. Sufficient volume in the vertical down-comer downstream of the gas accumulation location is needed to assure bubbly flow at the down-comer exit if a vertical down-comer exists.

   Westinghouse report FAI 09/130 (Reference 8) developed an analytical model to predict the distance the separated flow region (kinematic shock) would extend from the top of the horizontal elbow (Equation 5-6 of this report). This report demonstrated (Section 6.3.4) the validity of this analytical model by comparing the model predictions with measurements from gas transport testing conducted at Purdue University (Figure 6-1through Figure 6-4 of this report). As an alternative to the direct application of Equation 5-6, Figure 6-5 through Figure 6-8 were developed based on Equation 5-6, which provide the required vertical down-comer volume to ensure bubbly flow exists at the down-comer outlet.

2. If a horizontal pipe connects between the bottom of a down-comer and a pump entrance, a methodology should be applied that has a multi-dimensional two phase capability that has been verified by comparison to experimental data. Since phenomena in this region are not well understood, judgment may be a significant factor and a suitable safety factor should be added to predict behavior to reasonably ensure the prediction encompasses actual behavior.

   Westinghouse report WCAP-17537 (Reference 11) summarized the results of testing conducted by Westinghouse to establish dynamic venting requirements. As part of this testing, the air flow rate necessary to develop gas flow separation (kinematic shock) at the outlet of a vertical-to-horizontal elbow was determined as a function of water flow rate. This data was used to develop a relationship for the minimum required gas flux ratio to develop a kinematic shock at the elbow outlet (Equation 6-6) as a function of Froude Number.

   Westinghouse report WCAP-17271(Reference 3 and 4) summarize the results of gas transport testing in pump suction piping conducted at Purdue University. These results were used to develop a relationship (Equation 6-7) between the maximum gas flux ratio at the down-comer exit as a function on the vertical kinematic shock length as predicted by Equation 5-6.

   The testing conducted in support of WCAP-17537 measured the kinematic shock depth as a function of distance and flow rate. This data was used to establish a relationship

(Equation 6-21) for the required pipe inlet piping volume to ensure the kinematic shock does not encroach upon the pump inlet.

These relationships are summarized in Section 6.3.5 of this report.

3. Horizontal pipes may introduce other concerns. For example, flow stratification in horizontal pipes can lead to an accumulation of gas, such as in off-take or tee geometry. Once gas is accumulated, a subsequent instability can lead to a large surge in gas downstream.
4. Section 6.3.6 of this report utilizes flow regime maps for horizontal pipes developed from air-water test data (Reference 10) and from analytical considerations (Reference 14) to demonstrate that as long as the Froude number is equal to or greater than unity and the gas volumetric flux ratio is less than or equal to 0.25, then the gas cannot separate from the liquid into a stratified flow regime. The gas will be transported by the liquid in an intermittent (plug flow) or dispersed (bubbly flow) regime which will preclude an accumulation of gas, such as in off-take or tee geometry, which can lead to a subsequent instability resulting in a large surge in gas downstream.
5. If Froude number is greater than 2.5, there is a potential that a void will be transported as a slug.

   Section 6.3.7 of this report demonstrates based on 1) observations from the Purdue University testing that the slugs tended to be very unstable and break up in the vertical pipe, 2) the flow regime maps discussed in Section 6.3.6 indicate that a large slug would tend to quickly break up in the horizontal header if it made it to the bottom of the vertical down-comer, and 3) that the Purdue testing indicates that a vertical-to-horizontal elbow tends to hold-up gas at the elbow. Section 6.3.7 concludes that if the vertical down-comer is followed by an elbow and a horizontal run (that is, the vertical pipe does not go directly into the pump), it can be safely assumed a co-current slug would be broken up quickly, and the Froude number limit of 2.5 is not applicable. This limit remains applicable for pumps with vertically downward inlets when the gas accumulation location is immediately upstream of the pump inlet.

In order to facilitate implementation of the methodologies provided in WCAP-17271 and WCAP-17276, Sections 4, 5 and 1 provide detailed guidance for application of these methodologies in conjunction with the methods outlined in Section 6 to ensure implementation consistent with the limitations identified in the NRC SE on NEI 09-10. In addition, Section 11 of this report demonstrates this implementation through the use of a detailed worked example problem. Section 1 provides a road map of the evaluation process to facilitate use of the process.

The information in this report enables licensees to develop acceptance criteria to be used in operability evaluations for allowable gas volumes in safety related pump suction piping.

APPENDIX A - DESCRIPTION OF DYNAMIC VENTING TEST FACILITY

The test loop was constructed such that the effects of a 90° elbow connecting a vertically downward to horizontal section of piping, check valve and three orifices could be observed. A three dimensional piping and instrumentation diagram (P&ID) of the full test loop that was constructed and can be found below in Figure A-1. All elevations represent the vertical length from floor to pipe centerline. All lengths of pipe represent the total length between the start and end of a straight line section of pipe with fittings and impedance meters included in the total length. All pipe elbows, with the exception of a few elbows used in the loop, were clear, PVC, schedule 40 with an r/D of 2.5 and are labeled in Figure A-1. The elbows specified in Figure A-2 had the following specifications: 6" long sweep elbows had an r/D of 2.5, 4" long sweep elbows had an r/D of 2.0, and the short radius elbows had an r/D ranging 0.5 to 1.0. The pressure transducers were not shown in this figure since they varied throughout testing; only general pressure fitting locations were shown on the piping without dimensions. Figure A-2 shows the detailed locations of all instrumentation and pressure taps used for the 6- have been colored blue for convenience. Note that all dimensions listed in Figure A-1 and Figure A-2 are within +/- ¼". Extra care was taken when measuring the distance between each impedance meters due to the importance in the data analysis. Table A-1 shows exact distances between the centerline (C-C) of each meter with a measurement accuracy of +/- 1/8".

Table A-1 Distance between Impedance Meters

Impedance Meters	C-C Distance (in)
VM8 – VM9	84.25
VM10 – VM11	96.25
PW1 – PW2	84.50

Two separate air injection locations were used throughout testing. Air injection location 1 was used for tests involving the 4" and 6" 90° elbow and air injection location 2 was used for tests involving orifices and a check valve. An additional air injection location, not shown in Figure A-1, existed on the top header of the loop near the outlet of the first white long sweep elbow. Both air injection location 1 and 2 have been labeled in the loop P&ID in Figure A-1 and air injection location 1 is shown in greater detail in Figure A-1 and Figure A-2. All air flow rates were monitored by the air flow meter (AFM) listed in Table A-2.

Impedance measurements were acquired at the outlet and several feet downstream of each flow restriction (elbow, orifice and check valve). Note that the impedance meters (VM) in Figure A-1 are referred to as Double Ring Impedance Meters (RIMP).

Differential pressure measurements were acquired across each flow restriction and also across the piping downstream of the flow restriction in most tests. A pressure measurement was also acquired upstream of the flow restriction being tested. All pressure taps were placed on the side of the pipes to avoid air entering into the tubing.

Figure A-1 and Figure A-2 show detail of the tested pipe geometry. The liquid flow rate was monitored downstream of the pump. The tank was kept near atmospheric conditions to act as a gas separator, which maintained water solid conditions through the pump and liquid flow meter. All piping that was not part of each test section consisted of 6" clear, PVC, schedule 40, with a limited section at the outlet of the pump being 4", PVC, schedule 40 pipe.

All instrumentation was calibrated through a vendor which complies with National Institute of Standards and Technology (NIST) traceable standards. The make, description, model number, serial number, and calibrated range of each instrument are included in Table A-2 below. All impedance meters (VM 7-11) and PW(1&2) were fabricated and calibrated by Westinghouse.

All uncertainties for the corresponding instruments listed above in Table A-2 are listed below in Table A-3. More details about the calibration uncertainties can be found in the equipment datasheets that are stored in the calibration database listed above.

Table A-2 Instrument Calibration Information				
	Description	Model #	Serial #	Range
AFM	Sage Metering Air Flow Meter	SIG-200-DC24-AIR-RG3	44155A-29954	0-600 SCFM
AFM	Sage Metering Air Flow Meter	SIG-200-DC24-AIR-RG3	44155B-29954	0-200 SCFM
AFM	Sage Metering Air Flow Meter	SIG-200-DC24-AIR-RG3	44155C-29954	0-20 SCFM
DP 1	Rosemount Pressure Transmitter	3051CD2A22A1AB4M5Q4	2129435	0-9.03 psi
DP 2	Rosemount Pressure Transmitter	3051CD2A22A1AB4M5Q4	2129436	0-9.03 psi
DP3	Rosemount Pressure Transmitter	3051S1CD4A2E12A1AB4M5Q4	0357661	-10-50 psi
MFM	Yamatake Magnetic Flow Meter (Converter)	MGG14C-RH4A-1B1N-YAH	R-A1440-A1-011	0-1250 GPM
	Yamatake Magnetic Flow Meter (Detector)	MGG18F-100PA11LS1AHA-X-Y	R-91589-41-124A	0-1250 GPM
P1	Rosemount Pressure Transmitter	3051S1CG4A2E12A1AB4M5Q4	0357662	-14.2-150 psi
TC	Omega Type T Thermocouple with 6" length probe and 0.25" diameter probe	NB1-CPSS-14U-6	VT-980224-05	0-200 °C
VM(7-11)	Westinghouse			
PW(1&2)	Westinghouse			

Table A-3 Distance between Impedance Meters	
Impedance Meters	C-C Distance (in)
AFM	+/-1% of Reading +0.5% of Full Scale
DP 1	±0.065% of span= ± 0.006 psi
DP 2	±0.065% of span= ± 0.006 psi
DP 3	±0.025% of span= ± 0.015 psi
MFM	Q>498 gpm, error = 0.5% of rate Q<498 gpm, error = 0.1% of range
P1	±0.025% of span = ± 0.041 psi
TC	± 0.3 C
VM(7,8,9,10)	(0.5 + 3% of measured void fraction)%
VM11	(0.5 + 4% of measured void fraction)%
PW1	(0.7 + 3% of measured void fraction)%
PW2	(0.6 + 3% of measured void fraction)%
AFM	+/-1% of Reading +0.5% of Full Scale

Data from the AFM, MFM, DP(1-3), and P(1-2) were all be recorded on an IOTech DAQSCAN/2001 data acquisitions system (DAQ). Separate signal conditioning modules for the AFM, MFM, DP(1-3), and P(1-2) measurements were used to convert the instrument signals from a 4-20 milli-Amp (mA) signal to a 1-5 Volt (V) signal. A separate signal conditioning module was used to convert a 0-200 °C temperature reading to a 1-5 V signal. Dasylab was used to convert all readings from the IOTech DAQ system to the proper engineering units. Separate files for each set of tests (6" elbow, 4" elbow, orifice at low air flow rates, and orifice at high air flow rates) were created. Note that two different configurations of the AFM were needed for flows above and below 20 standard cubic feet per minute; thus two separate files were needed. Configuration information is provided in Table A-4.

Each set of impedance meters, VM(8&9), VM(10&11) and PW(1&2), depending on test set, had a 10 KHz electronic signal (1 V peak to peak) in the form of a sine wave provided across each of the impedance meter's electrodes. The electronic signal was provided by a Tektronix® Signal generator (Model AFG 3011). Both the voltage applied by the signal generator (V1) and the voltage across an impedance meter (V2), which was in series with a 981 Ω resistor, were measured by a National Instruments® (NI) PXI-6251 data acquisition board at a rate of 400 kHz. A high speed matrix switch was used to switch back forth between the two meters.

Calibration information for the NI data acquisition board, IOTech DAQSCAN/2001 data acquisitions system and signal conditioning modules can be found below in Table A-4.

Information as to which signal conditioning modules were connected to specific instruments (Instrum.) are also provided in the table below.

Table A-4 Instrument Calibration Information

Instrum.	Description	Model #	Serial #	Range	Error
N/A	IOTech DAQ System	DAQSCAN/2001	806352	-10 to +10 V	0.015% reading + 0.005 %range
AFM	Dataforth Signal Conditioning Module	SCM5B42-01	41494-11	4-20 mA	±0.1125% mA reading
All VM's	National Instruments DAQ Board	NI-PXI-6251	1413D1A	-10 to +10 V	1920 μV @ max Analog Input (10 V)
DP 1	Dataforth Signal Conditioning Module	SCM5B42-01	49369-9	4-20 mA	±0.1125% mA reading
DP 2	Dataforth Signal Conditioning Module	SCM5B42-01	41494-9	4-20 mA	±0.1125% mA reading
DP 3	Dataforth Signal Conditioning Module	SCM5B42-01	41494-11	4-20 mA	±0.1125% mA reading
MFM	Dataforth Signal Conditioning Module	SCM5B42-01	41494-12	4-20 mA	±0.1125% mA reading
P1	Dataforth Signal Conditioning Module	SCM5B42-01	41494-15	4-20 mA	±0.1125% mA reading
P2	Dataforth Signal Conditioning Module	SCM5B42-01	41494-17	4-20 mA	±0.1125% mA reading
TC	Dataforth Signal Conditioning Module	SCM5B47T-07	11958-17	0-200 °C	±0.25% reading

a,c

Figure A-1 Dynamic Venting Test Facility

a,c

Figure A-2 6-Inch Elbow Test